UNIVERSITÉ DE SHERBROOKE

Faculté de génie

Département de génie civil

Modelling strategy to implement the local buckling and the non-linear behaviour of bolted connections in the analysis of steel lattice transmission towers

Stratégie de modélisation pour intégrer le flambement local et le comportement non linéaire des connexions boulonnées dans l'analyse des pylônes à treillis en acier de lignes de transport d'énergie

Thèse de doctorat
Spécialité : Génie Civil

Farshad POURSHARGH

Sherbrooke (Québec) Canada

April 2021

MEMBRES DU JURY

Sébastien Langlois, Prof.

Directeur

Frederic Legeron, Prof.

Co-Directeur

Charles-Philippe Lamarche, Prof.

Rapporteur et Évaluateur

Ghyslaine McClure, Prof.

Évaluateur

Simon Prud'homme, Ph.D

Évaluateur

ABSTRACT

The development of finite element method with the aid of powerful software has made it possible to analyze and design complicated civil engineering structures with more accuracy and reliability. Among these, electricity transmission line structures play an important role in our economy. Current practice in transmission line steel lattice tower design has many simplifying assumptions and cannot cover the real behaviour of towers under various loading conditions. Meanwhile, to qualify the design, a full-scale tower test has to be performed which is expensive and time consuming. Advanced numerical models have been developed in the past to simulate with more precision the behaviour of lattice towers. These models can limit and optimize the use of full-scale tests. However, some aspects of the non-linear structural behaviour of towers is still not efficiently taken into account in those advanced numerical methods.

In this research, an advanced numerical modelling and analysis procedure using the finite element method and predicting the behaviour up to failure of lattice towers made of steel angles is proposed. Two main subjects for non-linear modelling of towers are considered. Firstly, the local buckling failure of members using 1D beam elements is addressed by providing a new method to modify the material behaviour of the member. Secondly, a method is presented to predict the behaviour of various configurations of bolted steel member connections. The predicted behaviour then can be applied as a non-linear spring element to model the connections in the full tower. Using these methods less modelling effort, complication and time will be needed for tower projects and full-scale modelling. In addition, more accurate results are expected as we cover more non-linear aspects of the structure behaviour.

Keywords: Lattice steel tower, Angle section, Local buckling, Non-linear behaviour, Fiber beam element, Structure Failure, Bolt Slippage

RÉSUMÉ

L'évolution de la méthode des éléments finis et l'utilisation de puissants logiciels ont rendu possibles l'analyse et la conception des structures complexes de génie civil avec plus de précision et de fiabilité. Parmi ces dernières, les structures du réseau de transport électrique jouent un rôle important dans notre économie.

La pratique courante pour la conception des pylônes en treillis acier contient beaucoup d'hypothèses simplificatrices, et ne reproduit pas adéquatement le comportement réel des pylônes soumis à différents cas de chargement. Entre temps, pour qualifier la conception, un test à grande échelle est généralement réalisé, ce qui est très coûteux et long. Des modèles numériques avancés ont été développés dans le passé pour simuler avec plus de précision le comportement des pylônes en treillis. Ces modèles peuvent limiter et optimiser l'usage d'un test à grande échelle. Néanmoins, certains aspects du comportement structural non linéaire des pylônes ne sont pas considérés dans ces méthodes numériques avancées.

Ces travaux de recherche proposent une modélisation numérique avancée, une procédure d'analyse en utilisant la méthode des éléments finis et la prédiction du comportement à la rupture des pylônes à treillis composés de cornière d'acier. Deux sujets majeurs pour la modélisation non linéaire des pylônes sont considérés. Premièrement, la rupture en voilement local des membrures en utilisant un élément de poutre 1D est traité en fournissant une nouvelle méthode pour modifier le comportement du matériau de l'élément. Deuxièmement, une méthode est présentée afin de prédire le comportement des différentes configurations des connexions boulonnées dans les éléments en acier. Le comportement prédit peut être appliqué en tant qu'élément ressort non linéaire afin de modéliser les assemblages dans le pylône. L'utilisation de ces méthodes diminuera l'effort de modélisation, les complications et le temps nécessaire pour des projets de pylône et

permettra la modélisation à grande échelle. En outre, des résultats plus précis sont attendus étant donné que le comportement non linéaire des structures est davantage pris en compte.

Mot clé : Pylônes à treillis en acier, profilé de cornière, voilement local, comportement non linéaire, élément poutre multi-fibres, ruine des structures, glissement de boulons.

Acknowledgments

I would like to first thank my supervisors Prof. Sebastien Langlois and Prof. Frederic Legeron, for their continuous support and guidance along this way. Without their support and advices to improve this study, it would be impossible for me to achieve this success. My sincere gratitude to Prof. Langlois, who helped me on reviewing this thesis and related articles.

This study is conducted based on research fund from RTE/Hydro-Quebec and Natural Sciences and Engineering Research Council of Canada (NSERC), so I acknowledge all the financial support from these organizations to conclude this program.

Immense experience and knowledge of Dr. Marc Demers, on designing the experimental specimens and testing procedure as well as his comments and encouragement is also highly appreciated. In addition, my special thanks to Dr. Kahina Sad-Saoud, for helping me with experimental results, modeling of specimens and her help on improving the articles.

Finally, my special thanks goes to my Father, Mother and Wife. Words cannot describe what you have provided and sacrificed for me during this journey.

TABLE OF CONTENTS

LIST OF TABLES

LIST OF FIGURES

CHAPTER 1 INTRODUCTION

1.1. Analysis and design of transmission line structures

Transmission lines are important elements of the power systems of modern countries such as Canada. To maintain economic activities, transmission lines must be reliable. At the same time, the geometry of towers should be optimized to control the cost of these very long constructions.

Lattice steel towers are widely used all over the world to support conductors. The structural integrity of towers is a key factor in the reliability of a transmission system. To minimize the risk of disruption to the power supply as a result of tower failure, the reliability of towers needs to be properly evaluated.

A lattice transmission tower is a complex structure, and its design is characterized by the special requirements from electrical and structural points of view. The former determines the general shape of tower in terms of the height and the length of its cross-arms that carry the conductors.

The towers can also be classified according to their location in the line and the way the conductors are attached to the support regardless of the number of wires and circuits. Conductors can be either anchored to the supports or suspended depending on the configuration of the insulator chains. The tangent tower which is primarily designed to be located on straight lines, and normally uses suspension insulators. Typically, 90% of the transmission line is made of tangent towers with suspended supports in flat terrains. Thus, optimized design of tangent towers would minimize the total weight of the steel required in the project. If the line is deviated at a small angle, another type of tower, named angle tower, should be used. Angle towers are designed to resist the permanent transverse load induced from the deviation angle and light angle towers are typically in suspension. In some

conditions the angle of deviation in line can be about 30 to 60 degrees. Dead-end is another type of tower which can be utilized. In such towers, the conductor is discontinued and anchored on both sides of the tower, they are typically the strongest among all types of towers. The construction of each transmission line project is an engineering challenge, and, in certain conditions, the design of unusual towers such as river-crossing towers or highway crossing towers may be necessary. These types of tower are known as special towers.

1.2. Current design recommendations

There are different modelling assumptions in the standard method of analysis and design. There is not a general agreement on the way elements are modelled. One assumption is to consider members as linear structural elements which are connected to each other by frictionless joints acting like hinges. Thus, the tower is idealised as a space truss. Moreover, the influence of end bending moments in members is ignored in the structural analysis, and the leg members, which are continuous, are assumed to be hinged at nodal points. The other common way is to model the tower as a frame-truss type, so the main members can also transfer moments.

Current design recommendations address some of the above issues by making corrections on the slenderness ratio of members. In this regard, members are designed under compression or tension, and flexural effects in compression are applied as modifications to L/r ratio. Although such assumptions simplify the analysis and design procedures, they do not account for the real behaviour of the tower under loading or failure. For example, according to **ECCS39** [1] the capacity of legs is derived from a basic buckling curve according to the equivalent slenderness ratio of member. The equivalent slenderness ratio is defined according to formation of bracing. **ECCS39** [1] mentions that the effect of eccentricity of axial loads transmitted from the bracing to the leg members cannot be disregarded, but it does not present a method to include the eccentricity in design.

For the design of bracing members, **ECCS39** [1] modifies the slenderness ratios to include the effects of framing eccentricity and the number of bolts at the connections, then the

designer should, again, refer to buckling curves and extract the brace capacity. Regarding the design of redundant members, the code recommends a percentage of load which is acting on main member. This percentage varies with the slenderness ratio of main member being stabilized by redundant.

1.3. Validation of design results

To validate the design results and to verify that the stresses in the members are in accordance with the analysis assumptions, a full-scale testing is typically required in the transmission line industry. The test is generally performed on the full constructed prototype of tower before fabrication.

Although the full-scale test provides a real insight to the designer about actual stress distribution, fit-up verification, behaviour of tower in deflected positions, and adequacy of connections, it is unable to confirm how the structure will react under dynamic loads, foundation settlement, and other loading or tower configuration than the one tested. This procedure is also very costly and time consuming.

1.4. Local buckling failure for angles

Slender steel sections are widely used in construction of different steel structures such as lattice structures for transmission line and telecommunication towers. Mainly two different types of instability can occur in the members. The first type is global buckling of member along its length which is based on member slenderness value and support conditions. Secondly, local buckling failure which is based on slenderness of the section and plate buckling behaviour. Both of these instabilities can be categorized as pure elastic or elasto-plastic buckling due to value of the stress developed in the member and slenderness values. In addition, the global buckling can be accompanied with local buckling which can make the analysis and design more complicated for these types of members. The global buckling behaviour is studied mostly in the literature and based on theoretical formulas, although the main challenge is evaluation of the member under elasto-plastic buckling and post-buckling capacity for local buckling.

All the steel design codes include equations to account for local buckling. In numerical models, local buckling can be reproduced using 2D shell or 3D elements. Non-linear numerical models have been developed in the last decades that can capture the complex behaviour of lattice structures up to failure. These models normally use beam elements which properly consider the global buckling and yielding of sections, but do not consider local buckling of angles due to geometrical limitations.

To address the local buckling, the **ECCS39** [1] document adopts a reduction on the yielding stress of members, which is directly related to the b/t (width to thickness) ratio of sections.

Other practical design codes such as **ASCE 10-97** [2], **Eurocode 3** [3] and **CAN/CSA S16** [4] present similar recommendations with minor differences in coefficients for the equivalent slenderness. Unfortunately, the design standards provide the recommendations only for individual members and connections, so load distribution and reactions between members in the overall structure are not considered.

1.5. Connection behaviour

Leg members in towers are connected via lap spliced bolted joints and the bracing members are connected to legs or to intermediate gusset plates via single leg bolted joints. The assumption of hinged joint does not represent the real joint behaviour and modelling connections as rigid is also inadequate as compared to real joint behaviour. The exact modelling of real joint behaviour is very difficult but there are some simplified methods available such as modelling the connection by a small beam element or spring, keeping in mind that the non-linear behaviour of connection starts from the early stages of the loading up to failure load.

The properties that make the behaviour of bolted joints complex can be split in several phenomena: eccentricity, rotational stiffness, joint slippage and local yielding. The tower connections are different from ordinary steel connections in other types of steel structures. In lattice transmission towers, the members are mostly connected directly via their flange or through the gusset plates which provide a connection flexibility. The slippage effect should be included in the numerical model, because lattice towers are constructed by bearing type

connections instead of friction type ones. Also, the post slippage behaviour as hole elongation should be also considered in the connection behaviour. Therefore, an efficient method is needed to include this phenomenon in the numerical model of full scale structures [5].

1.6. Objectives if this study

Although advanced numerical models have been proposed, they are not used in design and have rarely been used as an intermediate step between the design output and full-scale testing, or as a tool to help understand test results. Difficulties to precisely represent the local buckling behaviour of angles and the non-linear behaviour of connections have notably restricted their use in practice.

The aim of this project is therefore to define a workable analysis strategy for transmission line towers that considers the local buckling of angles and the non-linear behaviour of connections. In this research, a modelling strategy is developed and its ability to predict the failure loads and failure modes of lattice transmission towers is investigated. Model calibrations are performed by using data from recent tests and results of experiments on tower parts.

1.7. Contribution to industry

- **New method to include local buckling**
  Currently, local buckling behaviour can only be modelled using 2D elements which is complicated and long for modelling and analysis. In this study a new method is proposed to incorporate the local buckling behaviour in the finite element model of structures using fiber beam element by means of developing a stress-strain behaviour curve of steel.
- **A model to incorporate the connection behaviour**
  At this moment, there is not a simplified and robust method to include the non-linear behaviour and slippage effect in the finite element modelling of towers. In this study, a method is provided to simply predict the full force-displacement curve of complex

connections. This curve can then be integrated as a non-linear spring element in global finite element models of lattice towers.

1.8. Organization of the dissertation

- CHAPTER 2 covers a comprehensive review on the background and past studies conducted to investigate the non-linear behaviour of lattice towers and predict their failure modes due to local buckling and connection modelling.
- CHAPTER 3 presents the modelling methods used in this research such as defining the geometry and FE meshing process. Also, methods to properly model connections and fibre beam elements are investigated.
- CHAPTER 4 (1st article) proposes a method to incorporate the local buckling behaviour in the finite element model of structures using fiber beam element by means of developing a stress-strain behaviour curve of steel. In order to take into account this phenomenon, the stress-strain material behaviour of the member is modified in the finite element model. A stress-strain curve formula is provided for each class-4 member based on the local buckling slenderness value (λ_p) of the member.
- CHAPTER 5 (2nd article) a simple method is developed, which represents the complete behaviour of bolted connections. The method can be implemented in an efficient beam element model of a complete lattice tower with the aim to evaluate precisely their complex structural behaviour. The method is easy to implement for a large number of complex joint configurations. Hence, the behaviour of multi-bolt connections is obtained from the behaviour of one-bolt joints.
- CHAPTER 6 implements the features of chapter 5 for the modelling of joint behaviour in the modelling of a lattice tower section and compares the predictions of the proposed strategy with experimental results of a tower section.
- CHAPTER 7 presents the summary of this study, conclusions, and recommendation for future research.

CHAPTER 2 LITERATURE REVIEW

2.1. Advanced modelling techniques of transmission towers

In conventional design, transmission towers are modelled as a truss element [6] and in most of the cases, secondary braces are omitted from the analysis since they are assumed as redundant elements to reduce unbraced length of main members. In the majority of cases the members are assumed with pinned connections, such that tower models can be analysed as a 3D truss.

Lu *et al*. [7] summarized the results of the literature pertaining to the research findings on lattice transmission towers and line systems. The authors discussed the structural modelling and failure mode prediction for connection joints, individual members as well as structural systems subjected to static and dynamic loads. They also elaborated on steel lattice transmission tower models, and the pros and cons of different numerical modelling techniques. One of the main findings of the study was the need for development of specific modelling methods for lattice transmission towers and line systems. Moreover, they pointed out that more research needs to be done on advanced FEM techniques with the ability of modelling the behaviour of bolted connections and predicting their failure mode.

Using the truss elements can affect the accuracy of analysis [8,9]**,** as this type of element cannot consider the bending stresses and moments resulting from the real end connections. Lattice transmission towers are constructed using angle section members which are eccentrically connected. Therefore, secondary stresses arise due to eccentricity, joint rigidity and member continuity. One of the best known techniques is to utilize Beam-Column elements instead of Bar elements [10], which can incorporate most of the structural characteristics of lattice towers such as member continuity, asymmetric section properties, geometric and material non-linearity, as well as eccentric connections [11].

Another type of beam element that can be used to model the behaviour of angle section is the fibre beam element. In this case, the cross section of the beam column is subdivided into a finite number of elementary areas and the coordinates of the sub areas are determined with reference to the local principal coordinate system. The fibre beam element simplifies the number of degrees of freedom by assuming that Euler-Bernoulli hypothesis is respected (plane section before loading remains plane during loading). This type of element has the ability to provide the stresses in cross section [12].

In order to increase the accuracy of results and to perform more detailed analysis, some researchers used shell elements to model the members [5]. Shell elements allow calculating the stress and strain at every location of the tower and provide more detailing to modeled connections and eccentricities. A major drawback is the extensive time-consuming calculations with this type of element. Figure 2-1 shows the local buckling of a 220 kV bottom cross-arm in test and shell element modelling at failure.

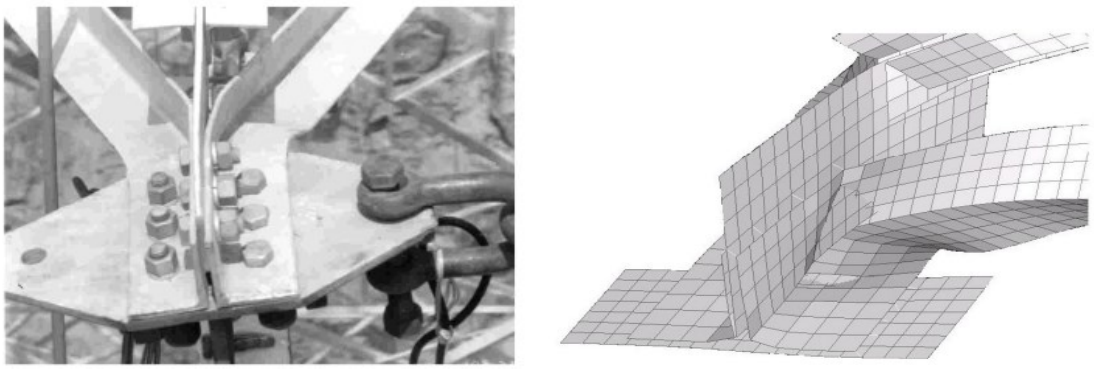

Figure 2-1: Local Buckling of cross-arm member and shell element modelling members [5]

Utilization of solid elements to model towers is another possibility, however, due to high number of degrees of freedom and required elements, this type of modelling generally is not practical. Solid elements are mostly used in mechanical parts where shell elements cannot cover the exact behaviour of the model through its third dimension, for instance the stress analysis of the part along the thickness. Nevertheless, there might be cases where solid elements need to be used such as local buckling and failure modelling in connections.

To benefit from both 1D and 2D elements, a combination of these elements can be used in models [13]. Figure 2-2 shows an angle member which is mostly modelled by beam elements, but over a short length in the middle shell elements were used. By the aid of this combination, it is possible to take into account local buckling or local plasticisation in certain parts of the model.

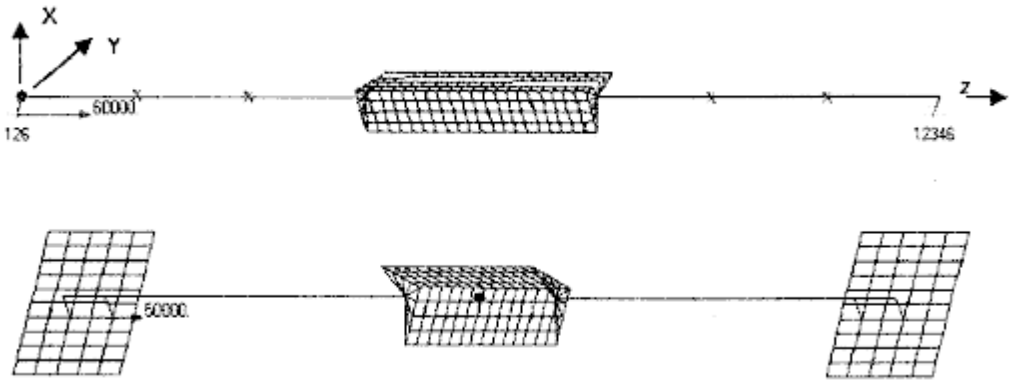

Figure 2-2: Combination of Beam and Shell elements [13]

Despite the use of beam elements which causes a faster and more economical modelling and analysis process, researchers [13] concluded that the accuracy of combined modelling is not as high as full shell modelling.

Recently another method to model large structures was proposed: the multi-scale approach. In this method the local connections and joints are simulated using shell or plate elements to cover more details and failure modes. The other components of the structure are modelled using truss or beam elements. Then all of these different scale modelling are coupled to form a multi scale FE model. The issue of multi-scale modelling is coupling of mixed-dimensional elements into one analysis model. As well the modelling effort to create these models is more extensive than a full beam or truss 3D model. Wang *et al.*[14] , used this method on a physical model of a transmission line tower. Solid elements were used to model connections including angle sections. They reported that, this method has great advantages to improve accuracy of local responses for this type of structures.

Langlois *et al*. [15] reported the techniques available to model the behaviour of steel lattice towers and recent presented advancements in knowledge. In addition, they recommended that the modelling technique and hypotheses for numerical analysis of lattice towers need to be carefully selected, despite availability of several options for improving modelling of the complex behaviour of steel lattice towers. Moreover, they pointed out that any unnecessary complexity of model can increase model uncertainties and thus need to be avoided if possible. In addition, they noted that complex models need to be validated by simplified models or performing experimental tests. They have also suggested that inevitable tolerances involved in fabrication and erection could influence the tower behaviour, and thus need to be considered when interpreting the results.

2.2. Consideration of non-linear behaviour

Comparing data from full scale tests with predicted results of linear analysis indicates that the behaviour of transmission towers under complex loading cannot be estimated using the linear analysis [16]. Electric Power Research Institute (EPRI) [17] showed that almost 23% of towers tested, failed below the design loads and often at unexpected locations. Moreover, available test data confirmed considerable discrepancies between member forces computed from linear elastic analysis and the measured values from full scale tests. To overcome this issue different types of non-linearity are defined in analysis such as geometric non-linearity, material non-linearity, joint behaviour and bolt slippage [18].

By including the Geometric non-linearity in the analysis, the effect of continuing changes in geometry of model and large deformations can be covered as the applied load is increased. The material non-linearity accounts for the effect of combined stresses on the elasto-plastic behaviour of member cross section. In most of the cases the material is defined by a bi-linear stress-strain relation, although definition of full behaviour is possible [5].

2.3. Connections and bolt slippage

The assumption of hinged joint does not represent the real joint behaviour and modelling connections as rigid is also inadequate as compared to real joint behaviour. On the other hand, in practice, angle members in towers are usually loaded eccentrically through one leg;

which causes a biaxial bending in addition to axial load (Figure 2-3). The combined action of axial and bending forces may cause a plastic hinge in cross-section. Furthermore the bolted leg of the angle can undergo a local deformation under the bearing force of bolts, causing displacement and rotation in connection and shear lag in member [5].

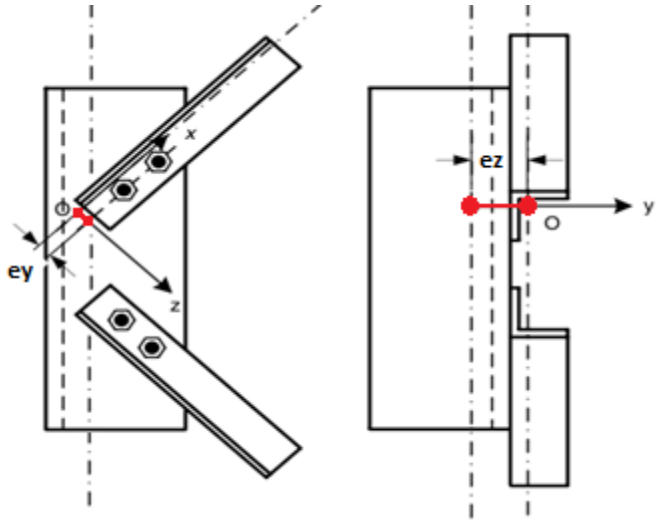

Figure 2-3. Joint eccentricities [5]

The exact modelling of this behaviour is very difficult, however there are some simplified methods available in the literature to model the connection behaviour such as modelling the connection by a small beam element or spring, considering that the non-linear behaviour of connection starts from the early stages of the loading up to failure load. One issue to model the connections is the rotational stiffness. To take into account the joint stiffness, Kang [19] showed that the connection rigidity has a considerable effect on the ultimate horizontal load capacity. The rigid connection increases the buckling capacity, so assumption of connection rigidity must be realistic, otherwise the buckling capacity of the structure may be over or underestimated.

Joint slippage is another aspect of the joint behaviour which has received a lot of attention, although a full model to predict the behaviour for multi-bolt connections and how to define the parameters to include it in a 3D model is not provided. Most of the bolt holes are larger than bolts to provide erection tolerance which makes the slippage inevitable. The slippage

may happen gradually or at a specific level of loading and it depends on different parameters such as: structural loading, workmanship, the constitutive properties of the bolts and connections including, corrosion, nature of the faying surfaces and bolt torqueing. Figure 2-4 depicts a joint before and after slippage.

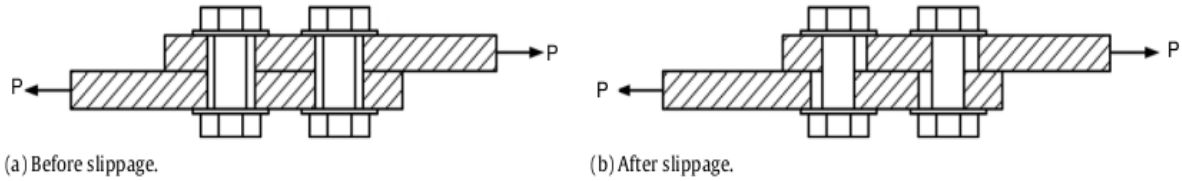

Figure 2-4. Bolted joint slippage effects [17]

Due to the lack of sufficiently reliable experimental data and the complexity of describing actual slippage in a real structure, very simplified models must be used. For example, in a study by Kitipornchai [20] the slippage is modelled as a random process. It was concluded that, joint slippage does not have a significant influence on the ultimate strength of the structure, but it has some effects on deflections. The slippage behaviour of some specific connections is studied by Ungkurapinan *et al*. [21], in this study the complete load-deformation curves of one to four bolt connections is reported (Figure 2-5). Unfortunately, there is not an extensive database of slippage parameters for angle member connections. A limited number of tests on specific angle sections and bolt arrangements could be found in the literature.

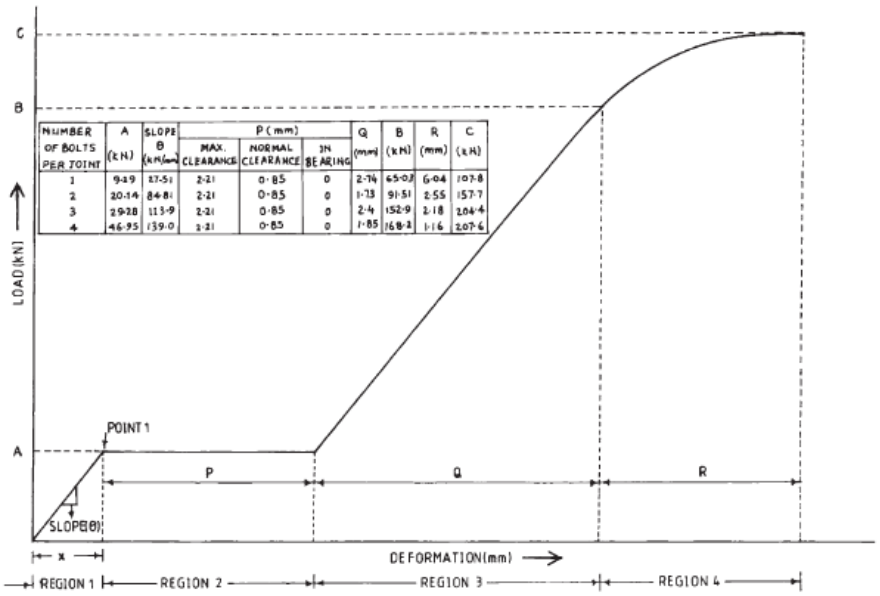

NUMBER OF BOLTS PER JOINT	A (kN)	SLOPE θ	P (mm) MAX. CLEARANCE	P (mm) NORMAL CLEARANCE	P (mm) IN BEARING	Q (mm)	B (kN)	R (mm)	C (kN)
1	9·19	27·51	2·21	0·85	0	2·74	65·03	6·04	107·8
2	20·14	84·81	2·21	0·85	0	1·73	91·51	2·55	157·7
3	29·28	113·9	2·21	0·85	0	2·4	152·9	2·18	204·4
4	46·95	139·0	2·21	0·85	0	1·85	168·2	1·16	207·6

Figure 2-5. Load-Deformation diagram for joints [21]

Knight *et al*. [22] concluded that joint effects cause the premature failure in towers and they must be considered in analysis. Results showed a good correlation with experiments when joint effects are considered.

Comparing numerical predictions with experimental results, Jiang *et al.* [23] described the effect of joints on structural analysis model. The results of the study showed that in predicting the tower sway displacement, joint slippage must be considered, this would dramatically increase the predicted tower deformation but would not affect its failure load, failure mode and sequence.

Ahmed *et al*. [24] numerically investigated the behaviour of transmission towers under working loads using the FEM by integrating the actual slippage behaviour of bolted joints reported by Ungkurupanian [25] into their non-linear joint model. They concluded that the slippage of tower-leg joint and bracing member joints can adversely influence the overall tower performance by either decreasing the ultimate capacity or increasing the vertical and lateral deflections under working loads. However, they have used a special loading scenario to model the frost-heave effect by applying axial forces directly under one leg which is

different than regular tower self weight or conductor forces. They pointed out that the joint slippage can favourably influence the tower performance when subjected to frost-heave induced displacements. This conclusion was justified by stating that the corresponding axial forces induced in the member are much lower than those corresponding to rigid joints (i.e. with no slippage). Moreover, based on their analytical results they concluded that incorporating bolted-joint slippage in the analysis of towers is important and it will affect the accuracy of the model.

Zhang *et al*. [26] considered the joint slippage and developed a finite-element model to predict the structural response of lattice steel structures. The efficiency of the model was compared against experimental results and a conventional model. They have shown that their proposed model can accurately predicts the structural response of lattice steel structures with joint slippage. They concluded that considering joint slippage can increase the displacement of lattice structures because of reduction in stiffness. Nonetheless, they noted that considering the effect of joint slippage had minor effect on the load-carrying capacity and failure mode. They also pointed out that the conventional model crucially overestimates the stiffness, underestimating the lateral displacement of lattice structures, because the effect of joint slippage is not considered in this model.

Tower capacity is also affected by joint slippage due to geometric non-linearity (global P-Delta effects). Therefore, the legs may experience additional bending and it would reduce the ultimate load bearing capacity of tower.

At this moment, there are some methods to include the non-linear behaviour and slippage effect in the finite element modelling of towers. Although the main problem is, these methods are difficult and time consuming to be implemented and they are not efficient enough for a large array of connection configurations. Also, the stiffness of connections in these methods needs to be evaluated by prototype specimens before implementing them in the models.

2.4. Tower configuration and elements

Finite element modelling of towers is not only implemented to address the needs of full-scale tower testing and failure analysis for the industry. There are other types of research which also benefit from a well defined and accurate numerical model. For example, the modelling of corrosion in the tower members using finite element analysis. Also, optimisation of geometry of towers helps the industry to save resources on construction and erection time. An accurate numerical model can help to improve these kinds of needs as well. Since in these cases, an efficient and more reliable numerical model can help for the assessment of structural behaviour of the modified or proposed geometry.

Li *et al*. [27] studied, the safety of transmission tower structure under corrosion damages by developing a simplified method. This model took into consideration the safety status of a single component and was able to scrutinize the safety index of the structure. Li *et al*. [27] have also shown that their model could anticipate the trend of safety reduction of the structural components and the layer structures, considering the corrosion characteristic of the tower site. Their model could also distinguish the structural components that have reached the dangerous state using numerical analysis.

Transmission line towers are mass produced and the policy of configuration design for them is based on the minimum weight philosophy [28]. There are limited numbers of studies to monitor the effect of tower configuration on its structural behaviour. For example, Kang [19] reported that cross bracing configuration in secondary bracing instead of single bracing, enhances the ultimate load capacity of structure.

Different bracing configurations are used in the tower design, the efficiency of the bracing system is studied by Prasad Rao *et al*. [29]. Five towers are tested and modelled by finite element method. Results showed that failures of towers are caused by buckling of compression bracing and legs. The effect of non-triangulated hip bracing pattern and isolated hip bracing connected to elevation redundant in "K" and "X" braced panels on tower behaviour are considered. Non-triangulated hip bracing caused the geometric instability in

the structure and leaded to premature failure. The authors concluded that, detailing deficiencies may have a significant influence on the behaviour of the structure, and introduction of force fitting construction deficiencies, imperfections, bolt hole clearances, etc. is difficult to be modelled.

2.5. Tower capacity prediction

The main controlling parameter in designing angle members in compression is the slenderness ratio of the members. Generally, leg members are designed with slenderness ratios ranging from 40 to 60. In this range the compression capacity is approximately equal to net tension capacity of the member, and they may fail by inelastic buckling [30]**.** Bracing members are designed with slenderness ratio lower than 200 that generally varies from 60 to 170.

The British Standards Institute [31], the American Society of Civil Engineers [32] and the bureau of Indian Standards [33] specify essentially the same method for evaluating the compressive strength of angle members in lattice towers, accounting for the effects of residual stresses, imperfections and end conditions. This method modifies the effective slenderness ratio of the member, depending upon the location of the member in the tower and the eccentricity of connection.

The modelling strategy should consider these factors and parameters in order to help the engineer and to facilitate the design of different tower configurations. Moreover, despite the advantages of finite element modelling, its adoption to investigate the steel towers should be carefully evaluated [8]**.**

The non-linear finite element analysis methods are effective for evaluating the strength of compression members and space structures. The beam element [34] which is used widely in this area is a 1D element with the ability of defining cross-section of the member from which the stresses can be obtained at different locations. Moreover, this method accounts for geometric and material non-linearity and it can predict the pre-ultimate behaviour and the limit loads. In this approach, loading is applied in small increments. At each loading level,

several iterations are performed to satisfy the equilibrium while the structural geometry is constantly updated. Consequently, the method can easily predict the buckling and post buckling behaviour of members as well as any instability.

Phill-Seung Lee [11] reported a comparison of large deformation analysis of a lattice steel tower with full scale tests. They tested two loading cases: (i) bending, (ii) flexure-torsion (Figure 2-6) and considered three connection models. Model-1, pin joints for one bolt connections and rigid joints for multi-bolt ones considering the eccentricity. Model-2, same as Model-1 but without connection eccentricity. Model-3, same as Model-1 but using all rigid connections.

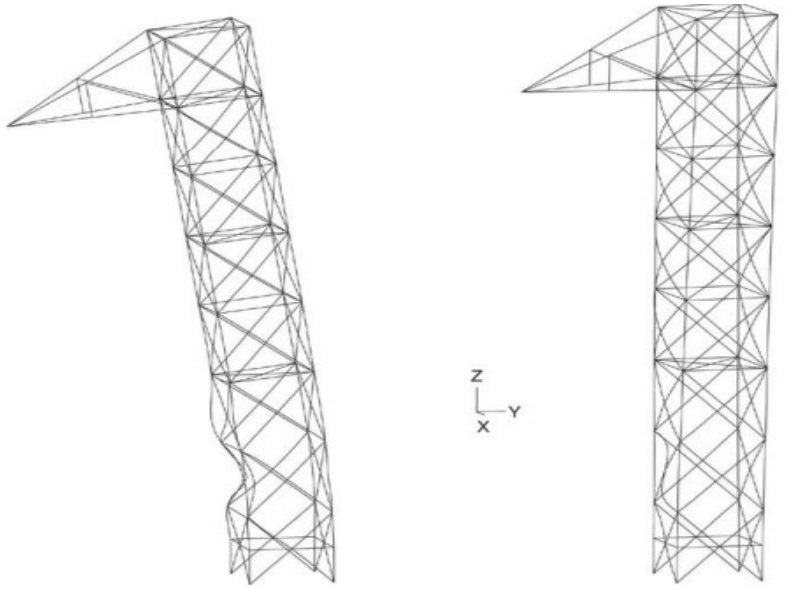

Figure 2-6: Deformed shapes in the bending (left) and flexure-torsion (right) cases [11]

In the bending case, the tower fails due to elastoplastic buckling, while in the flexure-torsion case, the tower collapses because of buckling of diagonal bracing members. In the bending case, the geometry and loading of tower is symmetric therefore the numerical model shows a symmetric failure, however the unknown imperfections caused the experimental results to have non-symmetric failure behaviour. The authors also mentioned that the load-

displacement curves have a good agreement in the linear elastic range, but they show high discrepancy when increasing the load (Figure 2-7 and Figure 2-8).

The following points were reported as the main reasons for the differences between the experimental and numerical results:

- The movement of foundation in experiments which is not modelled in numerical analysis.
- The presence of unknown geometric imperfections in the real tower.
- The behaviour of connections is very hard to be accurately modeled since they are neither perfectly rigid nor perfectly pinned.
- The effects of some local failures of the members cannot be predicted due to limitations of beam elements used in numerical model.
- Some dynamic effects were inevitably involved in the experimental results while the numerical results were obtained using static analysis

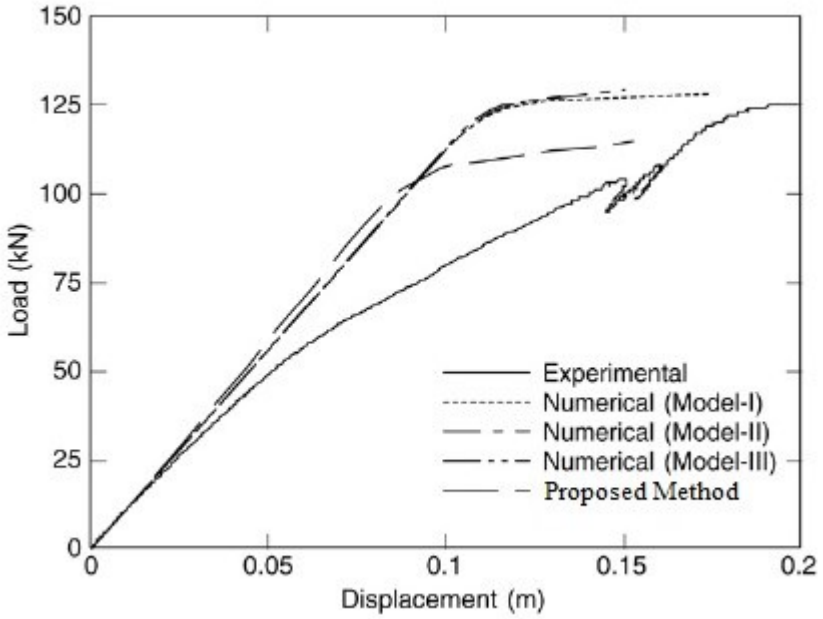

Figure 2-7: Load-Displacement curves of bending case [11]

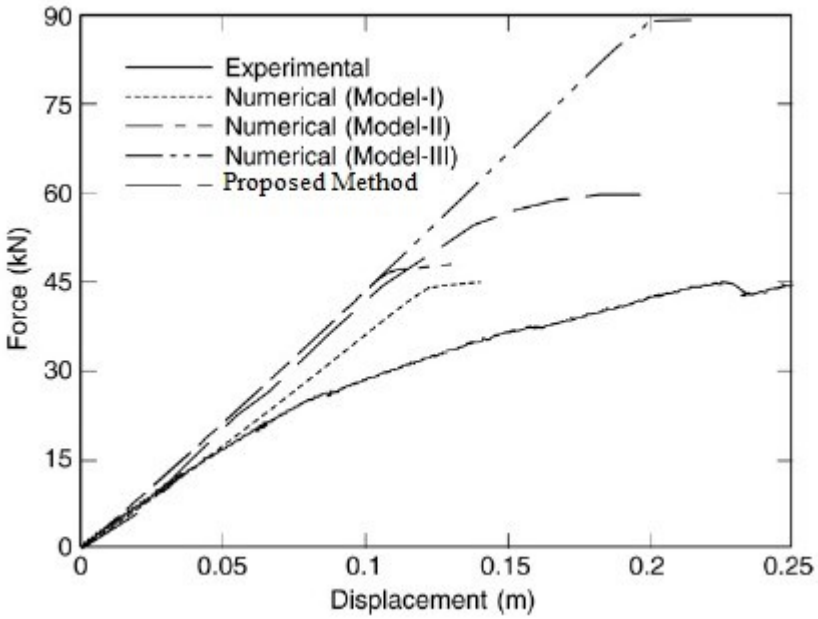

Figure 2-8: Load-Displacement curves of flexure-torsion case [11]

Prasad *et al*. [35] reported that 32 out of 138 full-scale tower tests at the Structural Engineering Research centre [CSIR-SERC] experienced different type of premature failures. To study the failure in detail, three towers were modelled and analysed by NE-Nastran non-linear finite element software. The entire tower was modelled using beam-column elements, however, to capture more details the failed compression bracings were modelled as plate elements (Figure 2-9).

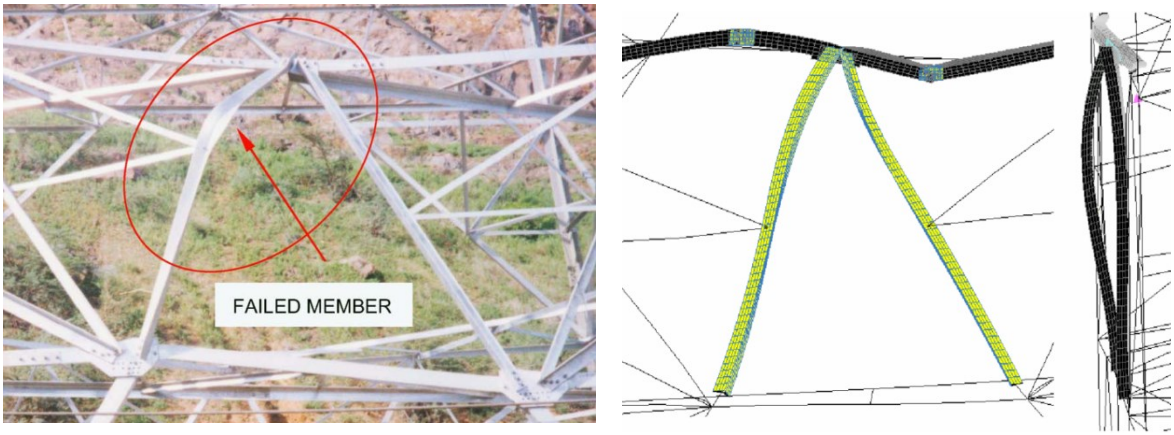

Figure 2-9: Failure modelling using plate elements [35]

The test failure pattern coincides with analysis failure pattern for both beam and plate modelling. Figure 2-10 and Figure 2-11 show the comparison of failure loads for leg and bracing members calculated based on different codes, Finite element analysis and tests. As shown, ASCE standard [32] always predict higher values than the experimental values and non-linear finite element analysis predictions were 7-14% higher than test results.

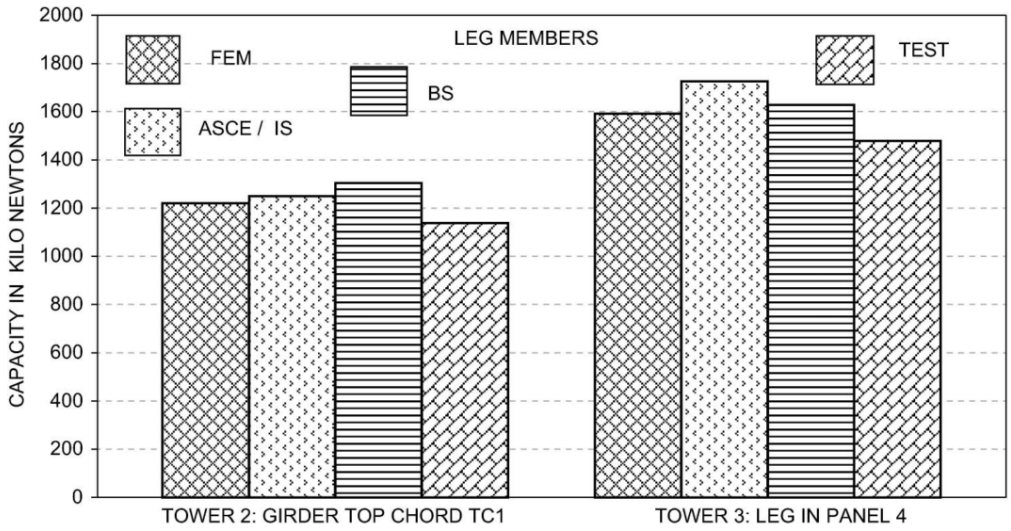

Figure 2-10: Comparison of load capacities for leg members [35] **(Note: FEM : Finite Element Model; ASCE** [32]**; BS** [31]**; IS** [33]**)**

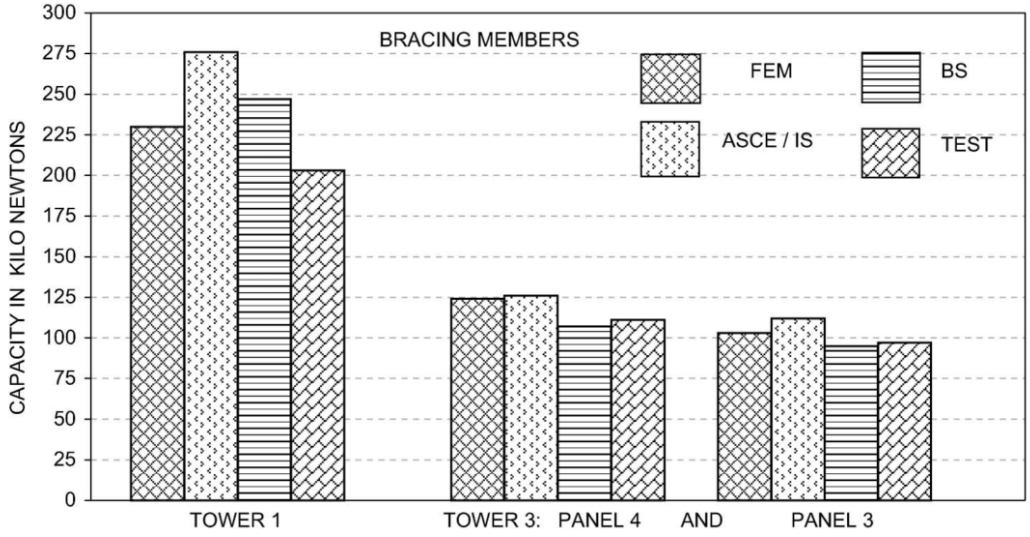

Figure 2-11: Comparison of load capacities for bracing members [35] **(Note: FEM : Finite Element Model; ASCE** [32]**; BS** [31]**; IS** [33]**)**

Another study was performed by the same researchers [29] on five prematurely failed towers. They encountered over prediction of strength by non-linear analysis and concluded that FE analysis is still not a fully reliable method to predict tower strength and tests are still necessary for this purpose. However, it is indicated that the non-linear analysis is essential for understanding the behaviour, load carrying capacity, design deficiencies, and instability in structure.

Bouchard [36] developed a simple numerical procedure to improve the load capacity and the failure mode prediction of lattice towers. The critical elastic buckling stress (Fe) is determined by a linear buckling analysis rather than by method of effective length. The effects of connection eccentricity and stiffness is also considered in the model. Then the resistance of the element is calculated by using the procedure and equations from the standards. The author analyzed several cases to consider the different configurations of steel angle. The proposed model was compared with the results of experimental tests on 12 towers as well as with the results of different design standards. The author showed that the proposed method can accurately predict the load capacity of lattice towers. It was also noted that the proposed procedure can improve the precision of the calculation of the ultimate capacity and the mode of failure of the lattice towers.

Sad Saoud *et al*. [37] proposed a numerical model using beam elements to predict the load-carrying capacity of steel lattice towers under static loading. Their model was developed using the finite element package Code_Aster. The steel lattice towers were modeled using spatial beam elements considering both geometric and material non-linearities. They investigated the effect of eccentricities and initial out-of-straightness defects on the buckling response of lattice towers. They have concluded that both the ultimate carrying capacity and failure mode of lattice structures can be accurately predicted if the eccentricities are considered in the model. They have also reported that the predicted failure mode was not in agreement with experimental results when only out-of-straightness defects were considered in the model. Moreover, they pointed that the rotational stiffness of one-bolt connections could influence the ultimate capacity of lattice towers, however more research was recommended to be done in this regard.

2.6. Residual stresses and geometrical imperfections

An experimental investigation on 26 hot-rolled steel angles was performed by Adluri *et al*. [38] to investigate the distribution of residual stresses across the cross section. It is concluded that the maximum residual stress in section does not exceed $0.25F_y$. The researchers recommended to include the residual stresses in analysis and design of angle sections specially for inelastic buckling.

Performing numerical analysis using the finite element software Code_Aster, Gravel *et al*. [39] investigated the influence of residual stresses on the global performance of lattice towers. The multi-fibre beam elements were incorporated to model the elastoplastic angle members, and discrete elements. They considered both the eccentricity and the rotational stiffness of connections in their model and compared the numerical predictions with the results. They concluded that stiffening the connections around the bolt axis (KRY) could improve the ultimate load capacity of the section by up to 10%. Moreover, they pointed out that the ultimate capacity of the tower section was decreased by around 5% when the residual stresses were taken into account. In addition, they deduced that consideration of residual stresses had no effect on the failure mode.

Chan *et al*. [40] used an equivalent imperfection factor to include the residual stresses in their proposed second-order codified analysis and design. The factor accounts for combined effects of initial curvatures, residual stresses and P-Δ effects.

Despite the well documented research about value and distribution of residual stresses, there is not a common method to model the residual stresses in lattice towers.

2.7. Local buckling of sections

Prasad Rao [35] stated that out of 138 full scale tests, 32 towers faced different types of premature failures. These demonstrate the limits of the design method used in practice. In order to further study the failure mechanism, three towers were modeled and analysed using NE-Nastran non-linear finite element software. The geometric and material non-linearity

were used to attain the behaviour and limit loads. All tower components were modelled as beam-column elements. However, to obtain further details, the failed compression bracing was modelled as plate elements. Experimentally observed failure pattern agreed with the results of non-linear finite element analysis for both beam and plate modelling. However, non-linear finite element analysis predicted 7 to 14 percent higher failure loads compared to experimental results.

This type of non-linear model intends to capture the intricate and non-linear behaviour of steel lattice structures. However, it is not a practical design method, since it does not comply with the design code equations or more advanced methods such as direct strength method (DSM) [41–43] which evaluates the resistance of sections based on elastic buckling behaviour. It offers a one-step numerical model to characterize the pre- and post-buckling behaviour of the structure. This type of model is effective as alternative or complement to full-scale tests to comprehend the behaviour and verify the resistance of lattice towers. It was shown by recent research that, depending on the intent of the modelling, the following characteristics of lattice behaviour might need to be considered: joint eccentricity [36,37]**,** bolt slippage [44], and residual stresses [39]. It should however be noted that, in this type of model that normally simulates the elasto-plastic buckling of angle members, the possibility of local buckling of members is neglected.

Most recent research works in the modelling of angle members is either using beam elements or 2D shell elements. Angle sections may experience global or local buckling instability under compression load, depending on the slenderness and width to thickness ratio. Shell elements can signify the full three-dimensional behaviour of angle sections and specifically local buckling, with promising accuracy if the mesh is refined enough. However, the high number of members makes the use of shell elements impractical, especially in large and complex structures such as lattice towers. For example, Shan *et al*. [45], modeled angle members by non-linear plate elements. Both material and geometric non-linearities was considered in the study, however the analysis procedure was computer intensive thus time consuming. They determined that, 2D elements can only be used for small structures and as a research tool. This conclusion was also confirmed by other researchers [46]**.**

In slender angle sections having large width-to-thickness ratio, the global buckling deformation is accompanied by the local buckling of leg plates [47]**.** Consequently, this effect should be incorporated in the finite element model of the structure. Lee and McClure [46] established a L-section beam finite element model for elastoplastic large deformation analysis. It is stated that, the beam element is 2.4 times more efficient than shell modelling when the member length is equal to 4 meters, in terms of the computational time.

The fiber beam element is a very efficient element type that is utilized with success to model angle sections. This element can effectively integrate the stress and yielding effects in the member. Kitipornchai *et al*. [12,48] performed an analysis using non-linear fiber elements of angle sections under axial and bending loads. Numerical studies have been performed on a number of structures where the angle members were modelled as fiber elements. A number of different examples were presented to validate the fiber element model in predicting the ultimate behaviour of imperfect angle columns. The results obtained from the finite element model were compared to the results of experimental tests on two pairs of angle trusses with web members.

Vieira *et al*. [49] and Carrera *et al*. [50] suggested a 1D beam element to model the buckling of beams using analytical formulations. The results agreed with finite element models. They also reported a number of limitations for capturing the local buckling behaviour. It was stated that, more experiments are necessary to extend the proposed method.

More computational methods to determine the buckling loads of thin-walled sections were studied. Huang *et al*. [51], established a mathematical formulation. The angle section was selected as an example to perform numerical analysis of elastic and inelastic buckling using finite element models. Results from beam and shell elements were compared with the theoretical results. They concluded that, since the mathematical solution of higher order differential equations is complex, different method should be considered for the members with complicated deflections.

2.8. Types of elements to model lattice towers

As it was discussed in the previous section, lattice towers can be modelled using 1D elements such as bars or beams, 2D elements such as plate or shell and even 3D elements such as solid [13]. Figure 2-12 shows an angle member which is modeled by Truss, Beam, Fibre beam and Shell elements. Figure 2-13 illustrates a part of a tower which is modelled by 1D beam and 2D shell elements.

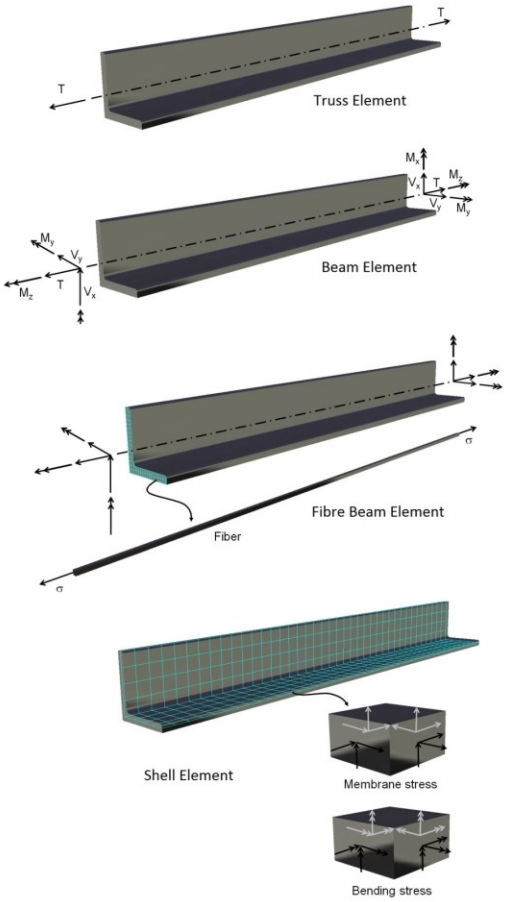

Figure 2-12: An angle section modeled by Truss, Beam, Fibre beam and Shell elements

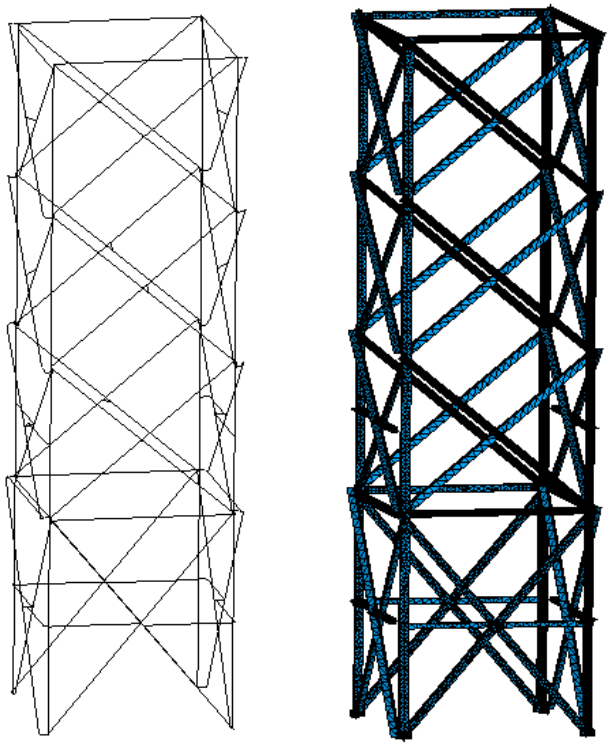

Figure 2-13: Modelling of a tower section by 1D and 2D elements

The meshing depends on the geometry of the model, failure mechanism and location. The existence of sharp edges or curved portions in the model requires a finer mesh. Moreover, a stress concentration field or local failure is expected in a specific part of the structure, a fine mesh should be defined in that location to achieve more accurate results. One should consider that fine meshing would lead to high number of elements and degrees of freedom in model, which may cause large matrices and excessive processing time and cost.

In this section different types of elements available in finite element software Code_Aster is investigated for tower modelling. The benefits and drawbacks of each element type is discussed as well. Since Code_Aster is a pure finite element solver without pre- and post-processing tools, in this study, SALOME package is used to create the geometry and meshing as well as post-processing the results.

SALOME software has enhanced algorithms to perform complex meshing compounds and sub-meshing abilities (Figure 2-14 and Figure 2-15).

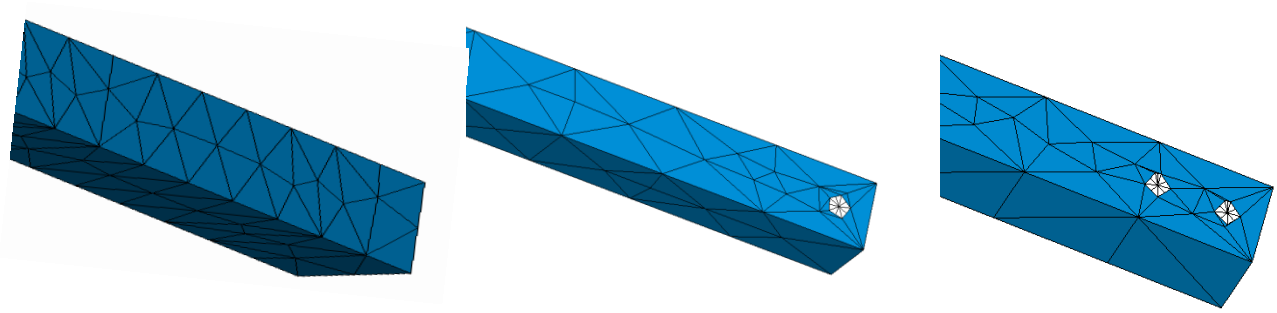

Figure 2-14: An angle member meshed in no, 1 and 2 end hole configuration

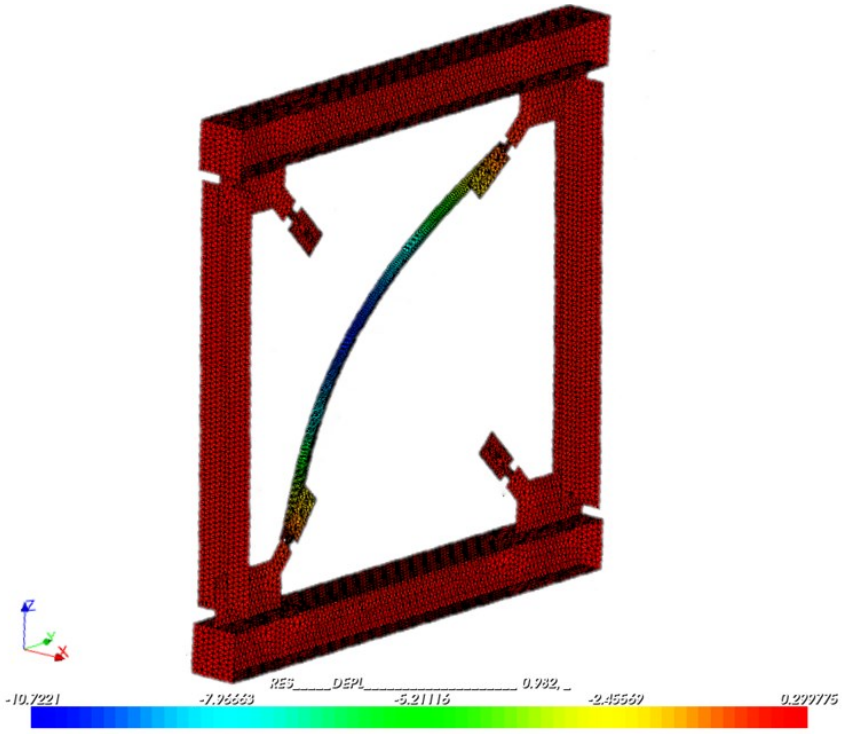

Figure 2-15: Buckling of an angle member inside the frame

SHELL3D, DKT and BEAM1D elements can be used to model the angle sections of towers. The selection of suitable element type for separate members is established by considering the member type, failure behaviour, required accuracy, loading condition and supports. To test and verify the modelling effort and calculation time needed in case of using plate elements, we have performed a preliminary study to model a full frame including a single brace in compression. As it is obvious from Figures 2-14 and 2-15, SALOME and Code-Aster are very powerful and capable of performing such analysis. Although the level of detail

and complexity of geometry and mesh as well as connection and bolt hole detailing, makes this option less practical compared to 1D beam elements.

There are two types of SHELL3D elements in the program Code_Aster, named QUAD9 and TRIA7 elements [Code_Aster Manual] as shown in Figure 2-16. Both elements have the ability to model large deflections and non-linear material, the former is a nine-node quadrangular element with eight edge nodes and one middle node, and the latter is a triangular seven-node element with six edge nodes and one middle node. Each edge nodes can support six displacement components (3 translations and 3 rotations), and the middle node only supports the rotational degrees of freedom. Another important characteristic of these elements is that they can be used on out of plane and uneven geometries.

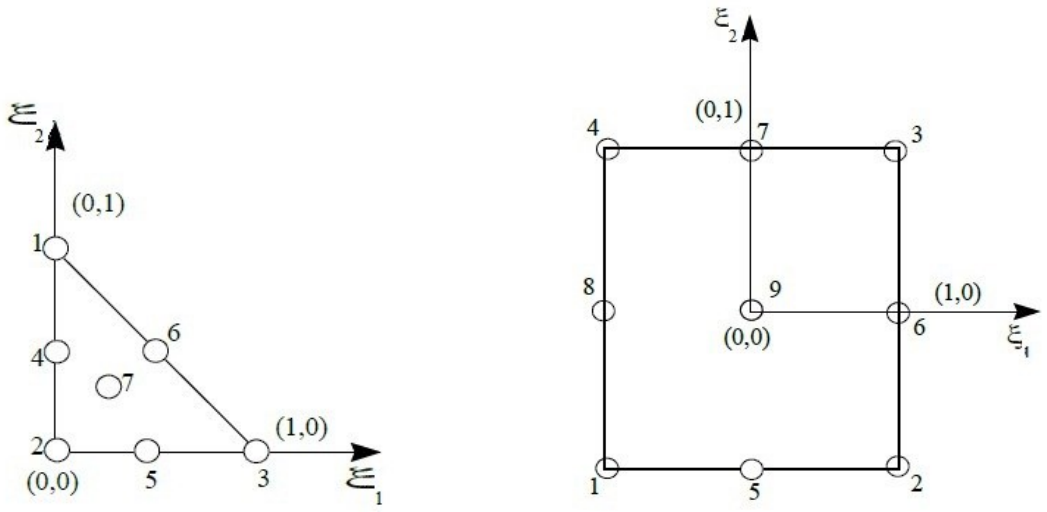

Figure 2-16: SHELL 3D elements in Code-Aster (Left: TRIA7, Right: QUAD9)

DKT elements, also known as plate elements, can be defined as triangular and rectangular elements with three or four corner nodes. They cannot model the curved and uneven geometries, nor do they support the large deformation effects.

Two node beam elements can be used to model the members as 1D element. In the Code_Aster software, there is the possibility of defining fibre beam elements. In this kind of element, the beam section is divided into definite longitudinal fibres which provide stress and strain output in the beam section. The advantage of fibre beam element to ordinary

Timoshenko beam element is the output of stress and strain fields of any section along the member. As a major drawback, this type of element is not capable of simulating Von-Mises yield criteria in section or local buckling and instabilities. In Figure 2-17 a tower section has been modelled by fibre beam elements, and the maximum axial stress in members is depicted as the results of the analysis. This model corresponds to the geometry depicted in Figure 2-13. As expected, using fibre beam elements enabled us to have faster modeling and analysis time.

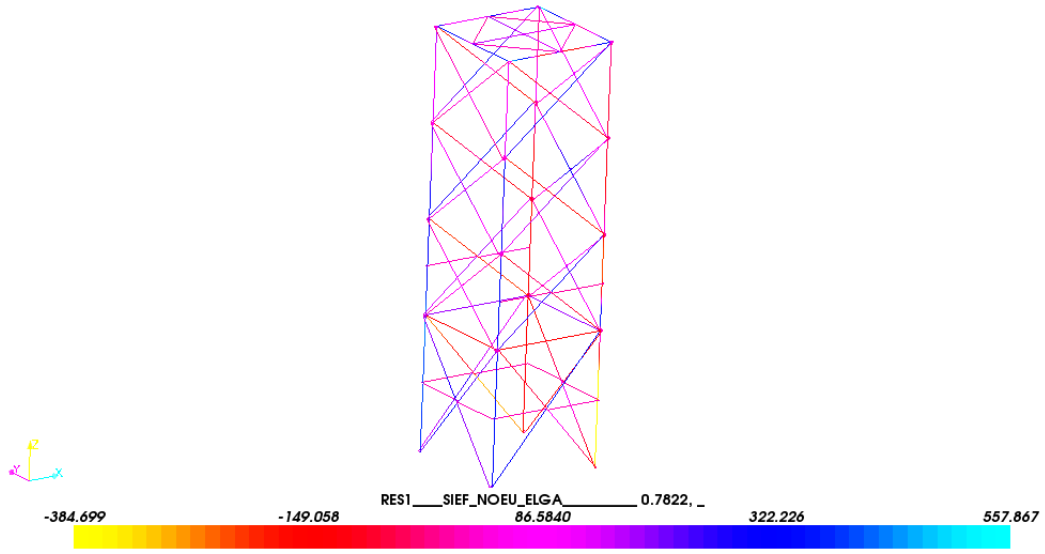

Figure 2-17: Tower modelling by fibre elements

The advantages of 1D element are the low computation time and simple geometric modelling. Below is the list of unavoidable drawbacks with such elements:

- There is no possibility of modelling geometric imperfections in angle member flange.
- Local buckling or sectional distortion cannot be predicted by fibre element (Figure 2-17).
- Calculation of yielding criteria (Von-mises or Tresca) and locating the yielding point are not possible.

Although the use of Shell elements fulfills the above disadvantages and adds accuracy to the model (Figure 2-18), shell models require rather a time-consuming calculation and post-

processing procedure due to high amount of degrees of freedom [45].

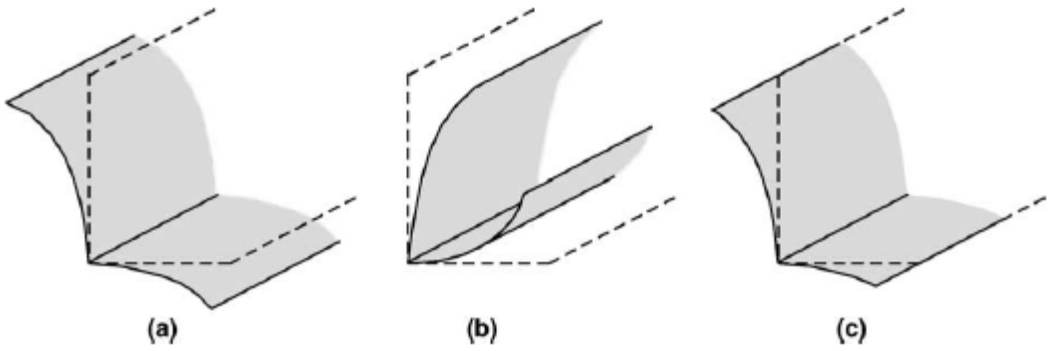

Figure 2-18: Local deformation of angles [45]

Existence of geometric imperfections and construction misalignments are another issue in construction of transmission line structures [11]. This effect causes a major gap between numerical and experimental results. In the case of 1D element, it is only possible to apply the overall member imperfection. If 2D elements are used, one would be able to consider the local imperfection of section flange. This method would have the ability to define different imperfection values for each member. Measuring this value for each member is not practical because individual investigation for imperfections is not possible in a complex massive tower in practice. Therefore, we can assume a constant imperfection value which is 1/1000 of member length according to codes [13]. Moreover, the towers are assembled part by part and generally there are some misalignment errors. These errors should be modelled on the geometry of tower body as well.

2.9. Mesh density

To achieve a reasonable mesh density, the accuracy of results and quantity of elements have to be balanced [5]. Depending on the internal forces of member, mesh density can be modified. For example, if the member experiences high bending moments, high density meshing should be used. The other effect is the load transfer at the location of joints and connections, which requires finer meshing [13].

Mesh density is also affected by the geometry of the model, such as curved edges and sharp corners. The number of elements should be increased to account for stress concentration at desired locations. Different mesh densities and distribution can be considered, to obtain accurate results and better convergence in non-linear analysis.

2.10. Conclusion

As it is evident from the literature, the accurate and efficient modelling of lattice towers still represent a major challenge. Different types of elements such as bars, beams, fiber beams, shells and solids can be considered to model the geometry. Each type has its own benefits and weaknesses based on the modelling effort and accuracy of results. The linear 1D elements are very efficient due to ease of modelling and less expensive calculation time. But these elements cannot provide some specific results such as stresses in the section, localized material yielding and not able to model the geometrical non-linearity like local buckling. Although fiber beam elements can address the problem of stress results in the section and at the same time the simplicity of a 1D element model, but these types of elements cannot consider the local buckling effect. The type of failure in member is a deciding factor to determine the element type. Among all failure models for angle members the most common failure modes are: (i) overall buckling, (ii) local buckling, (iii) plastic yielding in member. The element needed in the analysis should be able to reasonably represent these modes of failure.

Despite the aforementioned research effort, it is evident that there is a lack of a practical method for prediction of behaviour and strength of towers, or for prequalification process by numerical modelling.

Considering other analytical, numerical and experimental works in this field, the approach with fiber element is well adapted to analytically model the transmission tower structures but the main problem of using this type is the lack of ability to model local buckling.

Over the past decade, most research has emphasized that joint behaviour influences deflection most of the time, and failure mode and ultimate load in some cases. However, to

date, there is not a general method to predict the full connection behaviour for different bolt arrangements and include the non-linear behaviour containing slippage effect in the finite element modelling of towers.

CHAPTER 3 MODELLING STRATEGY

Based on the literature review, many modelling techniques have been used with various levels of accuracy. The research that has been conducted so far can be divided in the following categories:

- Connection behaviour
- Type of element
- Member failure modelling
- Geometrical and material non-linearity
- Initial imperfections
- Evaluation of the proposed strategy

In this chapter the proposed modelling strategy will be discussed in detail. The main focus will be on connection behaviour and local buckling failure modelling in members. These two aspects were shown to be particularly difficult to implement in a practical modelling method of complete lattice towers. The software Code_Aster is used for the analysis and SALOME graphic interface to model the structure and review the results. The procedure and properties of different experimental tests and verifications performed for this study will be addressed as well.

3.1. Connection detailing

It is recognized that the tower connections are different from ordinary steel connections in steel structures and bridges [21]. In lattice transmission towers, the members are mostly connected directly via their flange or through the gusset plates which provide a connection flexibility. In addition, the slippage effect should be included in the numerical model, because towers are constructed by bearing type connections instead of friction type ones. Other modes of failure could also happen such as bolt failure.

To model the joint eccentricities and flexibility, small beam elements are used. To consider slippage, Code_Aster has an effective command named ASSE_CORN. This command has the ability to model the slippage as presented in Figure 3-1.

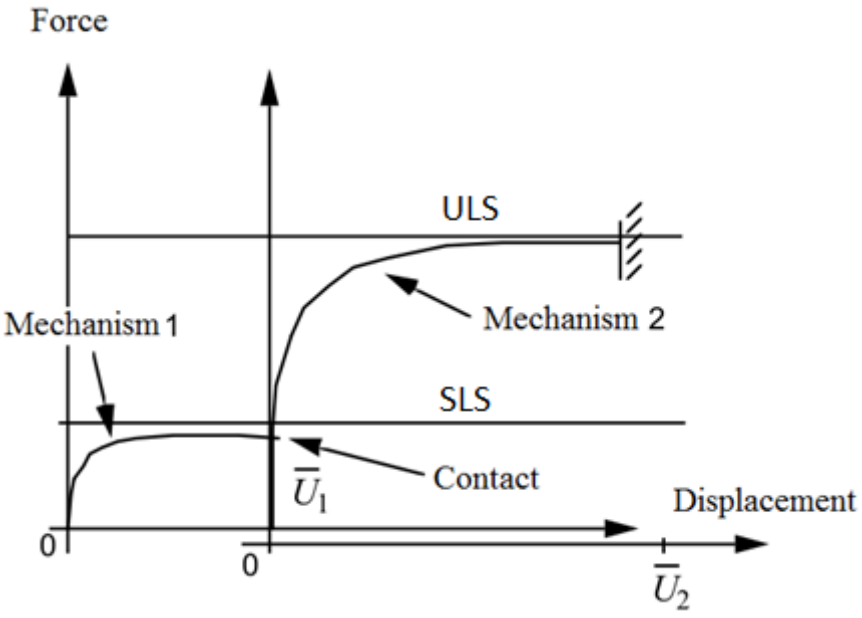

Figure 3-1: Joint slippage behaviour in Code-Aster

As it is obvious from Figure 3-1, the behaviour contains two mechanisms. The first mechanism models include the sliding of the connection up to contact point and serviceability limit state (SLS) force. After the contact point, the load transfers to bolts as shear force, the SLS limit is defined as the maximum load that causes the joint to stop sliding. The second mechanism models the plasticization of connection until failure which is the

ultimate limit state (ULS) load. The ULS load is the ultimate capacity of the connection, at which level the connection fails due to bolt breakage or tearing of flange.

A preliminary model made of shell elements was developed to address the ability of Code_Aster on the connection modelling and to compare the modelling and analysis effort in case of using 2D shell elements. The model is a simple two-member connection which are perpendicularly assembled. The vertical member acts as a stiff-leg member and the horizontal one as bracing. The eccentricity and slippage effects were included in this model as well as non-linear material and geometry modelling.

The results show that this method has the capability to model joint effects in our complicated towers. The geometry and meshing are performed in SALOME and the analysis is done with Code_Aster. Figure 3-2 shows the yielding stresses in model which is calculated by Von-mises criteria, and load-displacement graph of the model. The measured displacement is along the brace member, and the applied load is tensional load at the free end of horizontal angle member. The ASSE_CORN behaviour of code aster can also be used in compression although to avoid failure because of buckling and just to focus on connection behaviour, this model is studied under tension only force.

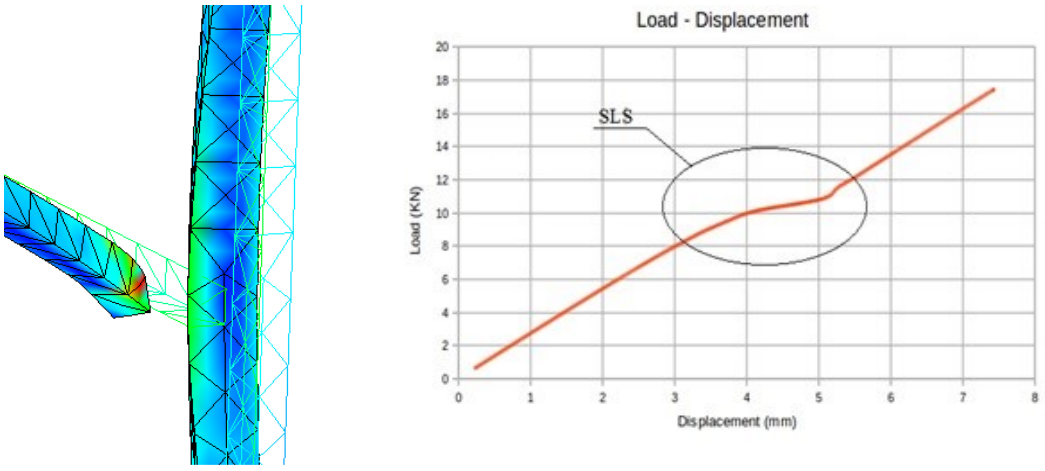

Figure 3-2: Behaviour of a simple connection analyzed by Code-Aster

In this preliminary study the members are modelled using 2D shell elements. A discrete 1D element with ASSE_CORN option of Code_Aster is used to connect the end of the brace

member to the leg. The connecting points are the nodes of triangular elements on ends of each member. A slippage value of 1mm is applied to the ASSE_CORN element to evaluate the behaviour and output results. In this test model, the connection plasticity is considered twice because of non-linear material of the shell elements which is combined with ASSE_CORN element behaviour. To avoid this issue the plasticised material around the holes needs to be removed from the analysis model. The connection eccentricities are addressed due to 3D geometry of members so there is no need to define rigid link elements to solve the eccentricity problem. Also, as it is obvious from Figure 3-2 (left side) using 2D elements provides the ability to visualise the stress distribution, member behaviour and deformation as a 3D view which is another positive point for this model. However, creating the geometry and analysis time are more extensive than using 1D elements. So, the method of using 1D rigid links to consider the connection eccentricity is more appropriate especially for large and complicated tower geometries. Figures 3-3a and 3-3b depict two types of connections for leg and brace members. Leg members are connected via lap spliced bolted joints (Figure 3-3a) and the bracing members are connected to legs via single leg bolted joints (Figure 3-3b). While the eccentricity of lap spliced joint to connect the leg members is negligible, the eccentricity of brace members which are connected through one flange need to be addressed in the numerical model using rigid links.

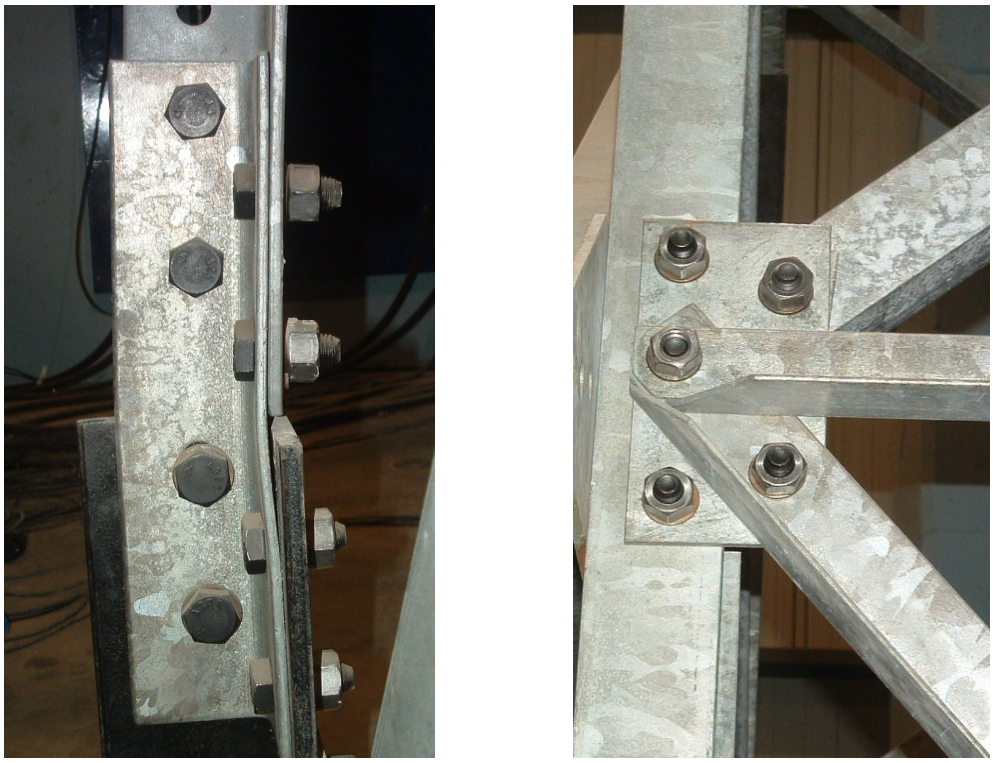

(a) Lap splice bolted joint (b) Single leg bolted joint

Figure 3-3: Joint types in towers

3.2. Methodology

3.2.1. Element type selection

The most effective and optimum element type or combination to model the towers is to be decided first as it conditions the remaining of the research. The proposed element type should consider the section shape and structural type of member. The element should have the ability of non-linear analysis and modelling the large displacement method (geometric non-linearity). Meanwhile, another priority is the optimization of element combination in order to obtain reasonable processing time and appropriate accuracy. According to our preliminary modelling efforts, Fibre beam and shell elements has shown acceptable results on simple angle members tested by Morrissette [52]. In this study the Fibre beam elements are implemented due to easier modelling and meshing as discussed in section 2.8 and Figure 2-

17. Also, these types of elements need less calculation time and can model yielding stress failures in the section.

The Fibre beam elements can also consider the penalizing effect of bending moments due to eccentricity of members. In this study, rigid link elements were used to model and apply the eccentricities to the member. So the bi-axial bending moment is applied to the Beam element because of the geometry of the model. Therefore, failure due to yielding or additional stresses because of bending moments in the member will be automatically considered in the fibre element behaviour.

Fibre beam element is limited to account for local buckling. To consider the local buckling, constitutive law has to include this effect if it is a behavior that is expected for the member. Also, to initiate global buckling, initial imperfection needs to be included in the modeling. It is recognized that the amplitude of initial imperfection can influence the failure mode and load capacity.

3.2.2. Material behaviour

There are two common methods of material modelling: bilinear and fully non-linear elasto-plastic stress-strain relationship. In the bilinear definition, material is modelled using only two-line portions. The first part models the behaviour up to yielding point according to Hooke's law and modulus of elasticity (E), after the yielding second part is the strain hardening part with a constant coefficient (E_t) known as hardening modulus. The bilinear model is a simplified stress-strain relation of material such as steel.

To input the exact stress-strain curve of material, the multi-linear material behaviour definition ability in Code_Aster is used. This command allows us to define stress-strain curve of the material point by point, which will result in more accurate output as well as covering the full behaviour of steel. Figure 3-4 compares the bilinear model with the real stress-strain curve of steel which is recorded from a uniaxial tension test. Coupon tests

should be performed on experimental specimens in order to transfer real stress-strain behaviour to numerical model.

In this study a bilinear material behaviour is used for the general model of the structure. However, to model the failure of the members subjected to local buckling, we have applied a full non-linear modified material behaviour as described in chapter 4.3.

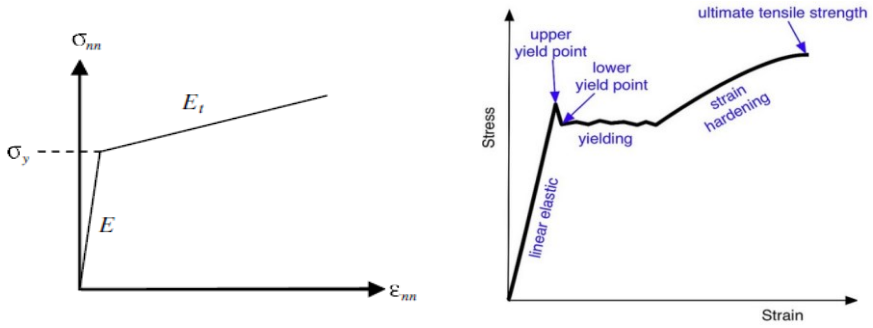

Figure 3-4: Non-linear material modelling (Left: bilinear relation, Right: real behaviour)

3.2.3. Local buckling of members

Depending on the type of member and section properties, we may encounter different types of failure. The proposed method should be able to cover plastic yielding as well as global and local instabilities. Figure 3-5 shows two failure scenarios which cannot be simulated by beam elements.

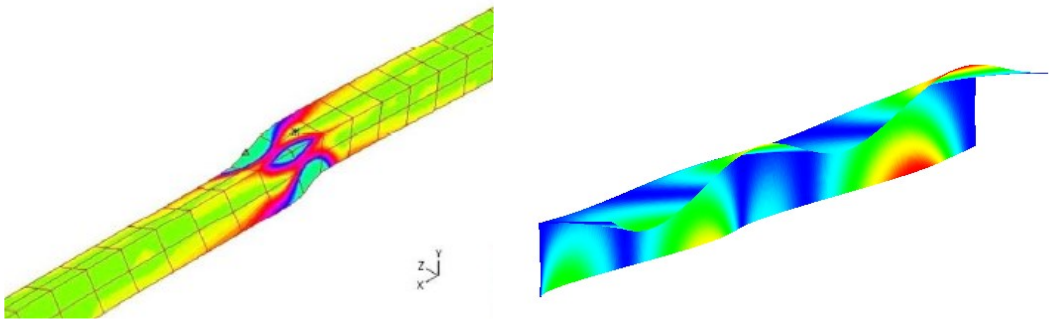

Figure 3-5: Local yielding and local buckling failures [46]

In this study, fibre beam modelling technique is used to model the 1D elements. The fibre beam element does not have the capacity to take into account local buckling which may be important in the behaviour of towers made of thin angle members. To account for local buckling, the modification of stress-strain law can be considered. The modification is conducted throughout the trial method and validating with real testing results.

As it is discussed in previous sections, local buckling of angle sections in lattice steel towers has not been very well researched in literature. More experimental tests need to be done to address this kind of failure mode and to find a proper method to include it in the finite element modelling.

To fill the current knowledge gap, one objective of this project is to propose a method to include the local buckling behaviour in the finite element model of structures using fiber beam element by developing a stress-strain behaviour curve of steel. To achieve this, forty-two slender section angle members were tested up to failure, and force-deflection curves were attained. Consequently, a local buckling slenderness ratio was defined by direct strength method [41] and equations were developed to correlate the slenderness ratio to two specific points on the stress-strain curve. Full stress-strain equations were then defined using curve fitting techniques to model the compressive behaviour of a slender angle with a given slenderness ratio. This material law is a way to introduce average normal stress based on member slenderness in range of inelastic local buckling. The angle shape normally is connected on one leg only and stress distribution is not uniform in the local zones close to connections. Therefore, it is difficult to introduce the method in a local zone of fibre element since all of the fibres would not follow the same constitutive law. Also, in joint regions where the angle section has a reduced net section, stress concentration may lead to local plate buckling phenomena which is not covered using this method. So the approach can be used mostly in global member level with high slenderness ratio of local buckling for the section.

Finally, the accuracy of proposed method was assessed against the test results of four full-scale X-braced frames of angle slender members tested by Morissette [52]. These tests are

explained with more details in section 4.3. The results are also compared to the admissible compressive stress calculated from different design standards.

Accordingly, the experimental program for the current project comprises testing of a total of 42 short angle members in pure compression. The tests were performed to evaluate the global stress-strain behaviour of angles failing due to local buckling. The local buckling slenderness ratio, λ_p, is introduced to characterize the sections undergoing local buckling, This ratio is used in the direct strength method [53] and was found useful to link the properties of the angle to the stress-strain behaviour. In this study, λ_p value is used as the main parameter which relates the local buckling behaviour of the member to a modified stress-strain material model. This material model is applied to the member in FE model to include the loss of stiffness due local buckling failure. The analytical and numerical approaches are presented in greater details in Section 4.2.1. Since the main objective of the tests was to extract the full behaviour of short angles based on their average stress-strain behaviour, we have not compared them to design values based on standards.

3.2.4. Non-linear behaviour of connection

The general objective of the suggested method is to propose an approach for predicting the full force-displacement curve of complex connections. This curve can then be integrated as a non-linear spring element in global finite element models of lattice towers.

The non-linear spring element used in this study can include the deflection due to slippage of connection and the near-field behaviour of plate in the vicinity of the bolt. The local behaviour of one-bolted connections, from loading to failure, is first predicted analytically. Then, the predicted load-deformation law is applied to numerical model to examine the non-linear response of plate assemblies with several bolts. Code_Aster has a powerful non-linear spring element that can model the connection behaviour. The methodology is to first predict the behaviour of one-bolted connection using equations available in the literature based on its properties and considering the near-field behaviour. At the second step, a series of specimens is tested in laboratory to validate the prediction model. The third step proposes a

method to categorize multi-bolted connections and predict their behaviour based on one bolt predicted model. This step is done with the help of a finite element plate model. At the next step, the method is evaluated by conducting experiments on several two-bolt joints. In the final step, predictions are compared to experimental results of four-bolt connections conducted by Cai [54]. The prediction method proposed in this study, allows to obtain the properties for a unique spring element that captures the overall non-linear behaviour of a given multi-bolted connection. This spring can easily be implemented at the end of a beam element in a complete lattice tower model.

An important part of the research is focused on how to define and include the joint effects in numerical modelling of towers. Angle member eccentricity and joint non-linear behaviour are considered in modelling. The eccentricity is modelled by rigid beam elements. Moreover, link elements are implemented to include the joint behaviour. The link element in Code_Aster has the ability to model the non-linear behaviour in three rotational degrees of freedom. However, the exact behaviour of connections for rotation should be defined as input parameters of link element.

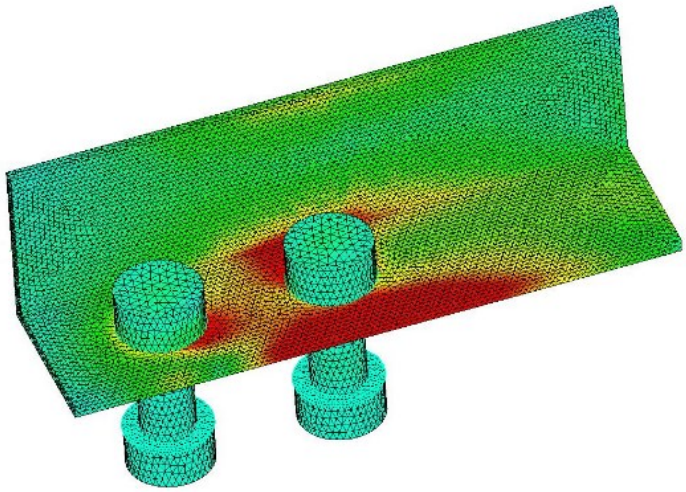

Figure 3-6: Finite element modelling of a connection by contact analysis

Figure 3-6 depicts a model which is meshed using 3D solid elements and contact analysis to verify the near field behaviour of the bolts. The contact analysis including the friction effects in the modelling is time consuming and the accuracy of results could always be questioned

as there is lack of experimental data to evaluate the performance of these connections. Therefore, the strategy adopted in this study is to measure the exact behaviour from experiments on prototypes of different connection assemblies. The results of these tests give us the bolt short-field behaviour and required parameters to include in the modelling. The results are in the form of force-displacement graphs. This method is based on predicting the behaviour of group of bolts based on one bolt so any arrangement of bolts can be considered. The near field behaviour of each bolt is considered separately, then it is possible to combine several bolts based on behaviour of one bolt in a FE model to predict the behaviour of group of bolts. Figure 3-7 depicts the layout of experiment for 1-, 2-bolt connection assemblies.

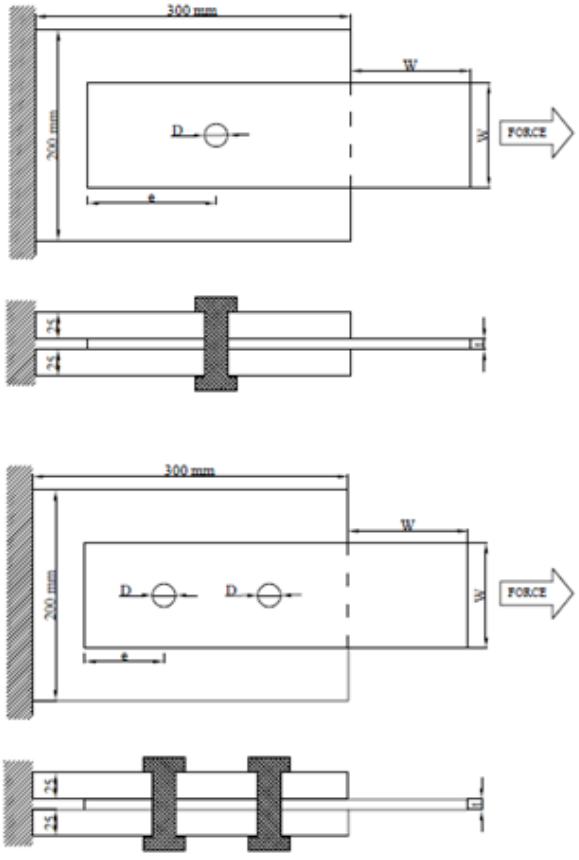

Figure 3-7: Experiment layout for 1-bolt and 2-bolt connections

In addition to bolt assembly, four parameters are investigated in experiments, D (bolt diameter), t (plate thickness), W (plate width) and e (end distance). The specimens are

deigned in a way that we can measure the near field behaviour of the bolts. Therefore, the connections are concentric and there is no shear lag phenomenon.

To select the proper parameters, the most common sections and bolt sizes in the industry are considered. Three major failure scenarios are assumed: (i) Bearing type (B), (ii) Shear block (S), (iii) Cleavage (C). Each specimen is designed to have a specific failure scenario, in order to have versatile failure types and behaviour in our tests. Table 3-1 and

Table 3-2 shows the experimental specimens and their configuration as well as predicted failure type according to CAN/CSA-S16 [4] design equations. The design equations provide the same limits for S and C failure types so in the table, C+S is for combined failure under those scenarios. Each test is repeated two times to ensure the precision of results. Accordingly, a total of 32 specimens are tested. The one-bolt specimens were used to validate the modelling method proposed in this study and the two-bolt specimens were designed to evaluate the prediction method for two bolts. These specimens were designed in a way that the near field behaviour of bolts is already predicted from the previous one-bolt tests.

Table 3-1: Properties of 1-bolt test specimens

Specimen No.	D (mm)	W (mm)	t (mm)	e (mm)	Failure Mode B (kN)	Failure Mode N (kN)	Failure Mode V (kN)	Failure Mode S (kN)	Possible Failure Scenarios
1	16	152	9.5	40.0	137	267	159	164	B
2	16	127	9.5	40.0	137	217	159	164	B
3	16	127	7.9	40.0	114	181	159	137	B
4	19	152	9.5	47.5	163	261	224	195	B
5	19	127	9.5	47.5	163	211	224	195	B
6	19	127	7.9	47.5	136	176	224	162	B
7	16	152	9.5	24.0	137	267	159	98	C+S
8	16	127	9.5	24.0	137	217	159	98	C+S
9	16	89	6.4	24.0	93	95	159	66	C+S

10	19	152	13.0	28.5	223	358	224	160	C+S
11	19	127	7.9	28.5	136	176	224	97	C+S
12	19	89	6.4	28.5	110	91	224	79	C+S

Table 3-2: Properties of 2-bolt test specimens

Specimen No.	Bolts	D (mm)	W (mm)	t (mm)	e (mm)	Failure Mode B (kN)	Failure Mode N (kN)	Failure Mode V (kN)	Failure Mode S (kN)	Possible Failure Scenarios
1	2	16	200	9.5	40.0	275	363	318	602	B
2	2	16	200	7.9	40.0	229	302	318	501	B
3	2	19	250	9.5	47.5	327	457	449	746	B
4	2	19	250	7.9	47.5	272	380	449	620	B

3.2.5. Initial imperfections

The modelling technique proposed should have the ability to include the initial geometrical imperfections. In other words, it should be able to apply different values of imperfection for each individual member in a tower. For research purposes, it is possible to measure the imperfections of members separately and apply them to the model, but for industrial application, we can propose a method to include imperfection for all of the members as per design codes. This can be achieved by using an initial imperfection value based on the length of the member applied to the geometry or an eccentricity at the connections. This will activate the main buckling mode in an incremental non-linear analysis [37, 39]. The initial imperfection can be a trivial perturbation load as well.

In this study an imperfection of (1/1000) length for members applied as a half sine along it for X-braced frame tests [51]. For the reduced scale tower section test, described in chapter 6, no imperfection is assumed in the numerical method. In this case, the connexion eccentricities were sufficient to trigger the global buckling behaviour [39].

3.2.6. Evaluation of the presented methods with experimental data

To verify the performance of the proposed method and its workability on lattice towers, two sets of different experimental data are used. At the first stage, the results of 4 experimental tests from a master's thesis [52] was considered as described in section 4.4.1. Morrisette has tested different angle sections with different connection assemblies up to failure level. The capacity of angle members has been measured in single and double bracing configurations. For the numerical model, only the bracing angle members and end connection plates are included in the model. It is assumed that the outside frame members are rigid in comparison to the angle members. Therefore, the end connection plates on top are supported by fixed supports with only unrestrained lateral displacement. The bottom supports are assumed to be fixed. The angle members are connected to these supports via two elements, first a rigid beam element to include the member eccentricity and second a non-linear spring to model the three-bolt connection behaviour. The properties of spring element are predicted using the method presented in this study for connection behaviour. The non-linear analysis phase is done with Code_Aster and the assumptions of non-linear material and large displacements are included in the procedure. As presented in chapter 4, the comparison of the model with these test results is used to validate the proposed method to model the local buckling behaviour of bracing angles.

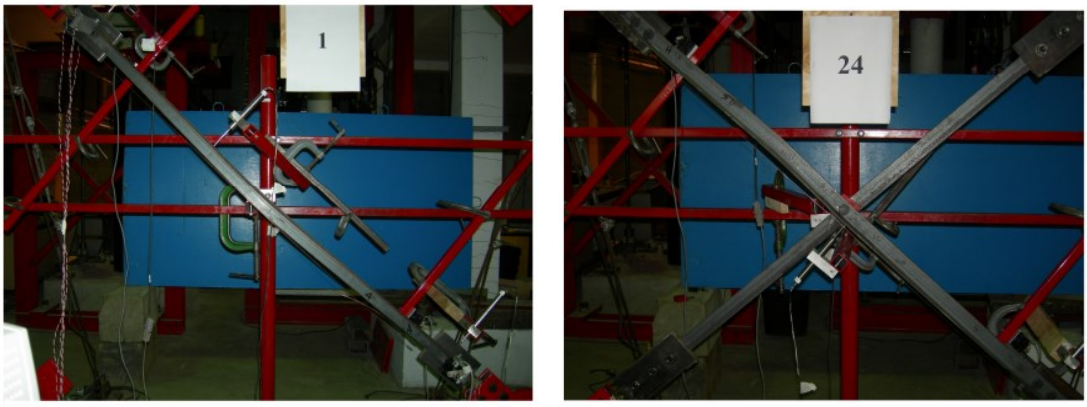

Figure 3-8: Single and double bracing configurations used by Morrisette [51]

As for the second type of experimental verification, the results of a reduced scale tower test [55] has been considered to verify the effect of connection behaviour in finite element model

using the method developed in this study. Figure 3-9 depicts the experimental test set up and the specimen.

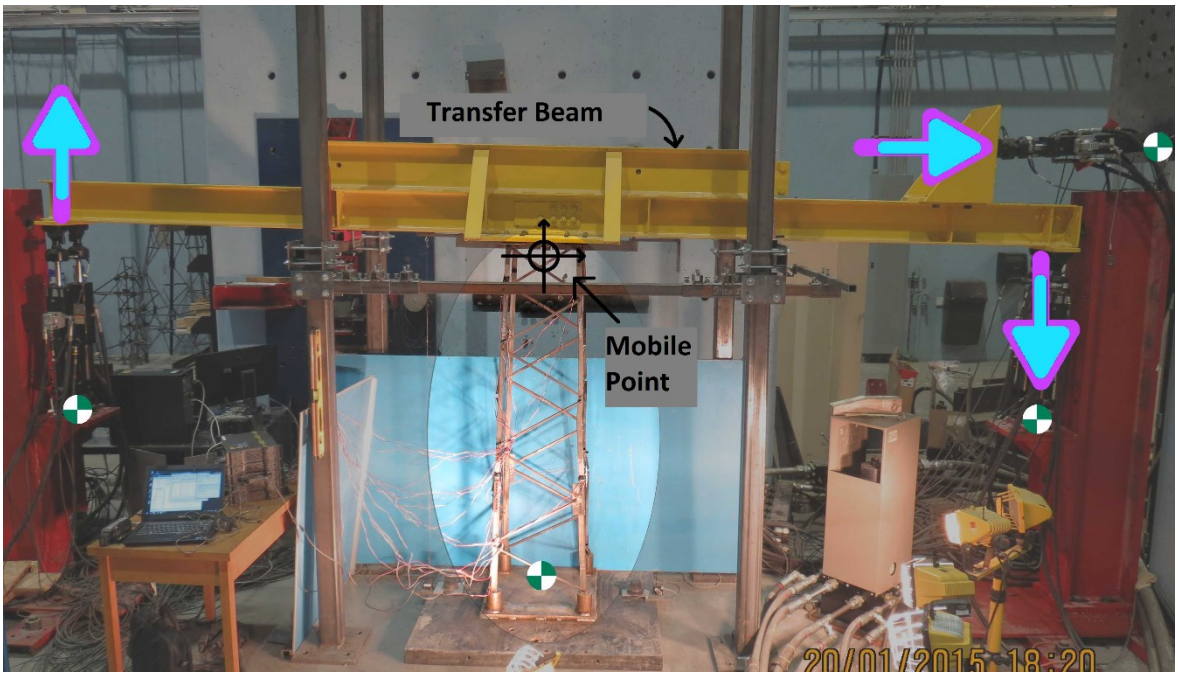

Figure 3-9: Reduced scale tower test [55]

In the numerical model the members are modelled using 1D fibre beam elements. Eccentricities of angle members are applied to the geometry using rigid links. An incremental push over analysis is performed based on non-linear material and large deformation assumptions. The brace connections of this structure are modelled using ASSE_CORN element to consider the non-linear behaviour including slippage. To define the parameters for ASSE_CORN element, the prediction method which is presented in chapter 5 is used. Finally, the Force-Displacement result of the numerical model is compared to experimental measurements to validate the accuracy of the modelling strategy. Full details of this verification are described in chapter 6. In this experiment, the local buckling is not critical and therefore, this validation focuses only on the effect of the non-linear connection behaviour.

CHAPTER 4 LOCAL BUCKLING FAILURE

Modelling the Local Buckling Failure of Angle Sections with Beam Elements

(Published in Journal of Advanced Steel construction – Vol. 15, No. 4)

Avant-propos

Auteurs et affiliation:

Farshad Pourshargh[a], Frederic P. Legeron[b,d], Sébastien Langlois[c]

[a] *PhD candidate at Université de Sherbrooke*

[b] *Eng., Ph.D. Formerly Professor, Civil Engineering Department, Université de Sherbrooke*

[c] *Eng., Ph.D. Assistant professor, Civil Engineering Department, Université de Sherbrooke*

[d] *Present affiliation: Vice President, Parsons*

Accepted: July 2019

Published: December 2019

Titre: Modelling the Local Buckling Failure of Angle Sections with Beam Elements

Abstract

Slender steel sections are widely used in construction of different steel structures such as lattice structures for transmission line and telecommunication towers. Local buckling may be the observed failure mode under compression loads for these slender sections and many experimental studies were done to evaluate their resistance. All of the steel design codes include equations to account for local buckling. In numerical models, local buckling can be reproduced using 2D shell or 3D elements. Non-linear numerical models have been developed in the last decades that can capture the complex behaviour of lattice structures up to failure. These models normally use beam elements which consider correctly global buckling and yielding of sections but do not consider local buckling of angles due to geometrical limitations. This article proposes a method which modifies the material behaviour of sections to involve the local buckling failure in the analysis. Forty-two experimental tests were conducted on short angles and a general stress-strain formula was defined based on the tests. The formula relates the local buckling slenderness ratio of the members to a material constitutive law accounting for local buckling. To validate the method, the numerical results were compared to those of four x-braced frame configurations using slender angle sections. The results show that the proposed method can accurately model the local buckling failure of fiber beam elements.

Keywords: Lattice steel tower, Angle section, Local buckling, Finite element model, Non-linear behaviour, Fiber beam element.

4.1. Introduction

Angle steel members are widely used in steel lattice structures for transmission lines and telecommunications. Lattice towers made of angle members have a complex structural behaviour mainly due to connection eccentricity, bolt slippage, local buckling and their impact on failure modes. The standard procedure for designing tower members is to build a simple linear model of the structure to determine forces in each member and then evaluate the resistance using design code equations. This type of analysis may not be correct because verification of the buckling resistance should be carried out as an integrated part of design not as an independent stage [40,56]. To overcome the limitation of this simple analysis, transmission line lattice towers are normally tested under different load conditions in full scale field tests before mass production.

Prasad Rao [35] reported that 32 towers out of 138 full scale tests at the Structural Engineering Research Centre [CSIR-SERC] experienced different type of premature failures which demonstrate the limits of the design method used in practice. To study the failure in detail, they modelled three towers and analysed them with NE-Nastran non-linear finite element software. The option for geometric and material non-linearity of the software was used to obtain the behaviour and limit loads. The entire tower was modelled using beam-column elements. However, to capture more details, the failed compression bracing was modelled as plate elements. The test failure pattern coincided with analysis failure pattern for both beam and plate modelling. However, non-linear finite element analysis predicted the failure load 7-14 percent above test results.

Another study was performed by the same researchers [30] on five prematurely failed towers. They encountered over prediction of strength by non-linear analysis and concluded that finite element analysis is still not a fully reliable method to predict tower strength and tests are still necessary for this purpose. However, it is indicated that the non-linear analysis is essential for understanding the behaviour, load carrying capacity, design deficiencies, and instability in structure. This type of non-linear model aims to capture the complex and non-linear behaviour of steel lattice structures. It is not a practical design method as such, because

it does not rely on design code equations or more advanced methods such as direct strength method (DSM) [41–43] to evaluate the resistance of sections. It provides a one-step numerical model to represent the pre and post buckling behaviour of the structure. This type of model is useful as an alternative or complement to full-scale tests to understand the behaviour and verify the resistance of lattice towers. Recent works showed that depending on the objective of the modelling, the following characteristics of lattice behaviour might need to be considered: joint eccentricity [36,37], bolt slippage [44], residual stresses [39], etc. However, in this type of model that normally simulates the elasto-plastic buckling of angle members, the potential local buckling of members is neglected. This article will focus on developing an efficient method to account for local buckling in non-linear models of lattice structures.

Currently, most research in the modelling of angle members is either using beam elements or 2D shell elements. Angle sections may undergo global or local buckling instability under compression load, depending on the slenderness and width to thickness ratios. Shell elements can represent the full three-dimensional behaviour of angle sections and specifically local buckling, with high accuracy if the mesh is refined enough. However, in the case of large and complex structures such as lattice towers, the high number of members makes the use of shell elements impractical. For example, Shan *et al*. [45], proposed to model angle members by non-linear plate elements. They included both material and geometric non-linearities in the study, but the analysis procedure was computer intensive and time consuming. They concluded that, 2D elements can only be used for small structures and as a research tool. It has also been confirmed by other researchers [46].

In the case of slender angle sections with high width-to-thickness ratio, the global buckling deformation is accompanied by local buckling of leg plates [47] and this effect should be incorporated in the finite element model of the structure. Lee and McClure [46] developed a L-section beam finite element for elastoplastic large deformation analysis. It is mentioned that, considering the computational time, the beam element is 2.4 times more efficient than shell modelling when the member length is equal to 4 meters.

The fiber beam element is a very effective element that is used with some success to model angle sections. This element can properly incorporate the stress and yielding effects in the member. Kitipornchai *et al*. [12,48] reported an analysis with non-linear fiber elements of angle sections under axial and bending loads. Numerical studies have been done on a number of structures and the angle members were modelled as fiber elements. They presented different examples to demonstrate the validity of fiber element model in predicting the ultimate behaviour of imperfect angle columns. The results obtained from the study were compared to experimental tests on two pairs of angle trusses with web members.

Vieira *et al*. [49] and Carrera *et al*. [50] proposed a 1D beam element to model the buckling of beams using analytical formulas. The results were in line with finite element models. Some limitations for capturing the local buckling behaviour were reported. Authors mentioned, more tests and experiments are needed to deal with extension of the method.

Other computational methods to calculate the buckling loads of thin-walled sections were also studied. Huang *et al*. [51], developed a mathematical formulation. They took the angle section as an example then numerical analysis of elastic and inelastic buckling was performed using finite element models. Comparison of results from beam and shell elements with the theoretical results was presented. It was concluded that mathematical solution of higher order differential equations is complicated and for the members with complicated deflections different method should be applied.

Considering other researches and experiments in this field, the approach with fiber element is well adapted analytically to model the transmission tower structures but a full local buckling behaviour that covers the pre and post buckling behaviour is not well defined.

The objective of this paper is to propose a method to incorporate the local buckling behaviour in the finite element model of structures using fiber beam element by means of developing a stress-strain behaviour curve of steel. For this purpose, forty-two slender section angle members were tested, and full force-deflection curves were extracted. Then, a local buckling slenderness ratio was defined by direct strength method [41] and equations were developed to relate the slenderness ratio to two specific points on the stress-strain curve. Considering

these two points, full stress-strain equations are then defined using curve fitting techniques to model the compressive behaviour of a slender angle with a given slenderness ratio. Finally, the proposed method was evaluated by comparing it to the test results of four full scale X-braced frames of angle slender members tested by Morissette [52].

4.2. Short angle specimens

4.2.1. Local buckling slenderness

The experimental program consists in testing 42 short angle members in pure compression. These tests were performed to evaluate the global stress-strain behaviour of angles failing due to local buckling. To characterize the sections undergoing local buckling, Table 4-1 introduces the local buckling slenderness ratio, λ_p, which is defined in equation (4-1). This ratio is used in the direct strength method [53] and was found useful to link the properties of the angle to the stress-strain behaviour.

$$\lambda_p = \sqrt{\frac{F_y}{\sigma_{cr}}} \tag{4-1}$$

In this equation, F_y stands for the yielding stress of steel and σ_{cr} is the critical elastic local buckling stress for the member which can be calculated using finite element software such as Code_Aster, ANSYS or ABAQUS. In this study a finite strip software CUFSM which is developed by Schafer [57] will be implemented to carry out critical elastic buckling load calculations. CUFSM which has been developed to accompany direct strength method is a finite strip elastic buckling analysis application. In the first step, geometry of the member is modelled either manually or from built-in cross-sections library. Then, general end boundary conditions and loading are applied to the member and the section is meshed automatically with finite strips. Finally, the analysis provides the buckling mode shapes of the member and the critical elastic buckling load for each mode. This software is freely available.

In practice, using FE analysis is time consuming for engineers. However, as a simplification, a mathematical relation can be developed relating the local buckling stress to the width to thickness ratio b/t, where b is the width of the angle leg and t is the thickness of the leg. Based on all the angle members that are reported in Table 4-1, a formula is presented to relate σ_{cr} value and (b/t) ratio:

$$(b/t) = \frac{\alpha}{\sqrt{\sigma_{cr}}} \tag{4-2}$$

Where α value is calculated to be 323 according to the curve fitting analysis shown in Fig.1. In this work the modulus of elasticity of steel was assumed to be 200,000 MPa. This simplification can be used when boundary conditions of angle member are fixed translation and free rotation. It should be noted however, that, as seen in Figure 4-1, the discrepancy in local buckling stress can be important, in particular at low b/t values.

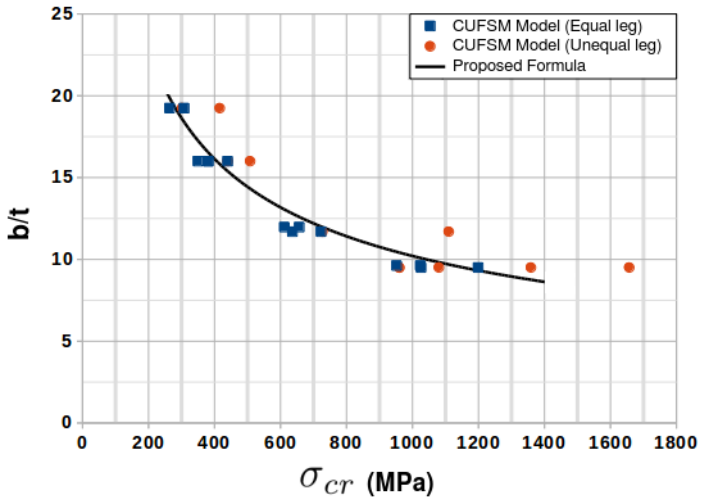

Figure 4-1: Calculated curve to relate σ_{cr} and (b/t) values

4.2.2. Experimental program

The objective of the experimental program is to provide test results on local buckling behaviour from various geometries of specimens. Forty-two short angle specimens, listed in Table 4-1, were tested under pure compression and then Force-Deformation behaviour was

measured. The leg width to thickness ratio, (b/t), of specimens was ranging from 9.5 to 19. According to (CSA-S16) [4] and Eurocode 3 [3]; all specimens are classified as class 4 sections which are subject to local buckling before reaching yielding in compression. The steel grade of the specimens is ASTM-A36 [58] and material properties are listed in Table 4-1.

Length of specimens was selected to avoid global buckling instability. Most configurations were tested on two identical specimens to evaluate the repeatability of results. The average of these identical tests where considered as final result to better represent the type of the sections in the market. Since the length of the specimens were short and they fail under local buckling mode the effect of geometrical imperfections and residual stresses are not considered. Although these effects are more important on global buckling mode which is not in the scope of this article. Taking the mentioned effects in consideration also adds more parameters to the prediction which makes it very complicated to reach out for a solution, so these effects are not investigated more in this article.

To provide continuous and uniform end conditions throughout the tests, the extremities of all specimens were accurately milled flat and strictly perpendicular to the axis of the angle. Specimens were supported by thick steel plate without hinge for the test. The alignment of the centroid of the angle on the line of action of the force was secured by top and bottom adjustment plates (Figure 4-2) bolted to the thick plates. To avoid any eccentric moment, the center of the force applied from machine coincided with center of gravity of the section. The angle shaped opening in each set of adjustment plates provided the required end restraints, fixed translation and free rotation.

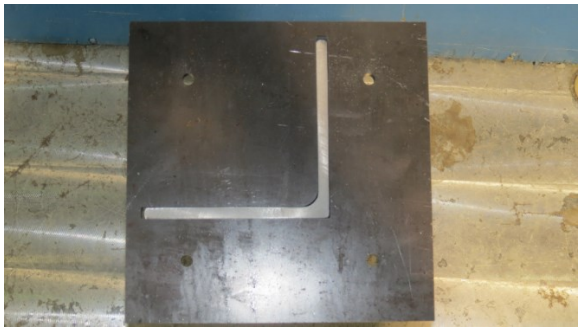

Figure 4-2: Adjustment plate in the supports

Table 4-1: Properties of short angle test specimens

Test	Section	Length (mm)	b/t	F_y (MPa)	F_u (MPa)	E (MPa)	σ_{cr} (MPa)	λ_p
1	L152x152x7.9	600	19.2	339	519	178000	264	1.13
2	L152x152x7.9	600	19.2	339	519	178000	264	1.13
3	L152x152x7.9	400	19.2	339	519	178000	308	1.05
4	L152x152x7.9	400	19.2	339	519	178000	308	1.05
5	L152x152x9.5	600	16.0	390	543	207000	381	1.01
6	L152x152x9.5	600	16.0	390	543	207000	381	1.01
7	L152x152x9.5	400	16.0	390	543	207000	440	0.94
8	L152x152x9.5	400	16.0	390	543	207000	440	0.94
9	L152x152x16	600	9.5	395	514	188281	1026	0.62
10	L152x152x16	600	9.5	395	514	188281	1026	0.62
11	L152x152x16	400	9.5	395	514	188281	1199	0.57
12	L152x152x16	400	9.5	395	514	188281	1199	0.57
13	L152X102X9.5	433	16.0	373	495	206297	508	0.86
14	L152X102X9.5	437	16.0	373	495	206297	508	0.86
15	L152X102X16	438	9.5	375	564	212700	1359	0.53
16	L152X102X16	439	9.5	375	564	212700	1359	0.53
17	L152X102X16	680	9.5	375	564	212700	1080	0.59
18	L152x152x9.5	598	16.0	392	541	201000	381	1.01
19	L152x152x9.5	597	16.0	392	541	201000	381	1.01
20	L152x152x9.5	598	16.0	392	541	201000	381	1.01
21	L152X102X9.5	718	16.0	371	492	208000	440	0.92
22	L152x152x9.5	850	16.0	380	526	210000	350	1.04
23	L152X102X16	800	9.5	375	563	212700	960	0.63
24	L152X102X16	300	9.5	375	563	212700	1657	0.48
25	L152X102X16	800	9.5	375	563	212700	960	0.63
26	L152x152x13	850	11.7	388	547	202626	636	0.78
27	L152x152x13	850	11.7	388	547	202626	636	0.78
28	L152x152x13	500	11.7	388	547	202626	723	0.73
29	L152x102x13	800	11.7	407	587	193387	727	0.75
30	L152x102x13	800	11.7	407	587	193387	727	0.75
31	L152x102x13	300	11.7	407	587	193387	1110	0.61
32	L152x102x7.9	800	19.2	405	557	204017	302	1.16
33	L152x102x7.9	800	19.2	405	557	204017	302	1.16
34	L152x102x7.9	300	19.2	405	557	204017	416	0.99
35	L76x76x6.35	400	12.0	379	526	203000	612	0.79
36	L76x76x6.35	400	12.0	379	526	203000	612	0.79
37	L76x76x6.35	300	12.0	379	526	203000	657	0.76

38	L76x76x6.35	300	12.0	379	526	203000	657	0.76
39	L76x76x7.9	400	9.6	388	555	203000	952	0.64
40	L76x76x7.9	400	9.6	388	555	203000	952	0.64
41	L76x76x7.9	300	9.6	388	555	203000	1024	0.62
42	L76x76x7.9	300	9.6	388	555	203000	1024	0.62

The compression jig was set up to perform the tests as shown in Figure 4-3 in a 500 kN hydraulic testing machine. The loading was displacement controlled at rates ranging from 0.12 to 0.3 mm/min according to the length of the specimen in order to reach the maximum load within 5 to 10 minutes. The test was continued up to the occurrence of a significant non-linear behaviour. Relative displacement of specimens was measured by a displacement transducer attached to the adjustment plate from bottom to top (Figure 4-3).

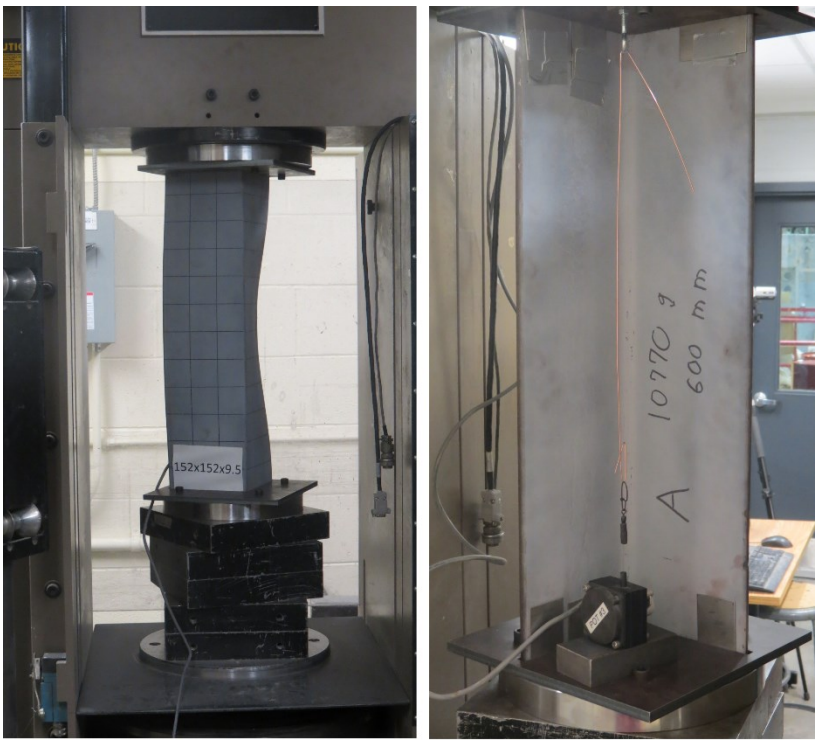

Figure 4-3: Test set-up and displacement transducer

4.2.3. Material property tests

Two or three coupons were cut and prepared from each batch of steel material and tested in tension according to ASTM A370-02 [59] standard. The value of F_y which is provided from

coupon tests was used to calculate λ_p for each specimen. The values are indicated in Table 4-1.

4.3. Definition of material stress-strain behaviour

Based on the force-deflection results of short angle tests, 42 stress-strain material behaviours were extracted. Each material behaviour is related to the corresponding λ_p value of specimen. The values of σ(stress) and ε(strain) are calculated by assuming a homogeneous behaviour σ = P/A, $\varepsilon = \delta$/L, where: P is the applied force (N); A is the cross-sectional area (mm^2); δ is the vertical deflection of specimen (mm); and L = Length of specimen (mm).

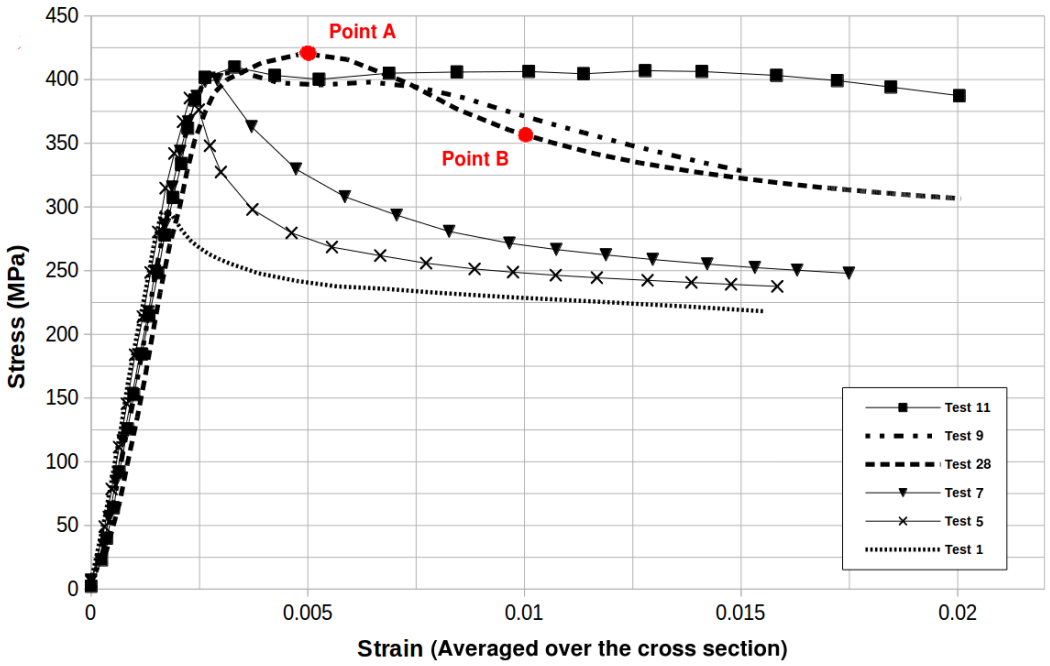

Figure 4-4: Measured stress-strain behaviour of six test specimens

Figure 4-4 shows the measured behaviour of six specimens. In order to characterize the behaviour of member in compression, it is assumed that the full stress-strain curve can be characterized by 2 points, A(ε_A,σ_A) the first peak in the curve and B(0.01,σ_B), Table 4-2 reports ε_A,σ_A, and σ_B values. Other points were also considered but based on accuracy of fitted curve the points above were selected. Using the short angle test results (Table 4-2) and curve fitting technique, equations (4-3) to (4-5) were developed to calculate the coordinates of points A

and B based on $\lambda_p$value. Since the number of tested specimens was limited, the range of values of λ_p for which the equations apply was limited to 0.57-1.20. This also affected the calculated values of σ_A in terms of material yield stress. Figure 4-5 illustrates the equations and distribution of test points.

$$\varepsilon_A = 0.0004965 \times (1 + \lambda_p{}^{-11.6})^{\frac{1}{5.8}} + 0.001521 \qquad 0.57 < \lambda_p < 1.20 \qquad (4\text{-}3)$$

$$\sigma_A = 407.9 \times (1 + \lambda_p^{20})^{-\frac{1}{10}} \qquad 0.57 < \lambda_p < 1.20 \qquad (4\text{-}4)$$

$$\sigma_B = 350.1 \times \lambda_p{}^2 - 903.9 \times \lambda_p + 809.1 \qquad 0.57 < \lambda_p < 1.20 \qquad (4\text{-}5)$$

Table 4-2: Results of short angle tests

Test	λ_p	ε_A	σ_A (MPa)	σ_B (MPa)
1	1.13	0.0017	298	228.0
2	1.13	0.0018	288	229.9
3	1.05	0.0022	313	234.0
4	1.05	0.0035	297	242.0
5	1.01	0.0023	389	248.0
6	1.01	0.0021	379	250.0
7	0.94	0.0028	401	269.7
8	0.94	0.0028	400	267.8
9	0.62	0.0032	407	371.2
10	0.62	0.0027	406	398.7
11	0.57	0.0032	409	406.6
12	0.57	0.0032	410	406.3
13	0.86	0.0029	367	271.7
14	0.86	0.0031	367	270.8
15	0.53	0.0035	350	374.0
16	0.53	0.0049	353	376.0
17	0.59	0.0022	350	350.7
18	1.01	0.0025	390	256.9
19	1.01	0.0026	384	254.8
20	1.01	0.0024	377	256.2
21	0.92	0.0024	371	254.0
22	1.04	0.0022	356	241.6
23	0.63	0.0030	422	376.0
24	0.48	0.0050	423	436.7

25	0.63	0.0035	425	392.0
26	0.78	0.0034	413	305.0
27	0.78	0.0032	413	301.8
28	0.73	0.0048	420	356.8
29	0.75	0.0036	414	332.2
30	0.75	0.0035	413	334.0
31	0.61	0.0070	450	453.0
32	1.16	0.0021	336	234.6
33	1.16	0.0021	319	245.1
34	0.99	0.0031	404	285.7
35	0.79	0.0029	418	292.6
36	0.79	0.0030	419	293.0
37	0.76	0.0034	411	329.0
38	0.76	0.0038	415	324.3
39	0.64	0.0031	431	406.8
40	0.64	0.0027	429	422.0
41	0.62	0.0030	432	427.0
42	0.62	0.0031	429	423.6

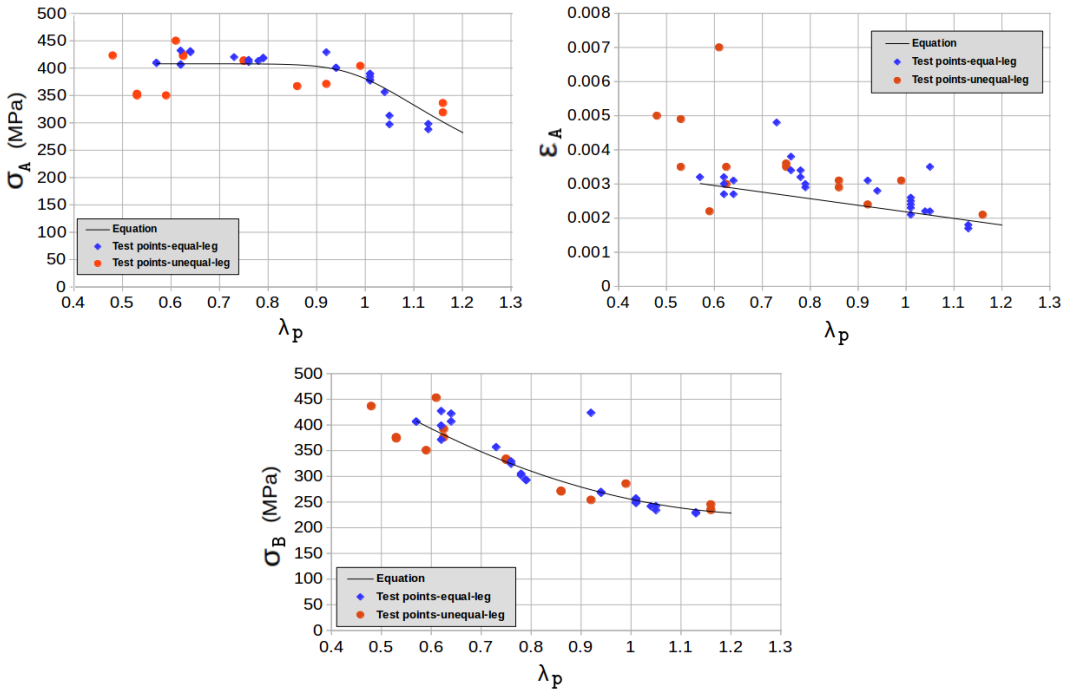

Figure 4-5: Equations (4-3) to (4-5) and distribution of test points

The coordinates of points A and B are used to calculate the three unknown parameters (C,D,k) that are used to define the stress-strain equation (4-6). Since the behaviour of steel

in the first steps of loading is completely elastic, the third criteria to calculate the parameters of equation is the slope of standard steel stress-strain material in elastic range which is assumed to be 200,000 MPa (Young's modulus). The main stress-strain equation is expressed as:

$$\sigma = \begin{cases} 200000 \times \varepsilon & \varepsilon \leq 0.0005 \\ C \times \varepsilon_m \times (\varepsilon_m + D \times \varepsilon_m{}^{(-k)})^{(-k)} & \varepsilon > 0.0005 \end{cases} \quad (4\text{-}6)$$

$$\varepsilon_m = 1000 \times \varepsilon \quad (4\text{-}7)$$

Equations (4-3) to (4-5) relate the λ_p value of any class 4 member to two characteristic points A and B of the stress-strain curve. Equation (4-6) then relates these two points to a complete and modified stress-strain curve that can be included in a beam element as material behaviour. The unknown parameters in the equation (C, D,k) were obtained by trial and error method. A simple script was developed to input the λ_p value. The script calculates the coordinates of points A and B based on equations (4-3) to (4-5). Then the points A and B are applied to equation (4-6) which provides the full stress-strain behaviour. Table 4-3 lists the parameters C, D and k that are calculated based on points A and B for each specimen and λ_p value. The output of equation (4-6) can be entered as a non-linear material behaviour in any finite element software. An alternative simplified solution would be to define the material as bi-linear stress-strain relation without using equation (4-6). The bi-linear behaviour could be defined by using the σ_A as F_y and the slope of the line connecting points A to B (AB) as E_t (Tangent modulus of material). Figure 4-6 compares the stress-strain curve calculated by equation (4-6) to the test results from short angle specimens for six different λ_p values.

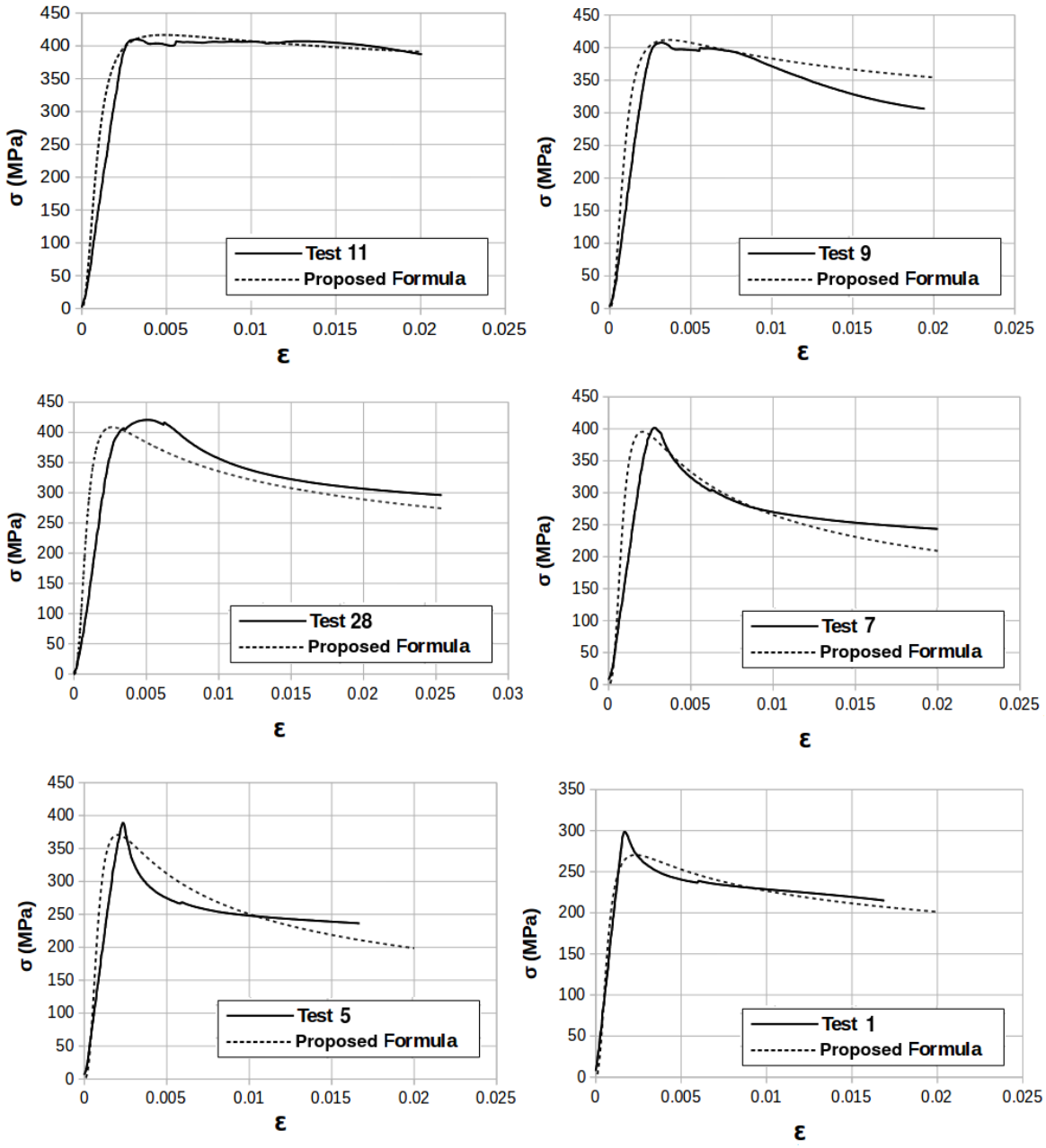

Figure 4-6: Comparison of stress-strain relationship between test results and equation (4-6)

Table 4-3: Calculated values of parameters for equation (4-6)

Tests	λ_p	C	D	k
1,2	1.13	440.289	0.563	1.272
3,4	1.05	526.022	0.625	1.329
5,6,18,19,20	1.01	563.891	0.653	1.346
7,8	0.94	601.782	0.692	1.349
9,10	0.62	512.091	0.831	1.123
11,12	0.57	479.906	0.844	1.068
13,14	0.86	602.713	0.729	1.315
15,16	0.53	449.86	0.848	1.018
17	0.59	493.722	0.840	1.091
21	0.92	605.266	0.702	1.343
22	1.04	536.673	0.633	1.334
23,25	0.63	517.363	0.827	1.133
24	0.48	441.128	0.847	1.004
26,27	0.78	583.226	0.764	1.263
28	0.73	565.003	0.786	1.224
29,30	0.75	572.487	0.777	1.240
31	0.61	506.351	0.834	1.113
32,33	1.16	409.118	0.538	1.246
34	0.99	578.983	0.665	1.351
35,36	0.79	585.562	0.760	1.269
37,38	0.76	575.722	0.773	1.247
39,40	0.64	523.266	0.824	1.143
41,42	0.62	512.091	0.831	1.123

As it is shown in Figure 4-6, the calculated curves are comparable to the experimental results and they have an acceptable accuracy. This is also demonstrated in Table 4-4 which compares the values of ε_A, σ_A and σ_B from Equation (4-6) and experimental work on short angles. The mean value of the differences is very close to 1.0 and the values of COV is reasonable for σ_A and σ_B parameters. The strain at peak is always difficult to capture in angles showing close to elasto-perfectly plastic behaviour. As a consequence, the COV value for ε_A parameter is relatively high. Despite the statistical comparisons in Table 4-4, it can be seen that the trend of stress-strain curve calculated by formula is in line with the experimental results and the inaccuracy on ε_A does not impact the close match of the predicted curve to the experiments.

Table 4-4: Comparison of parameters calculated with Equation (4-6) to test values for parameters ε_A, σ_A, σ_B

Test	ε_A (T)	σ_A (T)	σ_B (T)	ε_A (F)	σ_A (F)	σ_B (F)	$\frac{\varepsilon_A}{\text{(F/T)}}$	$\frac{\sigma_A}{\text{(F/T)}}$	$\frac{\sigma_B}{\text{(F/T)}}$
1	0.0017	298	228	0.0021	317	234	1.24	1.06	1.03
2	0.0018	288	230	0.0021	317	234	1.17	1.10	1.02
3	0.0022	313	234	0.0020	358	245	0.91	1.14	1.05
4	0.0035	297	242	0.0020	358	245	0.57	1.21	1.01
5	0.0023	389	248	0.0020	376	252	0.87	0.97	1.02
6	0.0021	379	250	0.0020	376	252	0.95	0.99	1.01
7	0.0028	401	270	0.0019	397	269	0.68	0.99	1.00
8	0.0028	400	268	0.0019	397	269	0.68	0.99	1.00
9	0.0032	407	371	0.0036	412	383	1.13	1.01	1.03
10	0.0027	406	399	0.0036	412	383	1.33	1.01	0.96
11	0.0032	409	407	0.0046	416	402	1.44	1.02	0.99
12	0.0032	410	406	0.0046	416	402	1.44	1.01	0.99
13	0.0029	367	272	0.0022	406	291	0.76	1.11	1.07
14	0.0031	367	271	0.0022	406	291	0.71	1.11	1.07
15	0.0035	350	374	0.0042	418	428	1.20	1.20	1.14
16	0.0049	353	376	0.0042	418	428	0.86	1.19	1.14
17	0.0022	350	351	0.0042	414	397	1.91	1.18	1.13
18	0.0025	390	257	0.0020	373	251	0.80	0.96	0.98
19	0.0026	384	255	0.0020	376	252	0.77	0.98	0.99
20	0.0024	377	256	0.0020	376	252	0.83	1.00	0.98
21	0.0024	371	254	0.0021	401	274	0.88	1.08	1.08
22	0.0022	356	242	0.0019	363	247	0.86	1.02	1.02
23	0.0030	422	376	0.0034	411	379	1.13	0.97	1.01
24	0.0050	423	437	0.0046	421	433	0.92	1.00	0.99
25	0.0035	425	392	0.0034	411	379	0.97	0.97	0.97
26	0.0034	413	305	0.0024	408	317	0.71	0.99	1.04
27	0.0032	413	302	0.0024	408	317	0.75	0.99	1.05
28	0.0048	420	357	0.0026	409	336	0.54	0.97	0.94
29	0.0036	414	332	0.0025	408	328	0.69	0.99	0.99
30	0.0035	413	334	0.0025	408	328	0.71	0.99	0.98
31	0.0070	450	453	0.0038	412	388	0.54	0.92	0.86
32	0.0021	336	235	0.0021	302	231	1.00	0.90	0.98
33	0.0021	319	245	0.0021	302	231	1.00	0.95	0.94
34	0.0031	404	286	0.0020	384	257	0.65	0.95	0.9
35	0.0029	418	293	0.0024	408	314	0.83	0.98	1.07
36	0.0030	419	293	0.0024	408	314	0.80	0.97	1.07

37	0.0034	411	329	0.0025	408	323	0.74	0.99	0.98
38	0.0038	415	324	0.0025	408	323	0.66	0.98	1
39	0.0031	431	407	0.0033	411	374	1.06	0.95	0.92
40	0.0027	429	422	0.0033	411	374	1.22	0.96	0.89
41	0.003	432	427	0.0036	412	383	1.2	0.95	0.9
42	0.0031	429	424	0.0036	412	383	1.16	0.96	0.9
Average							0.93	1.02	1
COV (%)							30.29	7.56	6.53

Note: (T: Test, F: Formula) – Stress values are in (MPa)

4.4. Evaluating the method with experimental results

4.4.1. Experimental program

To evaluate the accuracy of the method, the numerical results were compared to those of experimental tests performed at Université de Sherbrooke [52] on four X-bracing frame configurations. The test set-up is a two-dimensional frame with the ability to include angle members acting as X-bracing. Figure 4-7 and Figure 4-8 present a sketch and a photo of the test set-up. A lateral load was applied to the frame which introduces compression and tension forces to the angles. The maximum capacity of the jack is 500 kN and it is mounted horizontally to a rigid supporting system. The frame was restrained by steel cables to avoid out of plane deflections. The beam to column connections were designed as pinned joints using a single bolt such that no bending moment was applied to the frame members and the lateral force induces direct axial tension and compression to the angles.

To measure the applied force to the angles, strain gauges were placed on end connection plates. Figure 4-9 depicts the geometry of the end plates, the thickness is 25.4 mm and two sets of plates were prepared for different bolt sizes of 12.7 mm and 15.9 mm. To ensure the accuracy of measured force, all assemblies of end plates and strain gages were calibrated separately. The recorded data from strain gauges mounted on the end plates, could then be transformed to applied force. In addition, displacement transducers were implemented to measure the lateral and out of plane deformation of the frame and braces. The load was applied based on displacement control principle with a rate of 0.5 mm/min.

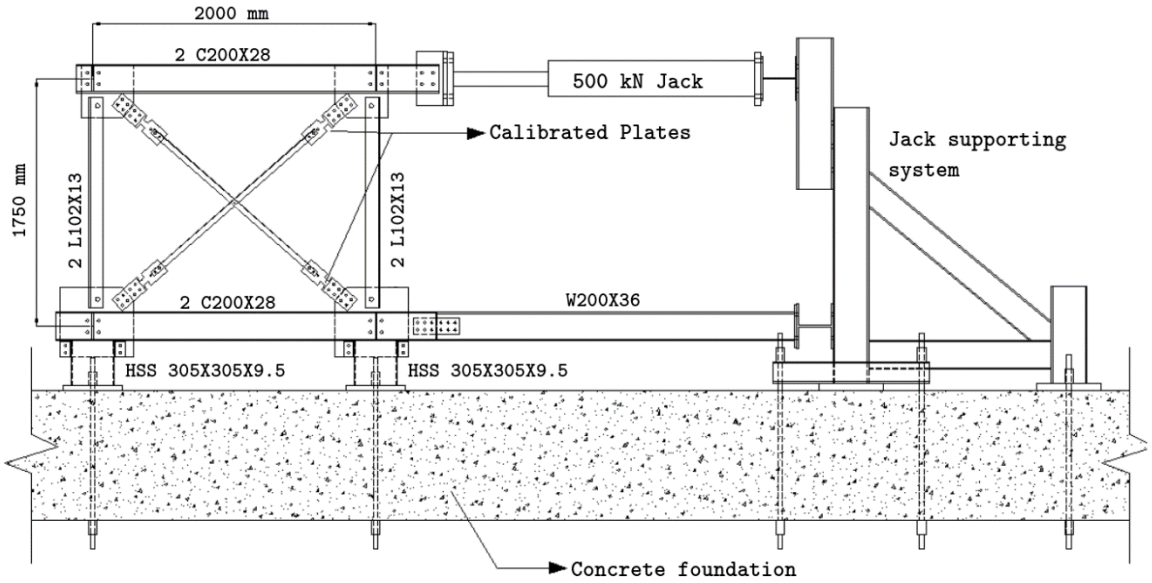

Figure 4-7: Schematics of the test set-up [52]

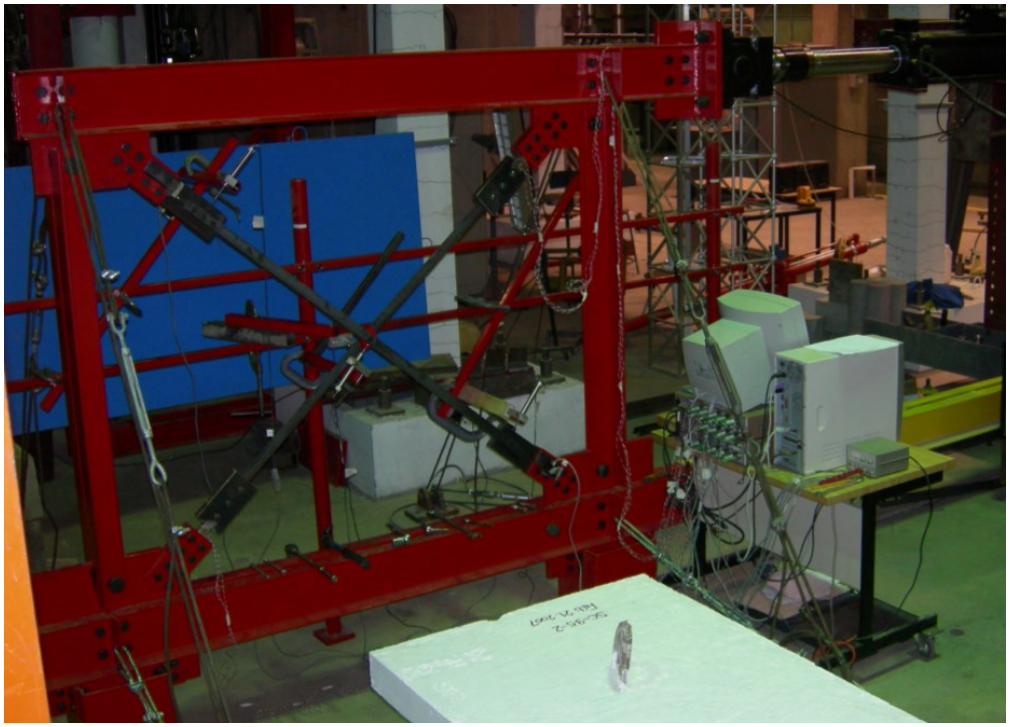

Figure 4-8: X-bracing test set-up [52]

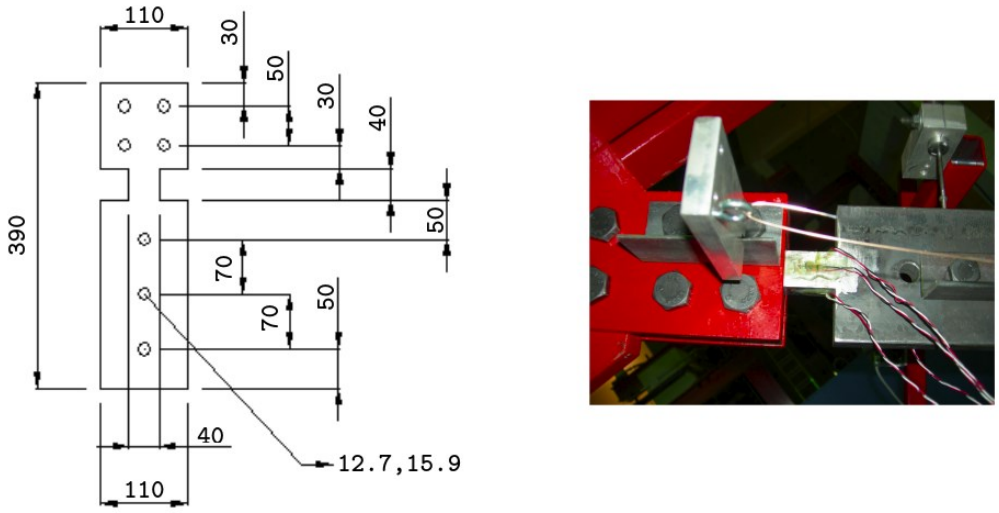

Figure 4-9: Geometry of the end plates and location of strain gauges (dimensions in millimeters) [52]

4.4.2. Test specimens

The X-bracing configuration involves two single angle sections under tension and compression. The target member is the angle under compression. Each angle is connected to the end plates using three bolts on one leg. The same leg is restrained in the middle of the member by a single bolt connected to the other bracing member which is under tension. A filler plate was provided to fit the space in between two angles in the middle and ensure that enough lateral support is present at the point of attachment (Figure 4-10). The two configurations were L38X38X3.2 and L44X44X3.2 angle sections. The repeatability of results was assessed by testing two specimens for both configurations. Table 4-5 lists the specimens and their properties based on tests conducted on coupons.

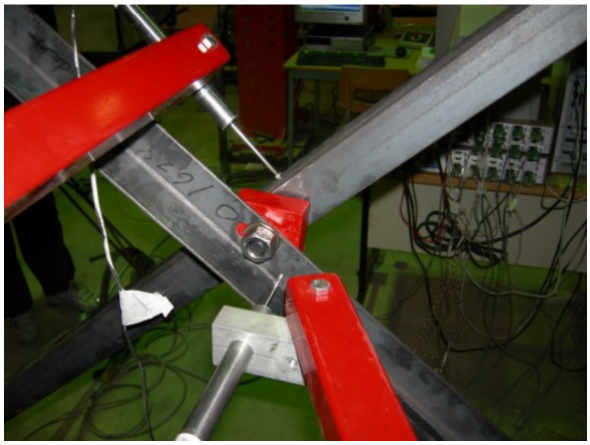

Figure 4-10: Lateral support of the angles in middle [52]

Table 4-5: Details of X-bracing test specimens

Test	Section	D(mm)	F_y (MPa)
1	L38X38X3.2	12.7	370
2	L38X38X3.2	12.7	392
3	L44X44X3.2	15.9	393
4	L44X44X3.2	15.9	393

Note: (D: Bolt diameter)

4.4.3. Finite element modelling of specimens

The four angle specimens of the previous section were modelled using Code_Aster software. Fiber beam elements are considered, and the optimum element size was evaluated to be 100 mm after conducting preliminary tests. To simplify the analysis, only the bracing angle members and end connection plates are included in the model. A preliminary deflection value of Length/1000 [60] at mid length of the braces is applied to the weak bending axis as global geometrical imperfection. It is assumed that the outside frame members are rigid in comparison to the angle members. Therefore, the end connection plates on top are supported by fixed supports with only unrestrained lateral displacement. The bottom supports are assumed to be fixed. The angle members are connected to these supports via two elements, first a rigid beam element to include the member eccentricity and second a non-linear spring to model the three-bolt connection behaviour. The properties of spring element considers the slippage and bolted connection behaviour based on formulas presented by Rex *et al*. [61]. To model the single bolt attaching the members at the middle of bracing system, it is assumed

that the middle nodes have identical displacement. However, the relative rotational displacement is released at this point.

The proposed method was applied to the analysis, firstly by calculation of σ_{cr} for each specimen which was done by Code_Aster (Figure 4-11). Since the boundary conditions of the members are not as mentioned in Section 4.2.1, equation (4-2) cannot be used and finite element modelling is implemented for this purpose. In the case of X-bracing tests, the angle member needed to be restrained at the middle to model the pinned connection. Since CUFSM could not apply this kind of restraint to the member, Code_Aster was used to perform the calculation. The bracing member under compression was modelled in Code_Aster using plate elements and mesh refinement was optimized using several trials. Each element had four corner nodes with six degrees of freedom and maximum element size was 4mm. Fixed boundary conditions were applied to the nodes located on one leg of the member on each end. To model the constraint in the middle of the brace member, a hinged support was applied to a node on the same supported leg (Figure 4-7). Then, the elastic buckling analysis was performed and σ_{cr} value was calculated for the brace member. This value was calculated for first local buckling mode shape.

The next step was to calculate the λ_p value for each specimen using equation (4-1). Table 4-6 summarizes the calculated σ_{cr} and λ_p values for each specimen. Then, the stress-strain curve is calculated using the two steps explained earlier: first equations (4-3) to (4-5) were used to calculate two points A and B on the curve given λ_p; second, parameters in equations (4-6) and (4-7) are calculated such that the stress-strain curve passes through these two points A and B. In the final step, the calculated curve is applied as material behaviour to the fiber elements of the members in compression. In this case the test was done under lateral force as a unidirectional push over load. So the compressional member was recognized from the beginning. In order to avoid penalizing the behaviour of tensional members, the modified material behaviour needs to be only applied to compressional members. In case of large structures which the behaviour of members can not be predicted from the beginning, it is advised to use special material behaviour of Code_Aster, which allows to define different stress-strain relation under tension and compression.

The non-linear analysis phase is done by Code_Aster and the assumptions of non-linear material and large displacements are included in the procedure.

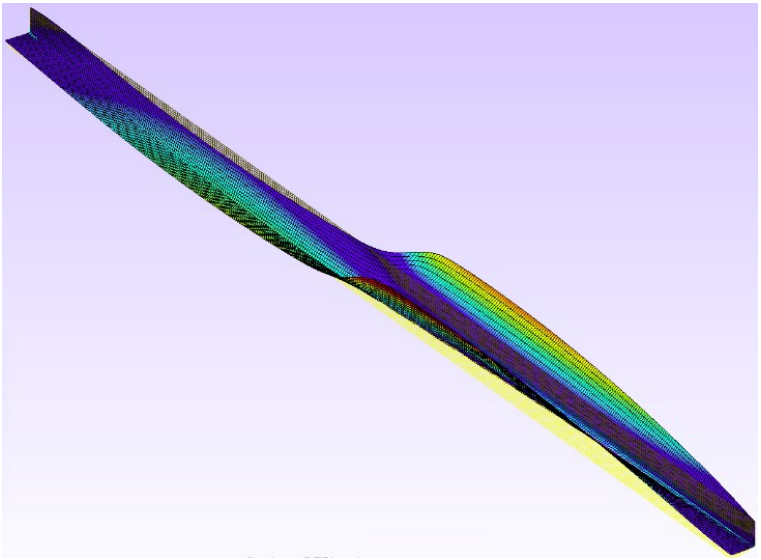

Figure 4-11: Local buckling mode of specimen (Test-3)

Table 4-6: Calculated σ_{cr} and λ_p values for test specimens

Test	σ_{cr} (MPa)	λ_p
1	295	1.11
2	295	1.15
3	234	1.29
4	234	1.29

4.4.4. Comparison of results and discussion

The experimental specimens failed due to local buckling phenomena, Figure 4-12 shows the final deflection for some of the test specimens. Figure 4-13 compares the failure stress of the experimental tests to the finite element models and member capacity based on ASCE 10-97 [32] and EC3 [3]. To clarify the effectiveness of the presented method, another set of analysis is performed without applying the proposed method to account for local buckling to the model. As it is obvious from the comparisons, neglecting the local buckling failure from the analysis, provides very high failure stresses. In the class-4 sections of this study, the local

buckling failure controls the member capacity. Even though the global buckling effect is included in the analysis due to large displacement option, it cannot take into account local failures which results in very high values of failure stress.

Table 4-7 reveals that the results of failure stress ($\sigma_{failure}$) for finite element model is much more accurate and consistent with the tests when the presented method is applied. The mean value of FEA to Test results is 1.02 when the modification of material behaviour is involved in the model. Despite the use of large displacement analysis, the above value increases dramatically to 1.54 if the effect of local buckling is ignored. This confirms that the procedure which is presented in this study offers an appropriate solution to model the local buckling behaviour of slender sections by beam elements.

Comparing the results of the presented method and design capacity of specimens based on ASCE 10-97 and EC3 shows that the method proposed yields results that are similar to the ASCE 10-97 and that are consistent (but less conservative) with EC3. The coefficient of variation (COV) is slightly less than for design codes. For test 4, the discrepancy between the finite element model and the experimental test reaches a maximum at 15 percent. This is also consistent with the maximum error obtained with ASCE 10-97. This error could be due in part to specific loading and boundary conditions used in the bracing tests which are not perfectly represented in the model and in the codes.

Figure 4-12: Local failure of test specimens (2 and 3) [52]

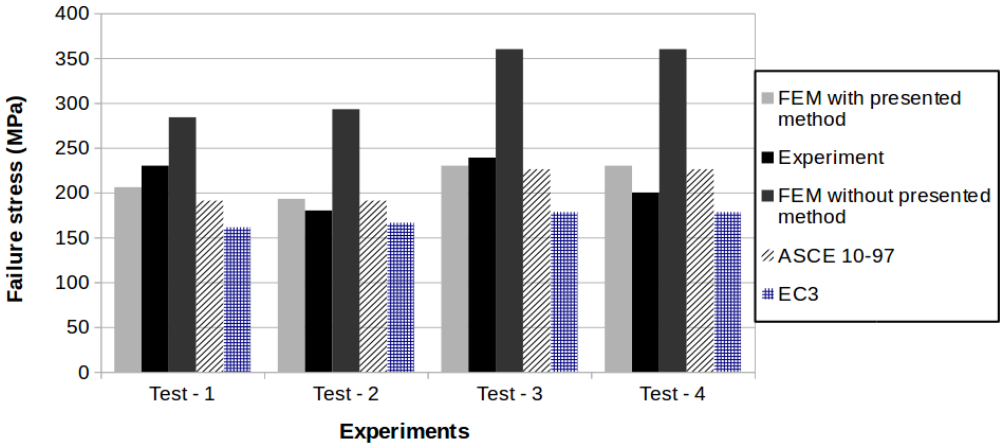

Figure 4-13: Comparison of failure stress results

Table 4-7: Accuracy of the analysis with and without including the presented method

Test	$\sigma_{failure}$ FEA (MPa)		$\sigma_{failure}$ test (MPa)	$\sigma_{capacity}$ ASCE (MPa)	$\sigma_{capacity}$ EC3 (MPa)	$\sigma_{failure}$ (FEA/test) ratio		ASCE/test	EC3/test
	w-lb	w/o-lb				w-lb	w/o-lb		
1	206	284	230	191	162	0.89	1.23	0.83	0.70
2	193	293	180	191	167	1.07	1.62	1.06	0.92
3	230	360	239	226	179	0.96	1.50	0.94	0.75
4	230	360	200	226	179	1.15	1.80	1.13	0.89
Average						1.02	1.54	0.99	0.82
COV (%)						11.00	15.4	13.2	13.3

Note: (w-lb: with local buckling, w/o-lb: without local buckling)

4.5. Conclusion

This article presented a new method to include the local buckling failure of class-4 members modelled by fiber beam finite elements. In order to take into account this phenomenon, the stress-strain material behaviour of the member was modified in the finite element model. A stress-strain curve formula was provided for each class-4 member based on the local buckling slenderness value (λ_p) of the member. Forty-two short angle specimens with λ_p values between 0.57 and 1.20 were tested first and the force-deflection behaviour of each specimen was recorded. Then the stress-strain behaviour was calculated for each of the λ_p

values of the tests. Based on the above stress-strain behaviours and curve fitting technique, a general formula was presented which relates the λ_p value to a specific stress-strain material behaviour.

In order to apply the method to a full-scale model, firstly the class-4 members are recognized and the related λ_p value is calculated. In the next step, the modified stress-strain curve is generated by the presented formula. Finally, the curve is assigned to the corresponding member as the material behaviour in the finite element software.

To evaluate the feasibility and accuracy of the method, it was implemented for four cross braced frame structures tested at Université de Sherbrooke. For the two configurations studied, class-4 angle sections were used as bracing members. The results were compared to two different fiber element models, with and without using the proposed method. It was observed that when considering the proposed method in the models, the mean ratio of model to test failure stress is 1.02, whereas this ratio increases to 1.54 when ignoring the method. Also, comparing the proposed method to design capacity calculated based on Eurocode and ASCE standards revealed that the new method provides more consistent results. Although the proposed method is not a practical design procedure, it may be considered to improve non-linear beam models of lattice towers that aim to complement and reduce the need for full-scale transmission tower tests.

The presented method to modify the material stress-strain behaviour is only valid for the interval of 0.57 to 1.20 of λ_p values. Future works are needed to expand this interval in order to cover more versatile class-4 sections such as un-equal leg angles. Also, the method was validated with only four bracing tests. Further investigations should be done to validate the proposed method on more complex structures and field-testing results.

4.6. Acknowledgments

The authors gratefully acknowledge the financial support from the National Sciences and Engineering Research Council of Canada (NSERC), RTE and Hydro-Québec.

CHAPTER 5 NON-LINEAR BEHAVIOUR OF CONNECTIONS

A simple method for a reliable modelling of the non-linear behaviour of bolted connections in steel lattice towers

Avant-propos

Auteurs et affiliation:

Farshad Pourshargh[a], Frederic P. Legeron[b,d], Sébastien Langlois[c], Kahina Sad Saoud[e]

[a]*PhD candidate at Université de Sherbrooke*

[b]*Eng., Ph.D. Formerly Professor, Civil Engineering Department, Université de Sherbrooke*

[c]*Eng., Ph.D. Associate professor, Civil Engineering Department, Université de Sherbrooke*

[d]*Present affiliation: Vice President, Parsons*

[e]*Civil Engineering Department, Université de Sherbrooke*

Submitted: Journal of Advanced Steel construction - December 2020

Published:

Titre: A simple method for a reliable modelling of the non-linear behaviour of bolted connections in steel lattice towers

Abstract

The behaviour of bolted connections in steel lattice transmission line towers affects their load-bearing capacity and failure mode. Bolted connections are commonly modelled as pinned or fixed joints, but their behaviour lies between these two extremes and evolves in a non-linear manner. Accordingly, an accurate finite element modelling of the structural response of complete steel lattice towers requires the consideration of various non-linear phenomena involved in bolted connexions, such as bolt slippage. In this study, a practical method is proposed for the modelling of the non-linear response of steel lattice tower connections involving one or multiple bolts. First, the local load-deformation behaviour of single-bolt lap connections is evaluated analytically depending on various geometric and material parameters and construction details. Then, the predicted non-linear behaviour for a given configuration serves as an input to a 2D/3D numerical model of the entire assembly of plates in which the bolted joints are represented as discrete elements. For comparison purposes, an extensive experimental study comprising forty-four tests were conducted on steel plates assembled with one or two bolts. This approach is also extended to simulate the behaviour of assemblies including four bolts and the obtained results are checked against experimental datasets from the literature. The obtained results show that the proposed method can predict accurately the response of a variety of multi-bolt connections. A potential application of the strategy developed in this paper could be in the numerical modelling of full-scale steel lattice towers, particularly for a reliable estimation of the displacements.

Keywords: Steel lattice tower, Non-linear behaviour, Bolted connection, Failure modes, Bolt slippage, Finite element modelling

5.1. Introduction

Steel lattice towers are widely used all over the world as transmission line supports. The structural integrity of such towers is a key factor in the reliability of a power transmission system. To minimize the risk of power supply disruptions that may occur because of tower failure, structural reliability of towers should be evaluated properly. In the standard simplified method of analysis and design, commonly used by tower engineers, lattice towers are idealized as linear trusses in which angle members are assumed to be connected to each other by frictionless joints acting as hinges. Moreover, the influence of end bending moments in members is generally ignored in simplified structural analyses, and leg members, which are supposed to be continuous, are assumed to be hinged in nodal points. Because of the simplifying assumptions used for design and analysis of lattice towers, it is a common practice among electric network operators to perform experimental tests on full-scale towers for the validation of new design concepts, which turns out to be a long and costly process.

Leg members in towers are connected via lap spliced bolted joints and the bracing members are usually connected to legs via single bolted joints to ensure a hinged connection. Assuming hinged joints does not represent their real behaviour and modelling bolted connections as rigid is also inadequate. In fact, an accurate numerical modelling of the behaviour of real joints is complex due to numerous interactions taking place locally.

The complex behaviour of bolted joints can be split into three categories: eccentricity, rotational stiffness and joint slippage. In practice, angle members in lattice towers are often loaded eccentrically, which causes a biaxial bending in addition to axial loads. The combined action of axial and bending forces may cause a plastic hinge in the cross-section and the bolted leg of the angle could undergo a local post-elastic deformation under the bearing force of bolts, causing displacement and rotation in the connection and shear lag in the member [5].

Additionally, most of the bolt holes are in practice slightly larger than the diameter of bolts, which makes joint slippage inevitable. The slippage may happen gradually or at a specific

level of loading and it depends on different parameters such as: structural loading, workmanship, the constitutive properties of the bolts and connections, nature and condition of the faying surfaces and bolt torqueing [19].

Because of the lack of experimental data and the complexity of describing the actual slippage phenomenon in a real structure, simplified models have to be used. For example, in a study by Kitipornchai *et al.* [20] the slippage is modeled as a random process. The authors concluded that joint behaviour does not have a significant influence on the ultimate strength of the structure, but it influences deflections. In a comparison of numerical predictions with experimental results, Jiang *et al.* [23] investigated the effect of joints on structural analysis model. The results of their study showed that to predict the tower sway displacement, joint behaviour must be considered. This will drastically increase the predicted tower deformation but will not affect its failure load, failure mode and sequence. To account for the joint stiffness, Kang *et al.* [19] found that the connection rigidity may have a considerable effect on the ultimate horizontal loading capacity of a lattice tower. The rigid connection increases the buckling capacity, thus the assumption on connection rigidity must be realistic. Otherwise, the buckling capacity of the structure may be over or underestimated. Knight and Santhakumar [22] concluded that neglecting the joint effects may be responsible for the premature failure in towers and must thus be considered in the analysis. The results of their study showed a good correlation with experiments when joint effects are considered.

Ungkurapinan et al [21] investigated the behaviour of various configurations of connections involving one to four bolts. Unfortunately, there is not a complete database of slippage parameters for angle member connections. Some limited numbers of tests are available on specific angle sections and bolt arrangements.

It is recognized that the tower connections are different from ordinary steel connections in other types of steel structures [23]**.** In lattice transmission towers, the members are mostly connected directly via their flange or through the gusset plates which provide a connection flexibility. In addition, the slippage effect should be included in the numerical model,

because lattice towers are constructed by bearing type connections instead of friction type ones.

The general objective of this article is to propose a simple method to predict the complex behaviour of bolted connections in steel lattice towers. The procedure detailed in this paper comprises two main aspects. First, the non-linear load-deformation behaviour of single-bolt connections is characterized based on their geometric/material properties and some construction details. This characterization includes the identification of the pre-slip, slip and post-slip regions of the behaviour. Then, the calculated behaviour is applied to finite element models of bolted assemblies, where the connections are represented using non-linear spring elements. The finite element method can involve multiple bolts with various arrangements. The accuracy of developed method is verified by conducting experimental tests on plate assemblies including single-bolt and two-bolt configurations. The prediction method is also compared to datasets from experimental tests performed on four-bolt connections provided by Cai and Driver [54] as well as a detailed three-dimensional finite element modelling of two-bolt connections considering multiple interactions between the assembled plates and the bolts.

The proposed method is intended to be easily implemented for a wide range of joint configurations and may find broader application in the context of numerical modelling of complete lattice towers with the aim of evaluating precisely their complex structural behaviour.

This article starts by presenting the approach developed for the representation of the behaviour of multi-bolt connections. Then, the experimental program investigating the response of different plate assemblies involving one or two bolts is briefly described. Finally, various configurations involving single and multiple bolts are examined and the obtained numerical results are compared with reference results.

5.2. Modelling and prediction of the non-linear behaviour of bolted connections

In the present study, a non-linear discrete element is employed to model the bolted connections. The paper particularly investigates the effect of varying the following geometric parameters: the plate thickness t_p, the plate width W, the bolt diameter D, the end distance of plate (distance from the center of the hole to plate edge) L_e, and the number of bolts n (the configurations analysed are summarized in Table 5-1 and Table 5-2). The non-linear spring element should also be able to include the deflection due to slippage of connection and the near-field behaviour of plate in the vicinity of the bolt. The local behaviour of single-bolt connections, from loading to failure, is first predicted analytically as described subsequently. Then, the predicted load-deformation law is applied to numerically model the non-linear response of plate assemblies using non-linear spring elements. Code_Aster, an open-source finite element software package developed by "Electricité de France" (EDF), is used in this research. Code_Aster has a powerful non-linear spring element that can model the connection behaviour. The methodology is to first predict the behaviour of single-bolt connection using equations available in the literature based on its properties and considering the near-field behaviour. At the second step, a series of specimens is tested in laboratory to validate the prediction model. The third step proposes a method to categorize multi-bolt connections and predict their behaviour based on one bolt predicted model. This step is done with the help of a finite element plate model. At the next step, the method is evaluated by conducting experiments on several two-bolt joints. In the final step, predictions are compared to experimental results of four-bolt connection tests which have been reported by a research at the University of Alberta, Canada [54].

Table 5-1: Properties of four-bolt specimens [54]

Section	D (mm)	W (mm)	t_p (mm)	L_e (mm)	*Fy* (MPa)	*Fu* (MPa)
A1G1	19	305.4	7.48	28.30	439	519
A2G1	19	305.4	7.52	29.27	439	519
A7G1	19	304.0	7.43	28.55	411	494
A5E1	19	248.5	7.55	31.00	343	487
A11E1	19	249.9	7.30	28.27	376	500
A8G2	19	304.5	7.44	27.08	411	494
A3R1	19	310.0	6.30	28.15	379	472
A9R1	19	311.6	6.54	27.56	369	478
A6E2	19	248.0	7.51	47.73	343	487
A12E2	19	249.5	7.34	44.00	376	500

Table 5-2: Properties of one-bolt test specimens

Configuration	D (mm)	W (mm)	t_p (mm)	L_e (mm)	F_y (MPa)	F_u (Mpa)	Failure Scenario
S1	16	152	9.50	40.0	396	555	B
S2	16	127	9.50	40.0	404	529	B
S3	16	127	7.90	40.0	417	560	B
S4	19	152	9.50	47.5	396	555	B
S5	19	127	9.50	47.5	404	529	B
S6	19	127	7.90	47.5	417	560	B
S7	16	152	9.50	24.0	396	555	C+S
S8	16	127	9.50	24.0	404	529	C+S
S9	16	89	6.35	24.0	370	578	C+S
S10	19	152	12.70	28.5	383	520	C+S
S11	19	127	7.90	28.5	417	560	C+S
S12	19	89	6.35	28.5	370	578	C+S

Note: (B: Bearing failure, C+S: Cleavage and End shear failure)

5.2.1. Prediction method for one-bolt connections

Figure 5-1 illustrates the typical force-displacement relationship of a bolted connection under uniaxial tensile load. This graph may be divided into two main regions: pre-contact and post-contact. The pre-contact region is characterized by a frictional load transfer followed by a significant bolt slippage and ends at the contact point defining the threshold value for establishing contact between the bolt and the plate. Beyond the contact point begins the post-contact region, in which the load is mainly transferred by bearing up to the failure of the joint.

To characterize the local response of a bolted connection, the values of the load at which bolt slippage occurs P_{slip}, the peak load $P_{failure}$, the elastic displacement reached before the onset of slippage $D_{preslip}$, the displacement at the end of the pre-contact region D_{slip} and the ultimate displacement $D_{failure}$ should first be determined based on the geometric and material properties of the connection and some construction details.

Once evaluated, the parameters defining the curve depicted in Figure 5-1 will be used in a two-dimensional finite element model, where the bolted joints are represented using spring elements, to deeply investigate the global response of assemblies. This may be done by assigning these values to the discrete elements through the non-linear behaviour law ASSE_CORN implemented in Code_Aster.

To determine the limit values associated with the pre-contact region, it is proposed to use equations developed by Rex and Easterling [62] to predict the slip behaviour of a single bolt bearing on a plate. They proposed the value of 0.193 mm for $D_{preslip}$ based on various experiments performed on a single plate assembled using one bolt. D_{slip} directly depends on the bolt hole clearance. Normally, the bolt holes are drilled larger than the diameter of bolts to satisfy the requirements in terms of erection tolerance. For example, common industry practices consider the value of 1.6 mm as a standard hole clearance in North American steel construction. Unless otherwise specified, the values of $D_{preslip}$ and D_{slip} in this work will be taken as 0.193 mm and 1.6 mm respectively.

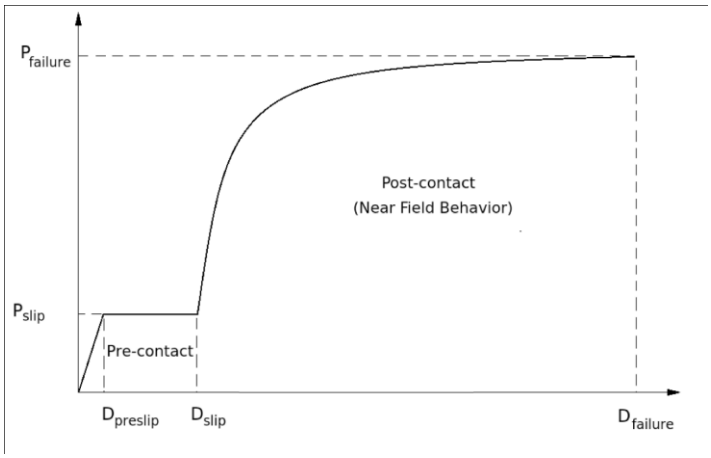

Figure 5-1: Behaviour of connection under axial load

The value P_{slip} is here calculated using the method of AISC code [63] as follows:

$$P_{slip} = K_s \times m \times n \times T_i \tag{5-1}$$

Where:

$$T_i = \frac{Bolt\ Torque}{C \times D} \tag{5-2}$$

And m = number of slip surfaces (two for the cases handled in this paper), n = number of bolts (one bolt in this case); K_s = slip coefficient (for a typical steel surface, K_s is taken as 0.33); C = nut factor (0.2, as given by [64]); and D = bolt diameter.

The amount of bolt torque in equation (2) is taken as 100 N-m, in accordance with the experimental tests carried out in this study.

For the post-contact region, the following empirical equation proposed by Rex and Easterling [61] will be used to predict the behaviour of a single-bolt connection [following equations use units of mm and kN]:

$$\frac{R}{R_n} = \frac{1.74 \times \bar{\Delta}}{(1+(\bar{\Delta})^{0.5})^2} - 0.009 \times \bar{\Delta} \tag{5-3}$$

in which, R is the plate load, and R_n the plate nominal strength which may be evaluated as follows:

$$R_n = D \times t_p \times F_b \tag{5-4}$$

And $\bar{\Delta}$ is the nominal deformation which is defined in Eq. (5-5).

In Eq. (5-4), the bearing/tear-out strength of the plate F_b is defined by the following relationship:

$$\bar{\Delta} = \frac{\Delta \times \beta \times K_i}{R_n} \tag{5-5}$$

$$F_b = F_u \times \frac{L_e}{D} \leq 2.4 \times F_u \tag{5-6}$$

$$K_i = \frac{1}{\frac{1}{K_{br}} + \frac{1}{K_b} + \frac{1}{K_v}} \tag{5-7}$$

$$K_{br} = 120 \times t_p \times F_y \times (D/25.4) \tag{5-8}$$

$$K_b = 32 \times E \times t_p \times (L_e/D - 1/2)^3 \tag{5-9}$$

$$K_v = 6.67 \times G \times t_p \times (L_e/D - 1/2) \tag{5-10}$$

In Eq. (5-5), Δ stands for the hole elongation and β denotes the steel correction factor, which is taken as 1.0 for typical structural steel. Equation (5-7) evaluates the initial stiffness of the connection K_i, from the bearing stiffness K_{br}, the bending stiffness K_b, and the shearing stiffness K_v. In this analysis, the modulus of elasticity E and the shear modulus G of steel are taken equal to 210,000 MPa and 80,000 MPa, respectively.

5.2.2. Prediction method for multi-bolt connections

The main contribution of this research is to predict the behaviour of multi-bolt connections based on the near field behaviour of one bolt. None of the literature reviewed considered the

prediction of full behaviour for the connections. In this section, the behaviour of multi-bolt connections is predicted. The behaviour of one-bolt joint is applied to a finite element model through a non-linear spring element. The properties of the spring elements are determined according to the method discussed in the previous section.

The finite element model is built using quadrilateral shell elements named "DKT" in Code_Aster. Each element has four nodes with six degrees of freedom and a bi-linear behaviour law is considered for the inelastic material. To avoid considering the near field behaviour twice, a rectangular portion of the plate is removed from the front side of the bolt. The length and width of this portion is equal to diameter of the bolt hole. The mesh size is adjusted considering geometrical complexity of the model, especially around holes. Mesh refinement is applied where needed based on a preliminary mesh size sensitivity analysis and the mesh size varies between 4 mm and 10 mm. Figure 5-2 compares the results obtained for a connection involving two bolts based on three mesh trials. In this case, since the non-linearity is mostly due to the spring elements, mesh size and density does not have a noticeable effect on the behaviour. The central nodes of bolts are represented as fixed support and a uniformly distributed tensile load is applied on the right side of the model. In reality, the near field zone is connected continuously to the surrounding area on the plate. To capture this, a rectangular cut out is created which provides extra nodes from the finite element model to connect the spring and avoid stress concentration. The rectangular shape also makes the mesh more structured. To illustrate this point, an example of a two-bolt connection is shown in Figure 5-3.

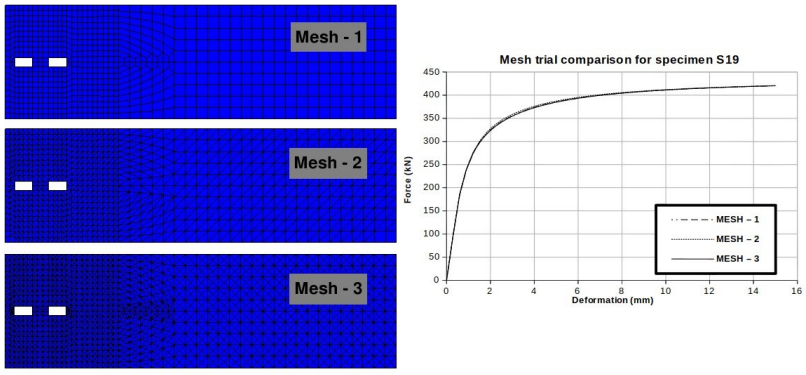

Figure 5-2: Comparison of different mesh refinement and sizes

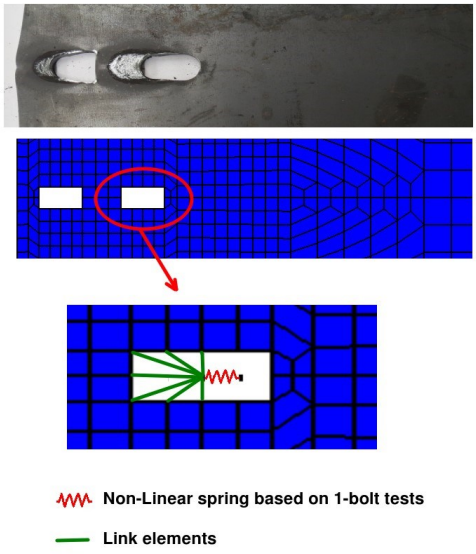

Figure 5-3: 2D modelling of a two-bolt connection using a plate and spring elements

The model is also able to consider different types of bolts with different diameters in the same connection. The near field behaviour of one bolt can be predicted first and then it will be assigned to non-linear spring elements, in any location on the plate. The efficiency of the proposed method is evaluated in section 5.4.3 by comparing to the tests on 4 two-bolt connection configurations.

The method proposed in this study is also verified by predicting the response of 10 four-bolt specimens which have been tested by Cai and Driver [54]. The researchers have used I-sections with bolt holes in the web, and the sections were loaded in tension to determine the capacity of connection. Figure 5-4 shows one of the specimens and the geometry of model which is proposed for the prediction. As one can notice, the four-bolt configuration presented in Figure 5-4 is not representative of lattice towers' typical connections. The main purpose here is to take advantage of the experimental results reported in the article by Cai and Driver [54] in order to evaluate the reliability of the method proposed in this paper. Three-dimensional shell elements of Code_Aster were used to mesh the model due to the complex geometry of the analysed samples. Each element has nine nodes with six degrees of freedom per node. The central node of bolts is modeled as a fixed support and a uniformly distributed tensile load is applied to the nodes located at the free end of the I-sections. The size of the near field zone in this case is equal to edge distance of the bolt hole. In this case, the spring

is connected to the sides of the zone since the end distance was too small to provide adequate support at the end of the rectangular holes (see Figure 5-4).

The prediction method and procedure for these specimens is the same as two-bolt specimens. First, the near field behaviour of one bolt is calculated using equations 1 to 3. Then the behaviour is applied to the four-bolt model through the non-linear spring elements. Properties of the specimens analysed are presented in Table 5-1 and Figure 5-5.

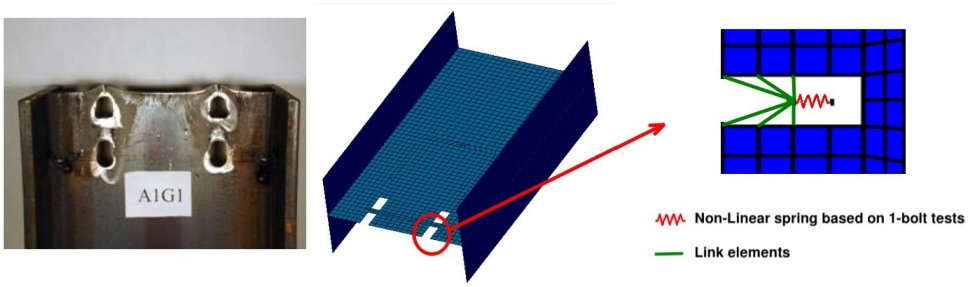

Figure 5-4: FE modelling of a connection involving four bolts

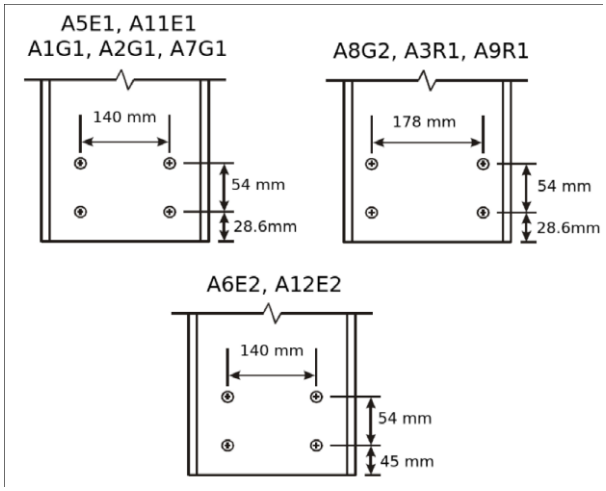

Figure 5-5: Configuration of four-bolt specimens [54]

5.3. Experimental program

This section reports the experimental investigations carried out on double lap connections. These tests will serve for the validation of the method developed in this paper for the prediction of the complex behaviour of multi-bolt connections.

5.3.1. Specimens

In this research, bolted plate specimens were tested under uniaxial tensile loading. The experimental program consists of twelve one-bolt and four two-bolt configurations. To ensure the quality and the reproducibility of the results, each configuration was tested twice. Figure 5-6 summarizes the dimensions and configurations of test specimens.

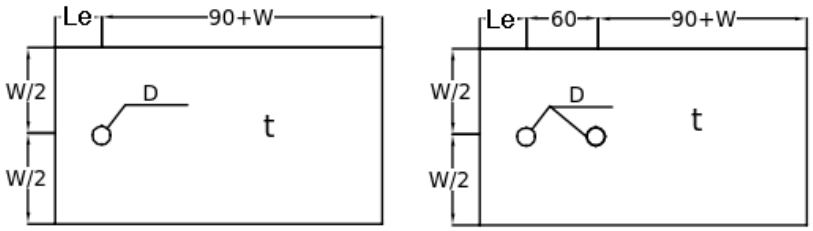

Figure 5-6: Configuration of the tested specimens

The one-bolt specimens were used to validate the analytical modelling method proposed in this article. A uniaxial load was applied to all of the specimens. The main variables are plate thickness, plate width, bolt diameter and end distance. The specimens were designed to fail under three different failure modes: (i) bearing; (ii) cleavage and (iii) end bearing [63]. The complete description of one-bolt specimens is provided in Table 5-2. Second group of specimens were designed to evaluate the prediction method for two bolts. These specimens were designed in a way that the near field behaviour of bolts is already predicted from the previous one-bolt tests. The objective is to define a prediction method for connections with more bolts based on near field behaviour of one bolt. The properties for this group of tests are provided in Table 5-3.

Table 5-3: Two-bolt test specimens

Configuration	Corresponding one-bolt configuration	D (mm)	W (mm)	t_p (mm)	L_e (mm)	F_y (MPa)	F_u (MPa)	Failure Scenario
S19	S1	16	200	9.5	40.0	387	516	B
S20	S3	16	200	7.9	40.0	452	482	B
S21	S4	19	250	9.5	47.5	374	521	B
S22	S6	19	250	7.9	47.5	390	465	B

Note: (B: Bearing failure)

5.3.2. Test set-up

The specimens were tested in a tension jig. To prevent the prying action of plates, the setup was prepared so as to apply only a uniaxial force on the specimens, without eccentricity or bending moments. Figure 5-7 and Figure 5-8 show the layout of experimental setup.

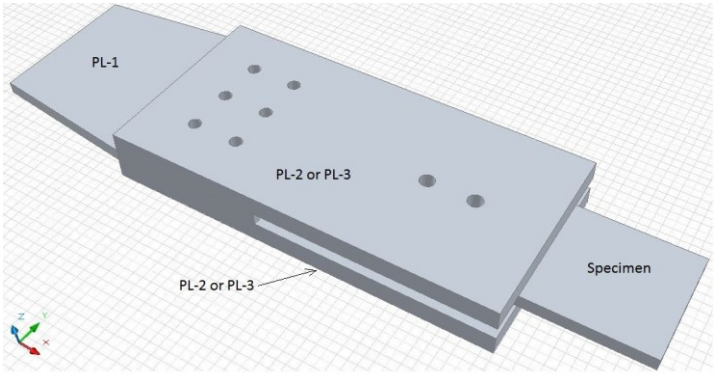

Figure 5-7: Layout of experimental set-up

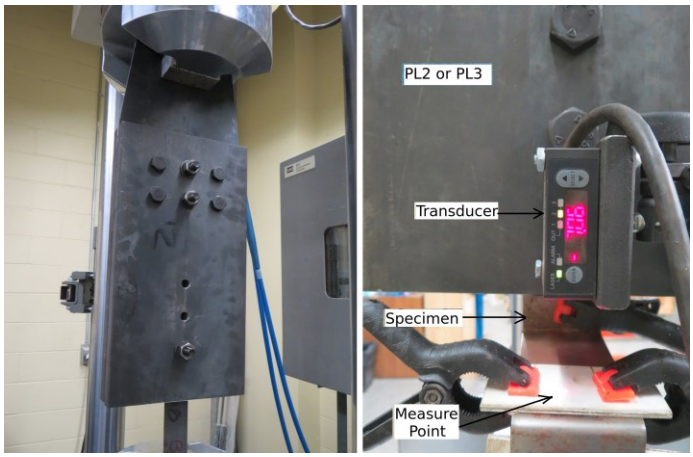

Figure 5-8: Final setup and transducer location

Plates PL-2 and PL-3 were used in all the test cases, but PL-1 was changed according to the thickness of each specimens. The thickness of plates PL-2 and PL-3 is 25mm and they are connected to PL-1 by six M16 bolts. The dimensions of the plates are 500 mm for length and 250mm for width. Each bolt was tensioned manually to a torque of 100 N-m to match common practice in the transmission line industry. To acquire accurate torque, a calibrated torque wrench was used. All the surfaces are normal bare steel without any preparation.

To measure the deformation of specimens, a high accuracy laser displacement transducer was used. The transducer rested on PL-2 or PL3 and the probe mounted on the specimen by using a small aluminium angle. Therefore, the relative deformation between the specimen and the connection plates was measured accurately. Figure 5-3 shows the set-up and location of displacement transducer.

An MTS hydraulic testing machine was used to apply tension to specimens. The capacity of the machine is 500 kN. The loading was displacement controlled with a loading rate of 1mm/min. The maximum value of displacement that was provided by the machine was set equal to the bolt diameter, although most of the specimens failed before this value was reached.

5.3.3. Material property tests

Two tension coupons were cut and prepared from each batch of steel material and tested according to ASTM A370-02 standard [57] standard. The values of yield strength F_y and ultimate tensile strength F_u of steel obtained from tensile coupon tests were used in the prediction method. These values are indicated in Table 5-1 and Table 5-2.

5.4. Results and discussion

5.4.1. Analysis of configurations involving one bolt

Figure 5-9a and Figure 5-9b depict the force-displacement curves of twelve one-bolt specimens (S1 to S12). These figures show that the proposed method can predict the full behaviour of the connections with high accuracy compared to the results obtained from the experimental tests. The predicted curve is also able to consider slip behaviour during the loading phase and the trend of the curve is similar to the behaviour of specimens. As shown in Figure 5-3, the specimens in this study were tested using a vertical test setup and the effect of gravity minimized the gap between the bolt and the contact surface of the hole. So in this case, to have a more realistic evaluation of the force-deflection relationship, the value of 1.6 mm gap is not introduced to the prediction method. As a result, the slippage behaviour is not significant in the predictions. The pre-tensioning force in the bolts also causes the slippage to happen gradually.

In Figure 5-9a and Figure 5-9b, the predicted curves are stopped at a displacement equals to bolt diameter because the method does not provide an estimate for final displacement. Even though the objective of this research is to predict the complete behaviour of connection, it is clear that the method can provide the values of ultimate capacity with a significant accuracy. Table 5-4 presents a comparison for the ultimate capacity between the prediction method and the experimental tests. The ratio of prediction to test capacity is on average 0.98. The following symbols are used in the tables, P_{ut} (ultimate capacity of test specimens), D_{ft} (final deflection of test specimens), P_{upr} (ultimate capacity predicted by the method). It is clear from Figure 5-9b, that while the maximum load is well captured for all failure modes tested

(B or C+S), the ultimate displacement is not captured accurately by the method for mode C+S.

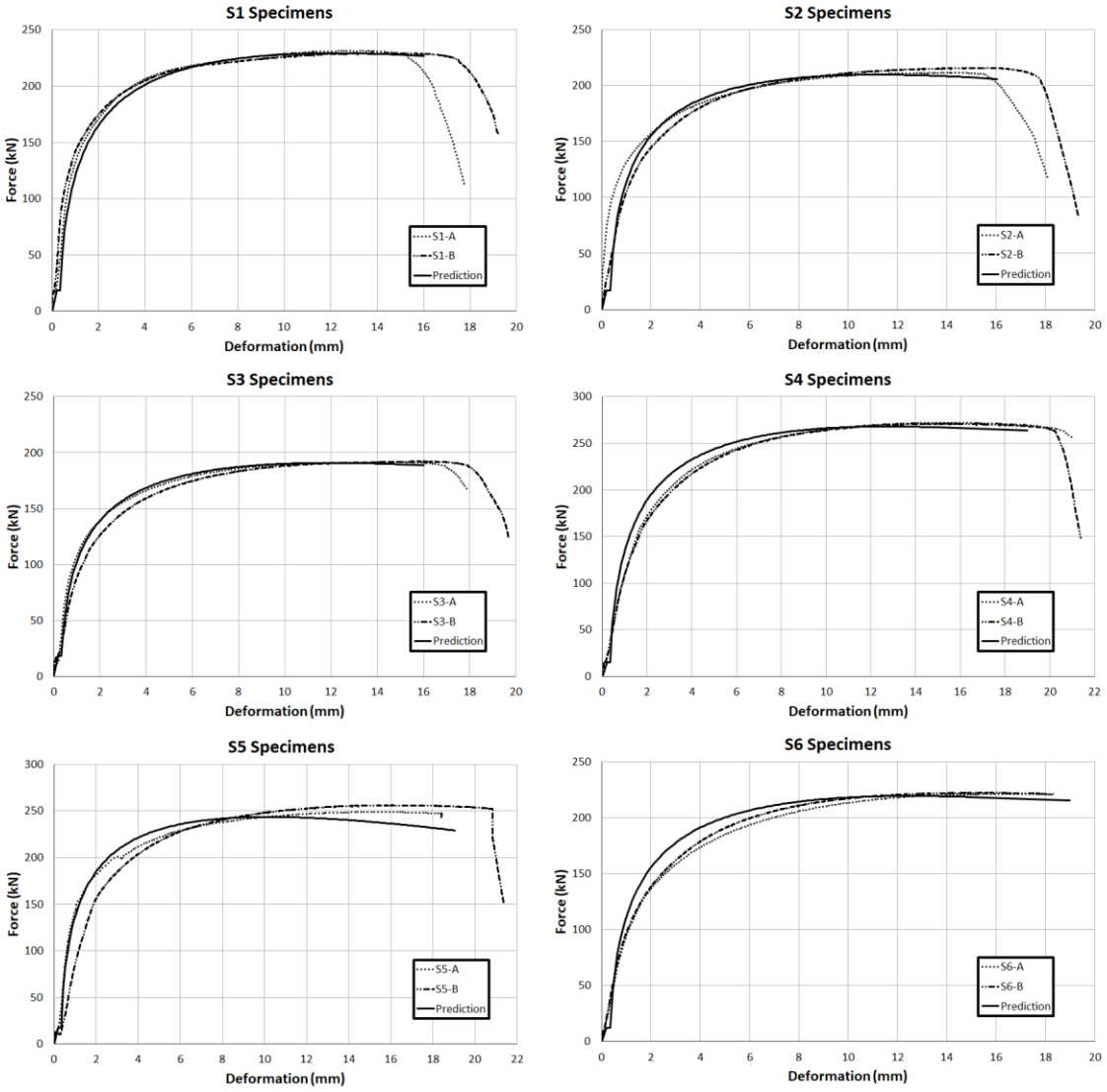

Figure 5-9a: Comparison of prediction and experimental behaviour of single-bolt connections

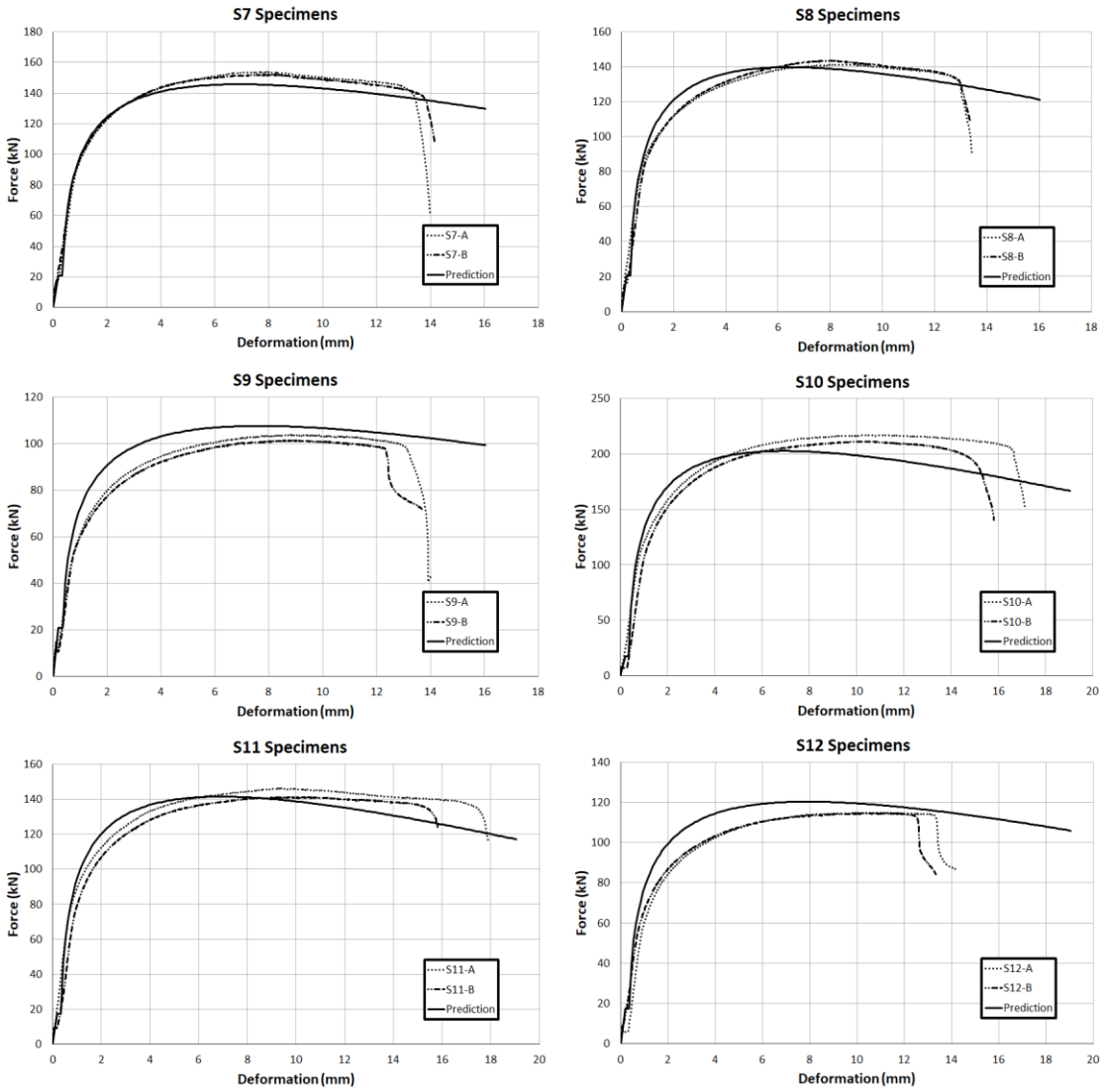

Figure 5-9b: Comparison of prediction and experimental behaviour of single-bolt connections

Table 5-4: Comparison of predicted and experimental ultimate capacity for one-bolt specimens

Specimen	P_{ut} (kN)	D_{ft} (mm)	P_{upr} (kN)	P_{upr}/P_{ut}
S1	230	16	219	0.95
S2	214	16	209	0.98
S3	192	17	188	0.98
S4	272	18	255	0.94
S5	253	18	244	0.97
S6	222	18	217	0.98
S7	153	13	146	0.95
S8	142	12	140	0.98
S9	103	12	107	1.04
S10	214	15	203	0.94
S11	144	15	142	0.99
S12	115	12	120	1.05
Average				0.98
COV (%)				3.6

COV: Coefficient of variation

5.4.2. Analysis of configurations involving two bolts

The method proposed for the prediction of the behaviour of connections with two bolts is derived using a finite element model. As described previously, the near field behaviour of each bolt was assigned to the model by means of a non-linear spring and the remaining parts of the specimen were modelled by shell elements. The prediction of specimen S19 has been performed based on the predicted near field behaviour of S1, which has the same bolt diameter, plate thickness, plate width and end distance. Similarly, the specimens S20, S21 and S22 have been predicted based on S3, S4 and S6 predictions, respectively.

In addition, a detailed 3D numerical modelling of the analysed two-bolt samples is performed in this case using three-dimensional solid finite elements. Figure 5-10 shows the geometry and mesh of the model. The numerical model is developed using Code_Aster and the adopted mesh scheme is constituted of 8-node isoparametric brick elements. To diminish the computational costs, each component of the connections is meshed individually with a fine mesh around the contact area and a coarse mesh elsewhere. In this formulation, the principle of virtual work is expressed in the current configuration accounting for finite strains. The inelastic behaviour of the structural steel composing the plates is approximated

by a multi-linear stress-strain relationship derived from the tensile coupon tests carried out on the analysed specimens (S19 to S22). In the absence of relevant details on the material behaviour of the high-strength bolts, they are modelled using a bi-linear elastoplastic constitutive law characterised by the modulus of elasticity E=200 GPa, Poisson's ratio ν=0.3, yield strength F_y=800 MPa, and the tangent modulus H=1 MPa. Finally, the von Mises yield criterion in conjunction with a linear isotropic hardening rule is adopted herein to simulate the plastic behaviour of the steel.

Plate PL-1 shown in Figure 5-7 is not represented in this modelling as it does not produce any direct effect on the behaviour of the connection. In accordance with the experimental tests, the uniaxial tensile loading is applied as an imposed displacement, while the surfaces of plates PL-2 and PL-3 are fully clamped in the side opposite to the loaded surface. The different parts constituting each connection are assembled using two bolts and the contact/friction behaviour, between plates PL-2/PL-3 and the bolts' head/washer, the three plates and the bolts' shank, and at interfaces between the central plate and plates PL-2/PL-3, is treated using the augmented Lagrangian method.

Figure 5-11 illustrates the comparison of the axial load-displacement results for the tests conducted on specimens with two bolts (S19 to S22). The numerical and experimental deformed configurations of the specimen S20, for instance, are shown in Figure 5-12. From Figure 5-12 it may be observed that the proposed method (Figure 5-12b) is in line with the experimental (Figure 5-12c) and the numerical (Figure 5-12a) deformed shapes.

As shown in Figure 5-11, good agreement is generally obtained between the developed method (using shell elements) and the experimental tests.

For specimen S21, the final displacement measured experimentally is smaller than the expected value. Since the operational capacity of testing machine was about 450 kN, this test was terminated to avoid damage to the machine. Also, one of the experimental tests performed on specimen S21 provided unreliable output due to misalignment of transducer. Therefore, only one experimental load-displacement curve is presented for this

configuration. By contrast, the numerical results obtained using 3D solid elements are somewhat different from the experimental ones.

Despite its simplicity, the proposed method thus appears to be computationally more efficient than a detailed numerical modelling using three-dimensional solid elements. Finally, Table 5-5 summarizes the ultimate capacity obtained with the proposed method. Average difference of connection capacity between the prediction method and experimental results is 2 percent.

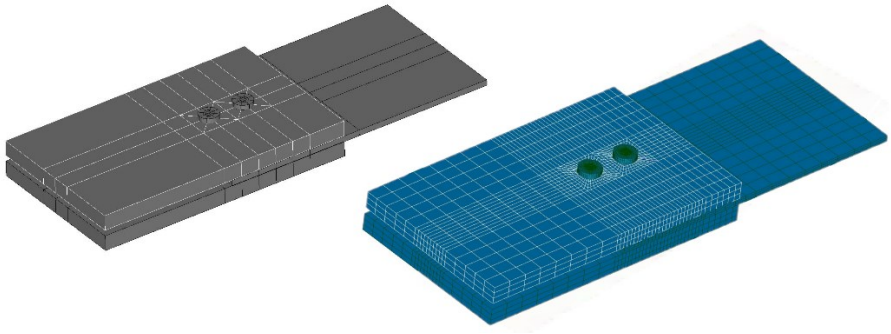

Figure 5-10: Numerical model of the two-bolt tests using 3D solid elements

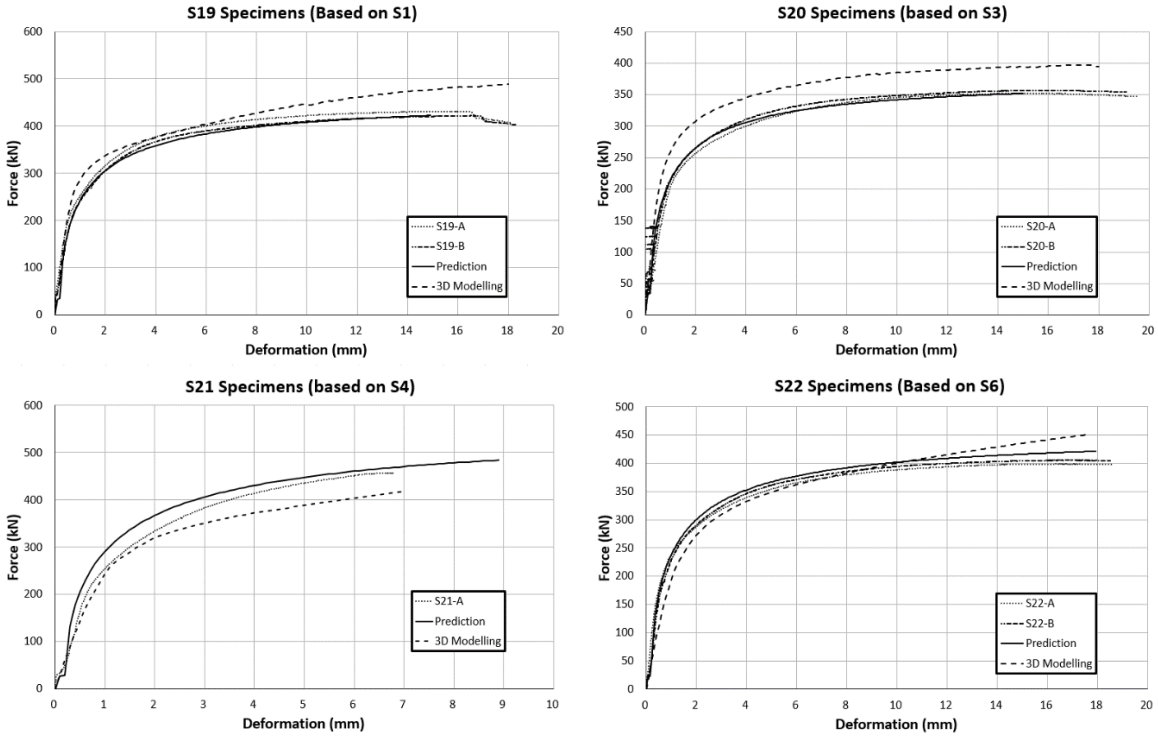

Figure 5-11: Comparison of two-bolt connections

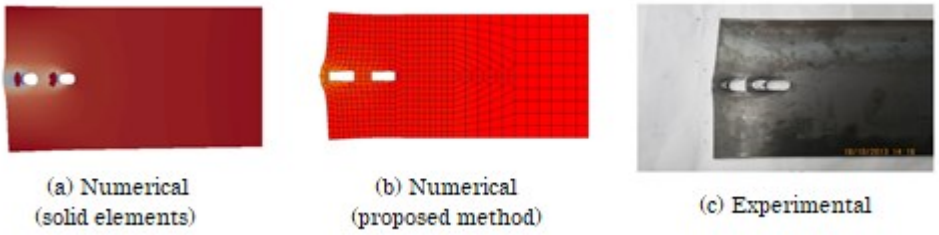

Figure 5-12: Deformed configuration of a two-bolt connection (specimen S20)

Table 5-5: Comparison of predicted and experimental ultimate capacity for two-bolt specimens

Specimen	P_{ut} (kN)	D_{ft} (mm)	P_{upr} (kN)	P_{u_3D} (kN)	$\frac{P_{upr}}{P_{ut}}$
S19	427	17	420	486	0.98
S20	354	19	363	397	1.03
S21	450	6.79*	475	417	1.06
S22	402	19	420	451	1.04
Average					1.02
COV (%)					3.31

P_{ut}: ultimate capacity of test specimens
D_{ft}: final deflection of test specimens
P_{upr}: ultimate capacity predicted by the method
P_{u_3D}: ultimate capacity of FE model using 3D solid elements
COV: Coefficient of Variation
* This specimen did not reach complete failure due to capacity of testing machine

5.4.3. Analysis of configurations involving four bolts

Figure 5-13 compares the predictions of four-bolt specimens with the tests results of the study from Cai and Driver [54]. Table 5-6 summarizes the results for the ten specimens considered in this study. Since the size of bolt hole for each specimen was not mentioned in their report, the amount of D_{slip} parameter is considered approximately to fit the experimental results. This set of tests also shows that the method can predict the behaviour of multi-bolt connections with acceptable accuracy. As it is observed from Table 5-6, the prediction method underestimates the ultimate capacity by 12 percent on average. The slippage behaviour of specimen A8G2 is obvious for both test and predicted results.

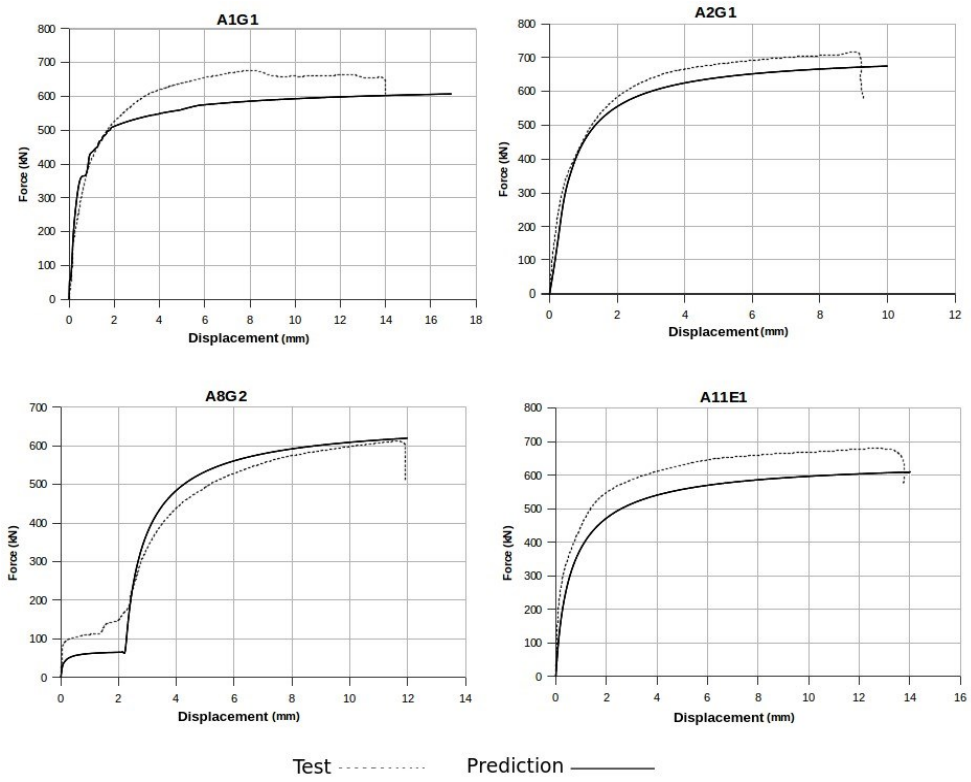

Figure 5-13: Comparison of four-bolt Specimens

Table 5-6: Comparison of predicted and experimental ultimate capacity for four-bolt specimens

Specimen	P_{ut} (kN)	D_{ft} (mm)	P_{upr} (kN)	$\frac{P_{upr}}{P_{ut}}$
A1G1	691	14	610	0.88
A2G1	724	9	675	0.93
A7G1	665	16	645	0.97
A5E1	698	9	600	0.86
A11E1	691	14	600	0.87
A8G2	622	12	611	0.98
A3R1	634	11	475	0.75
A9R1	633	16	500	0.79
A6E2	776	7	680	0.88
A12E2	793	16	715	0.90
Average				0.88
COV (%)				8.15

P_{ut}: ultimate capacity of test specimens
D_{ft}: final deflection of test specimens
P_{upr}: ultimate capacity predicted by the method
COV: Coefficient of Variation

5.4.4. Potential application of the proposed method in modelling of a steel lattice tower

Once the non-linear behaviour of multi-bolt connections is predicted using the method described in sections 5.4.2 and 5.4.3, one may take advantage of these results to accurately analyse the structural behaviour of lattice structures. Depending on the software used, this can be done by introducing the full curve of the connection's behaviour or, as it is done in Code_Aster, by introducing the key parameters defining the curves, as described in sections 5.4.2 and 5.4.3. The proposed method allows to obtain the properties for a unique spring element that captures the overall non-linear behaviour of a given multi-bolted connection. This spring can easily be implemented at the end of a beam element in a complete lattice tower model.

The parameters to be evaluated are P_{slip}, $P_{failure}$, D_{slip} and $D_{failure}$, and should be assigned to each spring element. Let us recall that the parameters $P_{failure}$ and $D_{failure}$ are the maximum capacity of the connection and the corresponding displacement, respectively. The values of P_{slip} and D_{slip} depend on the amount of slippage in the connections. If there is substantial and obvious slippage in the predicted behaviour, these values can be extracted directly from the curve. Otherwise, these values are assumed to be zero which means that near field behaviour initiates from the beginning and there is no slippage. Table 5-7 and Table 5-8 indicate the mentioned parameters to calibrate non-linear springs for two-bolt and four-bolt connections of this study.

Table 5-7: Parameters to calibrate the non-linear spring (two-bolt)

Specimen	P_{slip} (kN)	D_{slip} (mm)	$P_{failure}$ (kN)	$D_{failure}$ (mm)
S19	0	0	420	15
S20	0	0	363	15
S21	0	0	475	9
S22	0	0	420	19

Table 5-8: Parameters to calibrate the non-linear spring (four-bolt)

Specimen	P_{slip} (kN)	D_{slip} (mm)	$P_{failure}$ (kN)	$D_{failure}$ (mm)
A1G1	0	0	610	17
A2G1	0	0	675	10
A7G1	65	2.1	645	16
A5E1	0	0	600	9
A11E1	0	0	600	14
A8G2	66	2.2	611	12
A3R1	0	0	475	12
A9R1	0	0	500	15
A6E2	0	0	680	8
A12E2	0	0	715	15

5.5. Concluding remarks

This article presents a method to predict the full force-deformation behaviour of multi-bolt connections under uniaxial tension. The method is based on adding the near field behaviour of each bolt through a non-linear spring element in the finite element model of the connection. Several experimental tests on single-bolt connections were conducted and the results showed that their behaviour can be evaluated with existing theoretical and empirical relations. The near field behaviour is then applied as a non-linear spring to the finite element model of various connections. Next, the results for the finite element model were compared to experimental tests performed on two-bolt connections and to existing four-bolt tests. The method accurately predicted the full behaviour of one-, two- and four-bolt connections with different configurations and properties. It also allowed to match closely the ultimate capacity of the connection.

The proposed method allows to predict the full force-displacement curve of multi-bolt connections using a finite element model and starting from the geometry and mechanical properties of each individual bolt. This force-displacement curve for the multi-bolt connection can be used to calibrate a non-linear spring that will reproduce the connection behaviour in a large-scale tower model. For future work, more experimental tests with different bolt numbers and arrangements should be conducted. Also, tests on models should be performed to study the rotational behaviour of steel angle connections. Moreover, this study focused on bearing and end-shear failure. For the net section failure, another approach

needs to be developed. It is also recommended that the predictions of the present study be applied to a finite element model of a complex lattice tower and compared to full scale experimental tests.

CHAPTER 6 APPLICATION OF THE PROPOSED METHOD

In this chapter we implement the method proposed in chapter 5 for the modelling of joint behaviour in the numerical model of a lattice tower section and compare the predictions of the proposed strategy with experimental results of a reduced-scale tower section tested by Loignon [55] and described briefly in section 6.3

6.1. Numerical analysis method

The angle members of the reduced-scale tower are modeled using 1D fibre beam elements. These elements are defined in Code_Aster using POU_D_TGM element type. Based on a preliminary mesh refinement and convergence study, each member of the test section is meshed by using 15 elements. The mesh of the fibre sections is defined in a way that there are four equally sized square elements in the thickness of the section and same element dimension is used for the rest of the section. This type of element can model both non-linear geometry and material behaviours in the numerical model. Each fibre beam element is defined using two nodes with seven degrees of freedom, three for translation, three for rotations and one for warping effect.

Due to down-scaling of the tower geometry and sections, the local buckling slenderness ratio of the elements is small, therefore the local buckling method described in chapter 4 of this study is not implemented for this model.

A bilinear material behaviour is defined for the analysis. The material properties of the angle sections used for the model were determined from coupon tests and are listed in Table 6-1, where, E is the modulus of elasticity, Fy is the yielding stress and E_t is the tangent modulus.

Table 6-1: Material properties of the angle sections [65]

Section	Fy (MPa)	E (MPa)	E_t (MPa)
L12.7x12.7x3.18	462.4	193753	923.1
L19.1x19.1x3.18	396.1	204153	1154.8
L25.4x25.4x3.18	390.3	206600	1242.7

The analysis is performed considering both material and geometrical non-linear behaviour for the structure. In order to capture full non-linear behaviour of the structure, the system is solved using a Newton-Raphson method. The load pattern which led to the failure of experimental section, is applied incrementally to a fictive center node on top face of the numerical model; Fx = -8770 N, My = -7570 N-m and Fz = -4244 N, where Fx is the force in x direction, My is moment around y axis and Fz is the force in z direction (Figure 6-3). This fictive node is connected to the top of the leg members of section using rigid links. The numerical model is supported at the bottom of leg members using a fully fixed boundary condition for all of the translational and rotational degrees of freedom.

The failure mode of the test section was buckling of the main leg. The STAT_NON_LINE operator of Code_Aster is implemented for non-linear analysis. In the first time steps, the loading is applied based on a classical force-controlled approach and static incremental analysis. At the final load steps, the structure experiences an instability, so the algorithm of load application is switched manually to an arc-length method (Pilotage in Code_Aster) to capture more details such as snap-through or snap-back buckling and effectively analyzing post-buckling capacities [66].

6.2. Behaviour of the bolted connections

Three aspects of connection behaviour need to be considered in the analytical model. Connection eccentricity, rotational rigidity and axial behaviour containing slippage.

The angle sections for braces are connected through one flange to the leg members which causes eccentricity of forces applied to the connection. To consider the eccentricity in connection nodes, rigid link elements are used. These elements are modeled between the center of gravity of the brace section and the point of attachment to the leg member. More details are provided by Gravel [65] about the modelling technique to include connection eccentricities in the model.

Discrete linear spring elements (two nodes and six degrees of freedom per nodes) are used to define moment-rotation and force-displacement behaviour of the connection. One node of the discrete element is connected to the main leg member and the other node is connected to the end of the brace element. The translational stiffnesses KY, KZ are assigned high values to obtain a rigid behaviour. The out-of-plane rotation and torsional stiffness values (KRZ, KRX) are defined based on a detailed 3D finite element analysis including contact and solid elements [65]. The values of stiffness used in the numerical model are listed in Table 6-2. The axial non-linear behaviour of the bolted connection including the slippage is modelled according to the graph shown in Figure 5-4 using the ASSE_CORN relationship available in Code_Aster. The parameters defining the axial behaviour were determined using the method described in Chapter 5 and are summarized in Table 6-3 for this particular connection configuration. Figure 6-1 depicts the geometric properties of the end connection which is used. The in-plane rotational behaviour (KRY) of the brace members has a very small stiffness in that case because only one bolt per connection is used. Nonetheless, a non-linear force-displacement relationship was assigned using the ASSE_CORN relationship to follow the assumptions stated by Gravel [65].

Table 6-2: Stiffness values to define the discrete elements [65]

Degree of freedom	value
KX	Variable stiffness
KY	10E+10 (N/m)
KZ	10E+10 (N/m)
KRX	9.07E+03 (N-m/rad)
KRY	Variable stiffness
KRZ	1.80E+04 (N-m/rad)

One of the main values in the connection model is the estimation of the gap between the bolt and the bolt hole. Because of several conditions related to experiments and reality such as erection tolerances, human error, misalignment of parts, etc., this value is always very difficult to determine. Practically, bolt holes in towers industry are fabricated with a tolerance of *2mm* more than the nominal diameter of the bolt shaft. Therefore, *0.4mm* is the most realistic value for this reduced scale section test considering the bolt hole diameters and section shapes used. Although other values are also considered in the numerical model to evaluate the effect of slippage due to higher bolt clearance values.

In order to better understand the effect of this value on the model results and comparison with the results of the experimental tests, four different values have been assumed for the slippage parameter as *0.4, 0.6, 0.8* and *1 mm*.

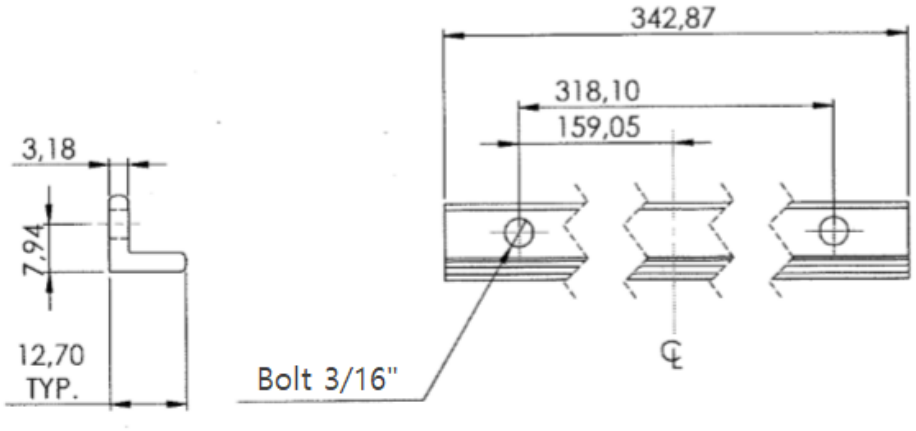

Figure 6-1: Dimensions used to predict the connection behaviour (units in mm)

Table 6-3: Parameters defining the non-linear behaviour law of the bolted connections

P_slip	3900 N
P_failure	18105 N
D_slip	0.4, 0.6, 0.8, 1.0 mm
D_failure	4.76 mm

6.3. Reduced-scale tower section test

A reduced-scale section of a tower has been constructed and tested based on the design of the H2 tower type used by RTE (Réseau de Transport d'Électricité – France). The real height of the structure is *32 m,* but the reduced-scale model has been down scaled to *8 m* due to limitations of laboratory (maximum height *12 m*). The sections also are scaled down to approximately 25% of its dimensions to be consistent with the structure. Figure 6-2 demonstrates the full tower specimen as it is constructed. The description of these tests is reported by Loignon *et. al.* [55]. For the purpose of this study a section of the structure is tested with height of *1.76 m* as shown in Figure 6-2.

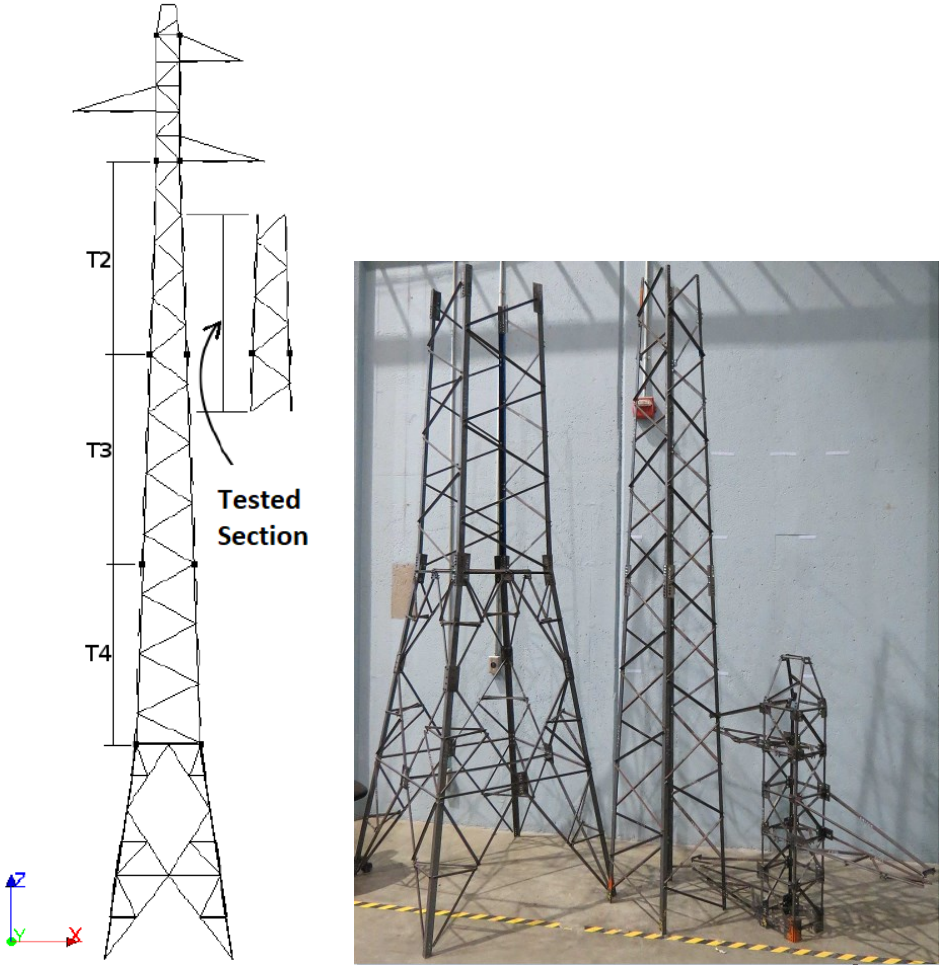

Figure 6-2: Reduced-scale test pylon [55]

The tower analyzed in this chapter was constructed from angle sections, using reduced scale cross sections. However, the design follows the geometrical philosophy of a real tower. For example, the leg members are constructed using larger sections than braces. Table 6-4 presents the full-scale and reduced tower angles. The sections selected are all equal legs angles. Due to constructability issues the scale factor of 1:4 was not respected fully for the experimental work. The thickness of the angle sections used is 3.18 mm, and bolt diameter is 4.725 mm. Figure 6-3 and Figure 6-4 present the drawings and details of the structure.

Table 6-4: Full-scale and reduced tower angles

Real scale	Reduced scale
L45x45x4.5	L12.7x12.7x3.18
L50x50x5	L12.7x12.7x3.18
L60x60x6	L12.7x12.7x3.18
L70x70x7	L19.1x19.1x3.18
L80x80x8	L25.4x25.4x3.18

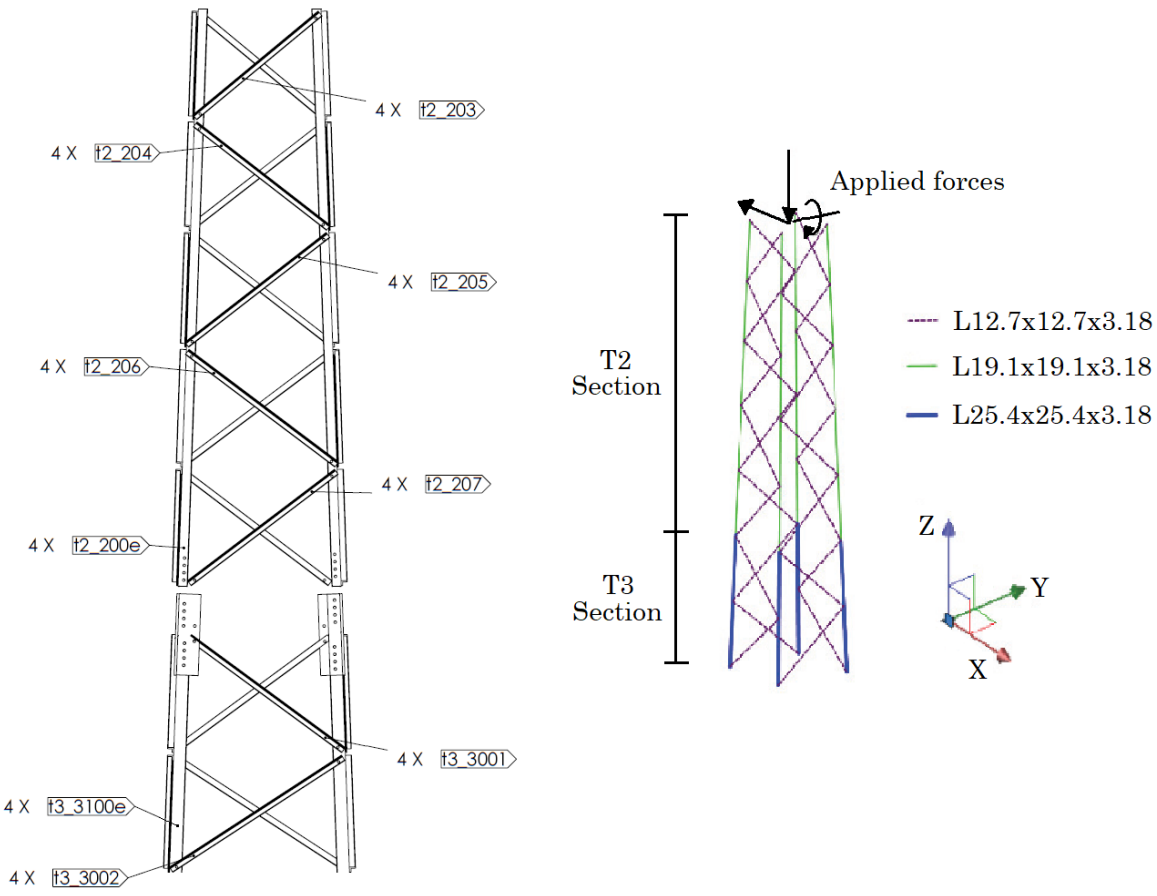

Figure 6-3: Details of the tested structure [55]

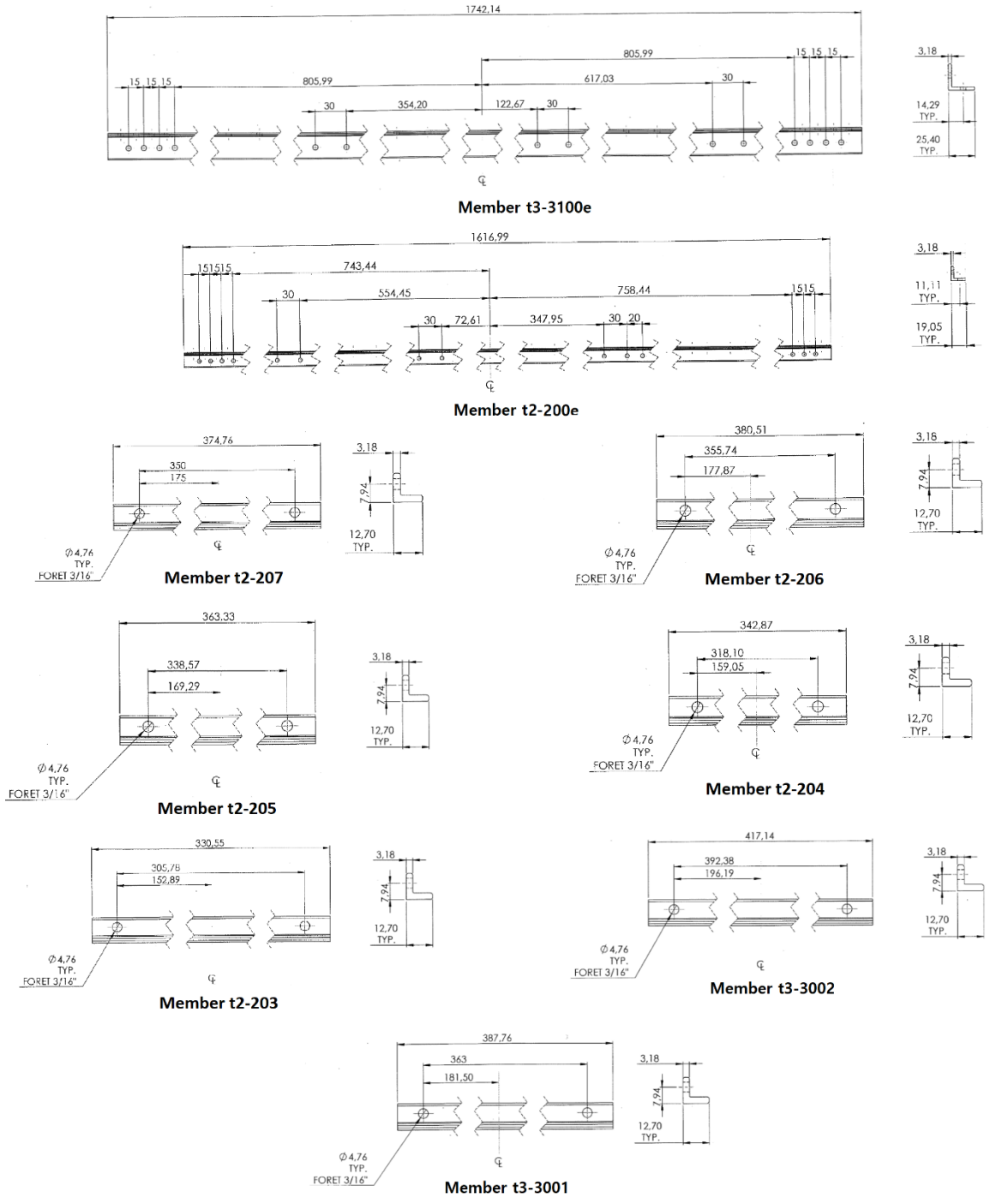

Figure 6-4: Details of the tested structure (units mm) [55]

6.4. Test procedure and instruments

The tested section of the tower measures *1.76* m in height, representing 22% of the total height of the entire reduced-scale tower. Figure 6-5 shows the studied tower section, which is made of a part of section T2 and a part of section T3 (Figure 6-3). To ensure the continuity of the section as it is in a full-scale tower, the legs are connected rigidly to the test base plate using welds. Full details of the procedure and instruments are report by Loignon *et. al.* [55].

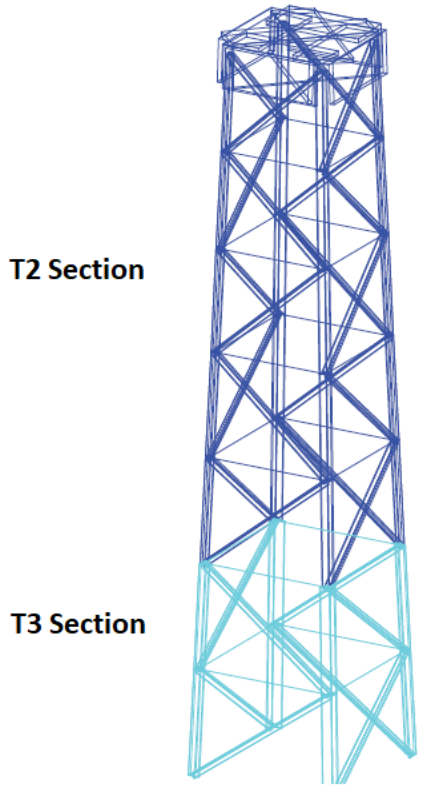

Figure 6-5: Tower section [55]

The test is repeated two times for this tower section. The forces are applied to the test section using a displacement-control method. Displacements are induced to the top of the specimen using a rigid transfer beam and three degrees of freedom. Hydraulic jacks were connected to the transfer beam to apply displacements and rotations to the top of the section (Figure 6-6). The displacements are increased gradually up to failure of the specimens. For both cases, the section failed because of global buckling of legs as illustrated in Figure 6-7.

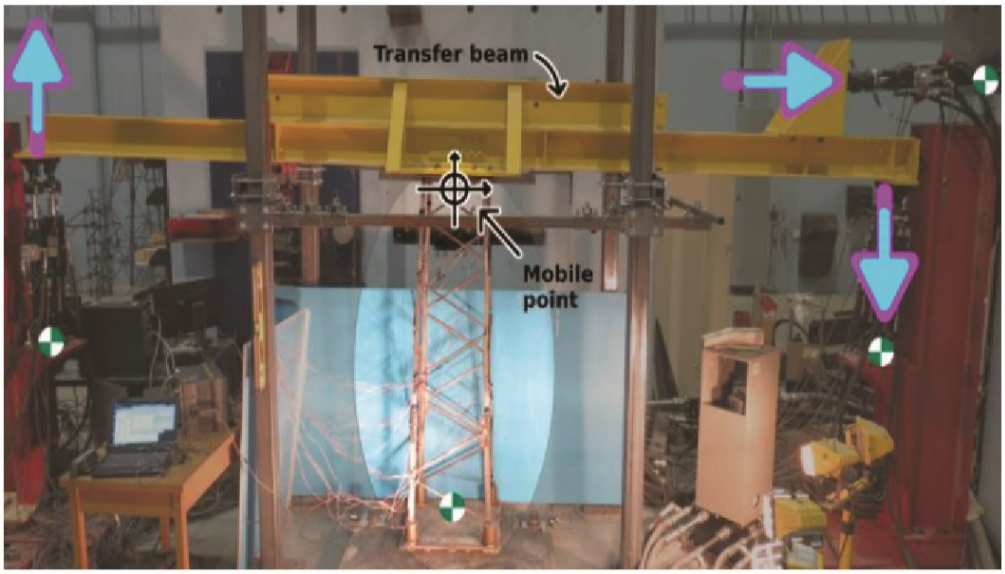

Figure 6-6: Transfer Beam to apply the forces [55]

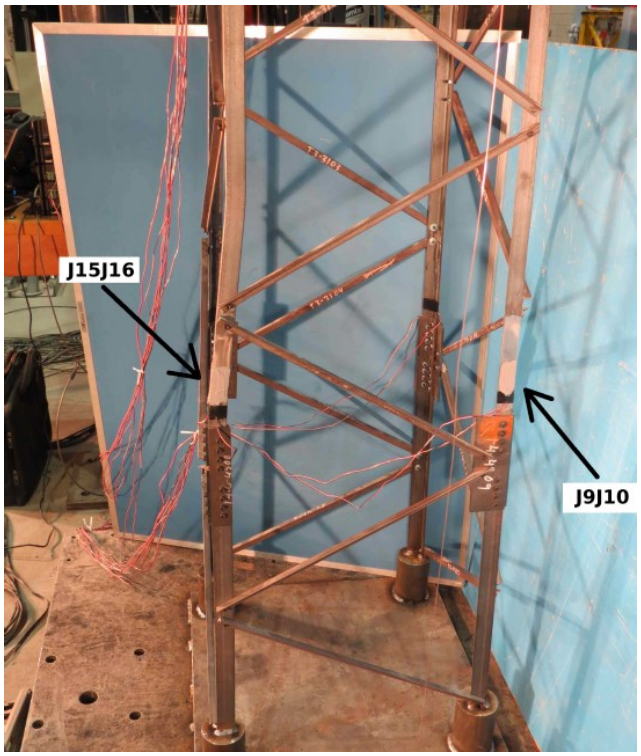

Figure 6-7: Failure of the structure due to buckling of legs [55]

6.5. Results comparison

In this section, the results of predicted force-displacement behaviour of the structure is compared to experimental results. Figure 6-8 compares the results of the experimental tests to predicted behaviour based on FE analysis. The full force-displacement behaviour of the section is presented. To emphasize the accuracy of predictions using the presented method, the behaviour of the model is also presented in the graph without considering the connection behaviour. In addition to general trend of the Force-Displacement behaviour, one can also compare the values related to instances of slippage and failure of the specimens. For example, around the horizontal force of 2.7 kN, both experimental and numerical models show a momentary higher displacement because of slippage while the force value is not increasing. This phenomenon is more obvious for the numerical models with higher slippage values.

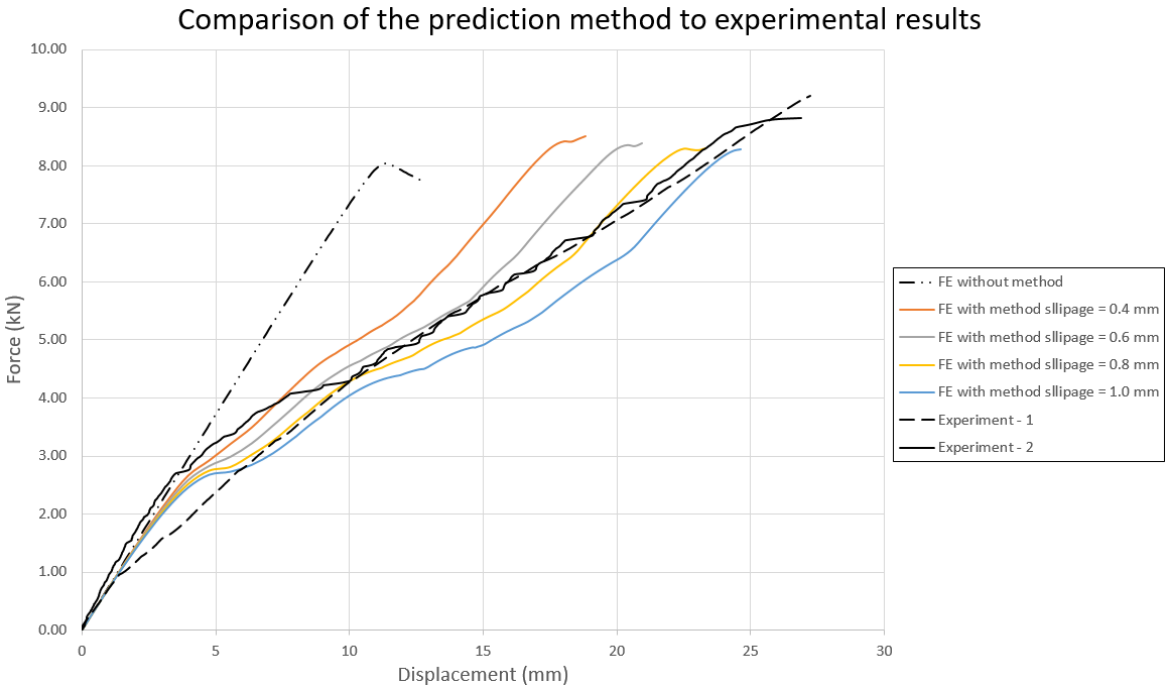

Figure 6-8: Comparison between the results of the experimental tests to predicted behaviour based on FE analysis

As it can be noticed from the results presented in Figure 6-8, the proposed method provides an acceptable accuracy comparing to experiments. While the behaviour without considering the connection behaviour provides smaller displacements, the prediction based on the method has clearly a higher accuracy.

The predicted displacement without considering the non-linear behaviour of connections is *12 mm* which is approximately half of the experimental value and is in line with findings of researchers such as Marjerrison [6] and Peterson [67]. The model shows very small displacement since the slippage and local deformations of the connection are not considered if the bolt slippage method is not applied.

The prediction based on the proposed method using four values of slippage shows a more realistic behaviour for the deformation of the structure compared to the calculations considering the linear behaviour of connections. Application of slippage values of *0.8* and *1.0 mm* provides higher deflections of the structure which aligns to the experimental results. However, it should be noted that a bolt slippage of 0.8 or 1.0 *mm* provides the most accurate results, whereas the expected value of slippage is actually lower. The additional displacement observed in the experimental tests could be due to other gaps, not considered in the model: at the attachment points of the section in the test bench and at the spliced connections on leg members. Overall, the proposed method is able to predict the trend of the force-displacement behaviour observed in the experimental results.

The numerical models failed due to buckling of main leg as shown in Figure 6-7 and Figure 6-9. It has been observed that the connection behaviour and slippage values do not affect the failure mode of the structure in this case. On the other hand, the consideration of the non-linear behaviour of connections does cause a small variation of the maximum failure load observed in the model as shown in Table 6-5. This table also shows the maximum load values obtained experimentally, which are averagely 6% higher than the loading obtained with 0.4 mm of slippage. In addition, the numerical model without using the method provides a difference of 11% for the value of maximum load.

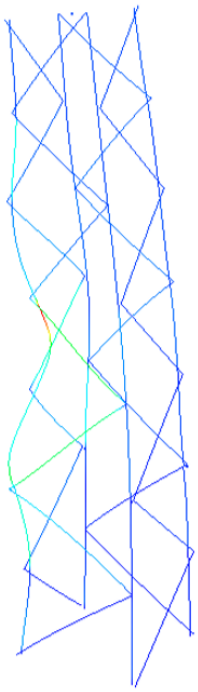

Figure 6-9: Failure mode of FE model due to main leg buckling

Table 6-5: Failure force for each case

Test case	Failure force (kN)
FE without method	8.02
FE with method slippage = 0.4	8.50
FE with method slippage = 0.6	8.38
FE with method slippage = 0.8	8.32
FE with method slippage = 1.0	8.29
Experiment - 1	9.16
Experiment - 2	8.77

CHAPTER 7 CONCLUSIONS AND FUTURE WORK

7.1. Summary and conclusions

The main objective of this work is to define a strategy to consider the local buckling of angles and non-linear behaviour of connections in a numerical model. A more accurate numerical model can provide an alternative for expensive and time-consuming full-scale tower tests. In addition to the accuracy, the numerical model needs to be also feasible in terms of modelling effort and analysis time. To achieve this, in this work fibre beam elements are implemented for modelling the tower members. The main issue of using beam elements is the lack of the ability to include the local buckling behaviour. In this study a new method is presented to address this shortcoming. The connection behaviour is also another aspect of tower modelling which affects the behaviour of the structure mainly in terms of displacements. Another simple method is also provided to predict the full Force-Displacement behaviour of the connections including slippage due to axial force.

Both of the aforementioned methods are verified using experimental tests on individual connections and angle members to ensure the accuracy of predictions. The methods are also applied to numerical models of x-braces and tower sections to study their effectiveness on a test structure.

Three major contributions were made by this research work. First, it investigated the feasibility of using a new method to take into account the local buckling failure of class-4 members modeled using fiber beam finite elements. Second, it proposed a method to predict the full force-deformation behaviour of multi-bolted connections under axial tension. Third, the connection behaviour predicted using the method described in this research was applied

to a reduced-scale tower section to verify the application of the method and compare it to experimental results.

To take into account the local buckling failure of class-4 members modeled using fiber beam finite elements. The stress-strain behaviour of the member's material was modified in the finite element model. A stress-strain curve formula was provided for each class-4 member based on its local buckling slenderness value (λ_p). In this regard, forty-two short angle specimens with λ_p values ranging from 0.57 to 1.20 were tested to measure their force-deflection behaviour. Subsequently, for each of the λ_p values, a stress-strain behaviour was calculated. Using the calculated stress-strain behaviours and curve fitting technique, a general formula relating the λ_p value to a specific stress-strain material behaviour was introduced.

In order to apply the method to a full-scale model, the class-4 members are identified and the related λ_p value is estimated. Subsequently, the presented formula is used to generate the modified stress-strain curve. This modified stress-strain curve is, then, assigned as the material behaviour of corresponding member in the finite element software.

To evaluate the feasibility and accuracy of the proposed method, it was applied to four cross braced frame structures tested at the University of Sherbrooke. Class-4 angle sections were used as bracing members for the two investigated configurations. The members had a low global slenderness value, therefore failure mode were assumed to be due local buckling phenomena. Two different fiber element models, with and without using the proposed method, were developed and the predictions were compared with experimental results. The comparisons confirm that implementing the proposed method in the finite element models, the mean ratio of model to test failure stress improved from 1.54 (without the proposed method) to 1.02. It was also found that the new method provides more consistent results in term of design capacity calculated based on Eurocode and ASCE standards.

The proposed method for connection behaviour is established by adding the near field behaviour of each bolt using a non-linear spring element in the finite element model of the

connection. Several experimental tests were performed on one-bolt connections and the results confirmed that their behaviour can be calculated using existing theoretical and empirical relations. The near field behaviour is then applied as a non-linear spring to the finite element model of different connections. Thereafter, the results for the finite element model were compared with experimental tests performed on two-bolt connections and to available four-bolt tests. It was shown that the proposed method can accurately predict the full behaviour of one-, two- and four-bolt connections having different configurations and properties. This method also allows to match the ultimate capacity of the connection. The proposed method allows predicting the full force-displacement curve of multi-bolt connections using a finite element model considering the geometry and mechanical properties of each individual bolt. This force-displacement curve can be utilized to calibrate a non-linear spring which will reproduce the connection behaviour in a large-scale tower model.

The main conclusions of this research are:

- Fibre beam elements can be used to model towers as long as local buckling and connection behavior is accounted for.
- It was observed that using the proposed method for local buckling, improves the mean ratio of model to test failure stress from 1.54 to 1.02.
- The proposed method for local buckling is not a practical design procedure, although it may be considered to improve non-linear beam models of lattice towers that aim to complement and reduce the need for full-scale transmission tower tests.
- The proposed method for axial connection behaviour allows to predict the full force-displacement curve of multi-bolt connections using a finite element model.
- The force-displacement curve for the multi-bolt connection can be used to calibrate a non-linear spring that will reproduce the axial connection behaviour in a large-scale tower model.
- Using the axial connection behaviour model presented in this research, the general trend of the Force-Displacement behaviour of a tower section can be predicted more accurately.

- The overall displacement of the tower due to slippage is predicted using this method with an acceptable accuracy comparing to experimental results.
- The predicted value of maximum failure load for the test section using the proposed method is 6% different than the experimental results. This value becomes 11% without using the method in the numerical model.

7.2. Limitations of this research

Although the proposed method may not be a practical design procedure, it may be considered to improve non-linear beam models of lattice towers that aim to complement and reduce the need for full-scale transmission tower tests. Moreover, the presented method to modify the material stress-strain behaviour is only valid for the interval of 0.57 to 1.20 of λ_p values. Thus, the validity of presented method should be checked for λ_p values outside this range.

Comparing the analysis and test results there are still some differences and gaps between the results. In this study a constant value of geometrical imperfection is considered since the real imperfections were not measured for the specimens. Meanwhile, the other cause can be due to existence of residual stresses which were not considered in this research.

7.3. Recommendations for future work

Despite the contribution made by this research, future works are needed to cover more versatile class-4 sections such as un-equal leg angles. Moreover, the proposed finite element method was validated with only four bracing tests. Further research should be directed to confirm the proposed method on more complex structures and field-testing results.

In addition, more experimental tests with different bolt numbers and arrangements should be conducted to validate the accuracy of the proposed method for predicting the full force-deformation behaviour of multi-bolted connections under axial tension. Moreover, tests on models should be performed to investigate the rotational behaviour of steel angle connections. Furthermore, this study focused on bearing and end-shear failure. For the net section failure, another approach needs to be developed. It is also recommended that the

predictions of the present study be applied to a finite element model of a complete lattice tower and compared to full scale experimental tests.

Prediction of value of gap between bolt and bolt hole in a structure is also very important. The evaluation of this parameter can be very complicated due to several factors related to the fabrication and installation of towers. Filed measurements could help to quantify the slippage value and use a single value, instead of a range of values. The slippage will obviously depend on the bolting procedure and may be modified in time.

As mentioned before, many factors come into play in steel tower design, especially uncertainties for the connections based on construction and workmanship. Studies on propagation of these uncertainties and how it affects the resistance would be useful to guide detailers to best joint design practices.

7.4. Conclusions

L'objectif principal de ce travail consiste à la définition d'une stratégie afin de considérer le voilement local des cornières et le comportement non linéaire des connections dans un modèle numérique. Un modèle numérique plus précis peut fournir une alternative pour les tests de pylônes à grande échelle qui sont coûteux et longs.

En plus de leurs précisions, les modèles numériques doivent être faisables en termes d'efforts de modélisation et de temps d'analyse. Afin d'atteindre cet objectif, dans ce travail des éléments poutres multi-fibres sont implémentés pour modéliser les membrures de pylône à treillis. La contrainte principale lors de l'utilisation des éléments poutres est l'incapacité

d'inclure le voilement local. Dans cette étude, une nouvelle méthode est présentée pour combler cette lacune. Le comportement des connections est aussi un autre aspect de la modélisation des pylônes à treillis qui influence le comportement de la structure, principalement en termes de déplacement. Une seconde méthode simplifiée est fournie pour prédire le comportement global force-déplacement des connections y compris le glissement due à l'effort axial.

Les deux méthodes susmentionnées sont vérifiées en utilisant des tests expérimentaux sur des connexions et des cornières individuelles, afin d'assurer l'exactitude de la prédiction. De plus, les méthodes sont appliquées à des modèles numériques de contreventement en X et de section de treillis dans le but d'étudier leurs performances sur une structure test.

Trois contributions majeures ont été réalisées par ce travail de recherche. Premièrement, il explore la faisabilité d'utiliser une nouvelle méthode qui tiendra compte de la rupture en voilement local de membrure de classe 4 modélisé par des élément finis poutres multi-fibres. Deuxièmement, il propose une méthode pour prédire le comportement complet force-déformation des connexions multi boulonnées sous une tension axiale. Troisièmement, le comportement de l'assemblage prédit grâce à la méthode décrite dans cette recherche a été appliqué sur une section de pylône à échelle réduite, dans le but de vérifier l'application de la méthode et la comparer aux résultats expérimentaux.

Ce travail de recherche a offert une nouvelle méthode afin de considérer la rupture en voilement local des membrures de classe 4 modélisé par des éléments finis poutres multi-fibres. Par conséquent, le comportement contrainte-déformation du matériau des membrures a été modifié dans le modèle éléments finis. L'équation de la courbe contrainte-déformation a été fournie pour chaque membrure classe 4, basée sur la valeur d'élancement du déversement local (λ_p). À cet égard, des essais sur quarante-deux cornières courtes ayant des valeurs de λ_p comprises entre 0.57 et 1.2 ont été effectués dans le but d'évaluer leur comportement force-déplacement. Le comportement contrainte-déformation a été calculé ultérieurement pour chaque valeur de λ_p. Grâce au comportement contrainte-déformation

calculé et la technique d'ajustement des courbes, une formule généralisée reliant la valeur de λ_p et le comportement contrainte-déformation du matériau a été produite.

Dans le but d'appliquer la méthode sur un modèle à grande échelle, les membrures de classe 4 sont identifiées et la valeur de λ_p est estimée. L'équation représentée est utilisée ultérieurement pour générer la courbe contrainte-déformation modifiée. Cette dernière est assignée comme comportement de matériau des membrures correspondantes dans le logiciel d'analyse par élément finis.

Afin d'évaluer la faisabilité et la précision de la méthode proposée, elle a été appliquée sur quatre cadres contreventés testés par Morissette [52] à l'Université de Sherbrooke. Des cornières de classe 4 sont utilisées pour les contreventements des deux configurations examinées. La membrure ayant un rapport d'élancement global faible, le mode de rupture est présumé être dû au phénomène de voilement local. Deux modèles distincts d'éléments multi-fibres ont été développés, un avec et l'autre sans l'utilisation de la méthode suggérée, les prédictions sont par la suite comparées aux résultats expérimentaux. La comparaison montre qu'après l'implémentation de la méthode proposée dans les modèles élément finis le ratio moyen du modèle par rapport à la contrainte de rupture expérimentale passe de 1.54 (sans l'usage de la méthode proposée) à 1.02. Il est aussi observé que la nouvelle méthode fournit des résultats plus cohérents en matière de capacité de conception, par rapport aux résultats des normes Eurocode et ASCE.

Par ailleurs, ce travail de recherche introduit une méthode pour prédire le comportement global force-déplacement des assemblages boulonnés sous une tension axiale. La méthode proposée est établie en ajoutant le comportement dans le champ proche de chaque boulon, en utilisant un élément ressort non linéaire dans le modèle élément finis des connexions. Divers tests expérimentaux ont été réalisés sur des connexions avec un boulon et les résultats confirment que leur comportement peut se calculer en utilisant des relations théoriques et empiriques existantes. Le comportement dans le champ proche du boulon est ainsi appliqué sous forme de ressort non linéaire dans le modèle élément finis pour différents assemblages. De ce fait, les résultats du modèle éléments finis ont été comparés avec des tests

expérimentaux réalisés sur des connexions à deux boulons et des tests à quatre boulons disponibles. Il a été prouvé que la méthode proposée peut prédire avec justesse le comportement global des assemblages avec un, deux et quatre boulons ayant des propriétés et configurations différentes. Cette méthode permet aussi d'harmoniser la capacité ultime de l'assemblage. La méthode proposée autorise la prédiction de la courbe générale force-déplacement des assemblages multi-boulonnés, en utilisant un modèle éléments finis qui considère la géométrie et les propriétés mécaniques de chaque boulon. Cette courbe force-déplacement peut être utilisée pour calibrer un ressort non linéaire, ce qui reproduira le comportement de l'assemblage dans un modèle de pylônes à grande échelle.

Les principales conclusions de cette recherche sont :

- Les éléments poutre multi-fibres peuvent être utilisés pour la modélisation des pylônes tant que le voilement local et le comportement des assemblages soient pris en compte.
- Il a été observé que l'usage de la méthode proposée pour le voilement local améliore le ratio moyen du modèle par rapport la contrainte de rupture expérimentale de 1.54 à 1.02.
- La méthode proposée pour le voilement local ne représente pas une procédure de conception pratique, en revanche, elle pourra être considérée pour améliorer le modèle non linéaire des poutres pour les pylônes à treillis visant à compléter et réduire le besoin pour des tests à grande échelle sur des pylônes de lignes de transport.
- La méthode proposée pour les connexions permet la prédiction de la courbe globale force-déplacement des assemblages à plusieurs boulons en utilisant un modèle éléments finis.
- La courbe force-déplacement pour un assemblage à plusieurs boulons peut être utilisée pour calibrer un ressort non linéaire qui reproduira le comportement de la connexion existante dans un modèle de pylône à grande échelle.

- En utilisant le comportement de l'assemblage défini dans cette recherche, la prédiction du comportement force-déplacement global pour les sections de pylônes sera plus précise.
- Le déplacement global des pylônes causé par le glissement est prédit en utilisant cette méthode avec une précision acceptable comparé aux résultats expérimentaux.
- En utilisant la méthode proposée, la valeur prédite de la charge de rupture maximale pour la section test a une différence de 6% avec les résultats expérimentaux. Cette valeur augmente àa 11% sans l'utilisation de la méthode dans le modèle numérique.

7.5. Limitations de cette recherche

La méthode proposée ne représente pas une procédure pratique de conception, cependant il est possible de la considérer afin d'améliorer les modèles non linéaires de poutre utilisés dans les pylônes à treillis, afin à compléter et réduire le besoin de tests à grande échelle pour les pylônes électriques. En outre, la présente méthode qui modifie le comportement contrainte-déformation du matériau n'est valide que pour des valeurs de λ_p comprises entre 0.57 et 1.2. Il est donc nécessaire de vérifier la validité de la méthode présentée pour des valeurs de λ_p en dehors de cette gamme.

En comparant les résultats des essais et de l'analyse, on distingue toujours des différences et écarts entre ces deux. Dans cette étude, un défaut de rectitude arbitraireest considéré car la valeur réelle d'imperfections n'est pas mesurée pour ces spécimens. Par ailleurs, une autre cause possible est l'effet des contrainte résiduelles qui nesont pas considérées dans cette recherche.

7.6. Recommandations pour des travaux futurs

Malgré la contribution réalisée par cette recherche, des travaux futurs sont nécessaires pour couvrir plus de sections variées de classe 4 comme les cornières à ailes inégales. De plus, la méthode éléments finis proposée a été validée avec une série de tests composée seulement de quatre contreventements. Des recherches supplémentaires devront être réalisées sur des structures plus complexes et des essais sur le terrain afin de confirmer la méthode proposée.

En outre, dans le but de valider l'exactitude de la méthode proposée, plus de tests expérimentaux ayant différents nombres de boulons et arrangements devront être menés pour prédire le comportement complet force-déplacement des assemblages boulonnés sollicités en tension axiale. De plus, des tests sur les modèles doivent être produits pour examiner le comportement en rotation des assemblages pour les cornières. D'autre part, cette étude a porté sur l'écrasement en pression diamétrale et la rupture de la pince en cisaillement des assemblages boulonnés. Pour la rupture de la section nette, une approche distincte serait à développer. Il est aussi recommandé d'appliquer les prédictions de la présente étude à un modèle éléments finis de pylône à treillis complet et faire la comparaison avec des tests expérimentaux à grande échelle.

La prédiction du jeu entre les boulons et les trous dans une structure est aussi importante. L'évaluation de ce paramètre est souvent très difficile à cause des nombreux facteurs reliés à la fabrication et l'installation des pylônes. Des mesures in situ pourraient aider à quantifier la valeur du glissement afin d'utiliser une unique valeur au lieu d'une multitude de valeurs. Le glissement dépend de la procédure de boulonnage et peut varier dans le temps.

Comme mentionné précédemment, plusieurs facteurs entre en jeu dans la conception des pylônes en acier, particulièrement l'incertitude des assemblages basés sur l'exécution et la construction. Les études sur la propagation de ces incertitudes et leur impacts sur la résistance sera très utile pour guider les ingénieurs à des meilleures pratiques de conception des assemblages.

REFERENCES

[1] European Convention for Constructional Steel Work, ECCS No.39: Recommendations for angles in lattice transmission towers, 1st ed., European Convention for Constructional Steelwork, [Bruxelles Belgium], 1985.

[2] ANSI/ASCE Standard, Design of latticed steel transmission structures, ANSI/ASCE Standard. (2000) 1–69. https://doi.org/10.1061/9780784413760.

[3] BS EN 1993-1-1, Eurocode 3—Design of steel structures, European Committee for Standardization (CEN), Brussels,. (2005).

[4] Canadian Standards Association, Limit states design of steel structures CAN/CSA S16-14, 2014.

[5] N.P. Rao, S.J. Mohan, N. Lakshmanan, A study on failure of cross ARMS in transmission line towers during prototype testing, International Journal of Structural Stability and Dynamics. 5 (2005) 435–455. https://doi.org/10.1142/s0219455405001672.

[6] M. Marjerrison, Electric Transmission Tower Design, Journal of the Power Division. 94 (1968) 1–24.

[7] C. Lu, Y. Ou, M. Xing, J. Mills, Structural Analysis of Lattice Steel Transmission Towers: A Review, Journal of Steel Structures & Construction. 2 (2016) 114. https://doi.org/10.4172/2472-0437.1000114.

[8] J.G.S. Da Silva, P.C.G.D.S. Vellasco, S.A.L. De Andrade, M.I.R. De Oliveira, Structural assessment of current steel design models for transmission and telecommunication towers, Journal of Constructional Steel Research. 61 (2005) 1108–1134. https://doi.org/10.1016/j.jcsr.2005.02.009.

[9] D.D. Cannon, Variation in design practice for lattice towers, in: Sess. Relat. to Steel Struct. Struct. Congr. ’89, 1989: pp. 268–277.

[10] F.G.A. Al-Bermani, S. Kitipornchai, Nonlinear analysis of thin-walled structures using least element/member, Journal of Structural Engineering (United States). 116

(1990) 215–234. https://doi.org/10.1061/(ASCE)0733-9445(1990)116:1(215).

[11] P.S. Lee, G. McClure, Elastoplastic large deformation analysis of a lattice steel tower structure and comparison with full-scale tests, Journal of Constructional Steel Research. 63 (2007) 709–717. https://doi.org/10.1016/j.jcsr.2006.06.041.

[12] S. Kitipornchai, F.G.A. Al-Bermani, S.L. Chan, Elasto-plastic finite element models for angle steel frames, Journal of Structural Engineering (United States). 116 (1990) 2567–2581. https://doi.org/10.1061/(ASCE)0733-9445(1990)116:10(2567).

[13] N. Prasad Rao, V. Kalyanaraman, Non-linear behaviour of lattice panel of angle towers, Journal of Constructional Steel Research. 57 (2001) 1337–1357. https://doi.org/10.1016/S0143-974X(01)00054-2.

[14] F.Y. Wang, Y.L. Xu, S. Zhan, Concurrent multi-scale modeling of a transmission tower structure and its experimental verification, Advanced Steel Construction. 13 (2017) 258–272. https://doi.org/10.18057/IJASC.2017.13.3.4.

[15] S. Langlois, S. Prud, F. Légeron, F. Pourshargh, Review of advanced modelling methods for lattice steel towers Montréal, 2016 CIGRE-IEC Colloquium. (2016) 9.

[16] S. Roy, S.J. Fang, E.C. Rossow, Secondary stresses on transmission tower structures, Journal of Energy Engineering. 110 (1984) 157–172. https://doi.org/10.1061/(ASCE)0733-9402(1984)110:2(157).

[17] R.A. LeMaster, Structural development studies at the EPRI transmission line mechanical research facility, Interim Report 1, EPRI EL. 4756 (1986).

[18] F.G.A. Albermani, S. Kitipornchai, Numerical simulation of structural behaviour of transmission towers, Thin-Walled Structures. 41 (2003) 167–177. https://doi.org/10.1016/S0263-8231(02)00085-X.

[19] W. Kang, F. Albermani, S. Kitipornchai, H.F. Lam, Modeling and analysis of lattice towers with more accurate models, Advanced Steel Construction. 3 (2007) 565–582.

[20] S. Kitipornchai, A.H. Peyrot, Effect of bolt slippage on ultimate behavior of lattice structures, Journal of Structural Engineering (United States). 120 (1994) 2281–2287. https://doi.org/10.1061/(ASCE)0733-9445(1994)120:8(2281).

[21] N. Ungkurapinan, S.R.D.S. Chandrakeerthy, R.K.N.D. Rajapakse, S.B. Yue, Joint slip in steel electric transmission towers, Engineering Structures. 25 (2003) 779–788.

https://doi.org/10.1016/S0141-0296(03)00003-8.

[22] G.M. Knight, A.R. Santhakumar, Joint effects on behavior of transmission towers, Journal of Structural Engineering (United States). 119 (1993) 698–712. https://doi.org/10.1061/(ASCE)0733-9445(1993)119:3(698).

[23] W.Q. Jiang, Z.Q. Wang, G. McClure, G.L. Wang, J.D. Geng, Accurate modeling of joint effects in lattice transmission towers, Engineering Structures. 33 (2011) 1817–1827. https://doi.org/10.1016/j.engstruct.2011.02.022.

[24] K.I.E. Ahmed, R.K.N.D. Rajapakse, M.S. Gadala, Influence of bolted-joint slippage on the response of transmission towers subjected to frost-heave, Advances in Structural Engineering. 12 (2009) 1–17. https://doi.org/10.1260/136943309787522641.

[25] N. Ungkurapinan, A study of joint slip in galvanized bolted angle connections, University of Manitoba, 2000.

[26] Y. Zhan, G. Wu, Q.L. Lu, Modeling the effect of joint slip in lattice steel structures, Journal of Performance of Constructed Facilities. 30 (2016). https://doi.org/10.1061/(ASCE)CF.1943-5509.0000797.

[27] J. Li, H. Xu, Q. Luo, G. Mei, Z. Zhou, B. Tang, J. Zhoug, Structural Mechanics Analysis and Safety Assessment of Transmission Tower, IOP Conference Series: Earth and Environmental Science. 170 (2018) 0–6. https://doi.org/10.1088/1755-1315/170/4/042087.

[28] G.V. Rao, Optimum designs for transmission line towers, Computers and Structures. 57 (1995) 81–92. https://doi.org/10.1016/0045-7949(94)00597-V.

[29] N. Prasad Rao, G.M. Samuel Knight, S.J. Mohan, N. Lakshmanan, Studies on failure of transmission line towers in testing, Engineering Structures. 35 (2012) 55–70. https://doi.org/10.1016/j.engstruct.2011.10.017.

[30] N. Prasad Rao, G.M.S. Knight, N. Lakshmanan, N.R. Iyer, Investigation of transmission line tower failures, Engineering Failure Analysis. 17 (2010) 1127–1141. https://doi.org/10.1016/j.engfailanal.2010.01.008.

[31] British Standards Institution BSI, BS 8100-3; Lattice towers ans masts; Part 3: Code of practice for strength assesment of members of lattice towers and masts, 3 (1999)

1–31.

[32] American Society of Civil Engineers, ASCE 10-97: Guide for design of steel transmission towers, American Society of Civil Engineers, Task Committee on Tower, Design. (1997) 47p.

[33] Bureau of Indian Standards, IS 802 (1995): Code of Practice for Use of Structural Steel In Overhead Transmission Line Towers, 1995.

[34] F. Albermani, S. Kitipornchai, R.W.K. Chan, Failure analysis of transmission towers, Engineering Failure Analysis. 16 (2009) 1922–1928. https://doi.org/10.1016/j.engfailanal.2008.10.001.

[35] N.P. Rao, ; G M Samuel Knight, ; S Seetharaman, ; N Lakshmanan, N.R. Iyer, N. Prasad Rao, G.M. Samuel Knight, S. Seetharaman, N. Lakshmanan, N.R. Iyer, Failure analysis of transmission line towers, Journal of Performance of Constructed Facilities. 25 (2011) 231–240. https://doi.org/10.1061/(ASCE)CF.1943-5509.0000161.

[36] P.L. Bouchard, Calcul de la capacité de pylônes à treillis avec une approche stabilité, Université de Sherbrooke, 2013.

[37] K. Sad Saoud, S. Langlois, A. Loignon, C.P. Lamarche, Failure analysis of transmission line steel lattice towers subjected to extreme loading, 6th International Structural Specialty Conference 2018, Held as Part of the Canadian Society for Civil Engineering Annual Conference 2018. (2018) 320–328.

[38] S.M.R. Adluri, M.K.S. Madugula, Flexural buckling of steel angles: Experimental investigation, Journal of Structural Engineering. 122 (1996) 309–317. https://doi.org/10.1061/(ASCE)0733-9445(1996)122:3(309).

[39] G. Gravel, P.L. Bouchard, S. Prudhomme, K. Sad Saoud, S. Langlois, Assessment of the effect of residual stresses on the mechanical behavior of steel lattice transmission towers, 6th International Structural Specialty Conference 2018, Held as Part of the Canadian Society for Civil Engineering Annual Conference 2018. (2018) 126–135.

[40] S.L. Chan, S.H. Cho, Second-order analysis and design of angle trusses Part I: Elastic analysis and design, Engineering Structures. 30 (2008) 616–625. https://doi.org/10.1016/j.engstruct.2007.05.010.

[41] B.W. Schafer, Advances in direct strength design of thin-walled members, Advances

in Strutures (ASSCCA'03). (2003) 333–339.

[42] N. Silvestre, D. Camotim, P.B. Dinis, Post-buckling behaviour and direct strength design of lipped channel columns experiencing local/distortional interaction, Journal of Constructional Steel Research. 73 (2012) 12–30. https://doi.org/10.1016/j.jcsr.2012.01.005.

[43] A.D. Martins, D. Camotim, P.B. Dinis, On the distortional-global interaction in cold-formed steel columns: Relevance, post-buckling behaviour, strength and DSM design, Journal of Constructional Steel Research. 145 (2018) 449–470. https://doi.org/10.1016/j.jcsr.2018.02.031.

[44] N. Prasad Rao, G.M. Samuel Knight, N. Lakshmanan, N.R. Iyer, Effect of bolt slip on tower deformation, Practice Periodical on Structural Design and Construction. 17 (2012) 65–73. https://doi.org/10.1061/(ASCE)SC.1943-5576.0000108.

[45] L. Shan, A.H. Peyroi, Plate element modeling of steel angle members, Journal of Structural Engineering (United States). 114 (1988) 821–840. https://doi.org/10.1061/(ASCE)0733-9445(1988)114:4(821).

[46] P.S. Lee, G. McClure, A general three-dimensional L-section beam finite element for elastoplastic large deformation analysis, Computers and Structures. 84 (2006) 215–229. https://doi.org/10.1016/j.compstruc.2005.09.013.

[47] Y.S. Park, S. Iwai, H. Kameda, T. Nonaka, Very low cycle failure process of steel angle members, Journal of Structural Engineering. 122 (1996) 133–141. https://doi.org/10.1061/(ASCE)0733-9445(1996)122:2(133).

[48] S. Kitipornchai, S.L. Chan, Nonlinear finite element analysis of angle and tee beam-columns, Journal of Structural Engineering (United States). 113 (1987) 721–739. https://doi.org/10.1061/(ASCE)0733-9445(1987)113:4(721).

[49] R.F. Vieira, F.B.E. Virtuoso, E.B.R. Pereira, Buckling of thin-walled structures through a higher order beam model, Computers and Structures. 180 (2017) 104–116. https://doi.org/10.1016/j.compstruc.2016.01.005.

[50] E. Carrera, A. Pagani, M. Petrolo, Refined 1D finite elements for the analysis of secondary, primary, and complete civil engineering structures, Journal of Structural Engineering (United States). 141 (2015). https://doi.org/10.1061/(ASCE)ST.1943-

541X.0001076.

[51] L. Huang, B. Li, Y. Wang, Computation Analysis of Buckling Loads of Thin-Walled Members with Open Sections, Mathematical Problems in Engineering. 2016 (2016). https://doi.org/10.1155/2016/8320469.

[52] É. Morissette, Évaluation des normes de calcul et du comportement des cornières simples en compression utilisées comme contreventements dans les pylônes à treillis en acier, Université de Sherbrooke, 2008.

[53] B.W. Schafer, Review: The Direct Strength Method of cold-formed steel member design, Journal of Constructional Steel Research. 64 (2008) 766–778. https://doi.org/10.1016/j.jcsr.2008.01.022.

[54] C. Qing, R.G. Driver, End tear-out failures of bolted tension members, Structural Engineering Report No. 278,. (2008) 1–154.

[55] S. Loignon, A, Légeron, F., Lamarche, C.-P. et Langlois, Développement d'un protocole d'essai hybride par sous-structuration pour les pylônes à treillis, 2018.

[56] S. Cho, S. Chan, Second-order analysis and design of angle trusses, Part II: Plastic analysis and design, Engineering Structures. 30 (2008) 626–631. https://doi.org/10.1016/j.engstruct.2007.04.022.

[57] B.W. Schafer, S. Ádány, Buckling analysis of cold-formed steel members with general boundary conditions using CUFSM: Conventional and constrained finite strip methods, in: 18th Int. Spec. Conf. Cold-Formed Steel Struct. -, Orlando, Florida, USA, 2006.

[58] ASTM International, ASTM A36 / A36M-14, Standard Specification for Carbon Structural Steel, 2014. https://doi.org/10.1520/A0036_A0036M-14.

[59] ASTM International, ASTM A370-02, Standard Test Methods and Definitions for Mechanical Testing of Steel Products, 2002. https://doi.org/10.1520/A0370-02.

[60] A. Beyer, N. Boissonnade, A. Khelil, A. Bureau, Influence of assumed geometric and material imperfections on the numerically determined ultimate resistance of hot-rolled U-shaped steel members, Journal of Constructional Steel Research. 147 (2018) 103–115. https://doi.org/10.1016/j.jcsr.2018.03.021.

[61] C.O. Rex, W. Samuel Easterling, Behavior and modeling of a bolt bearing on a single

plate, Journal of Structural Engineering. 129 (2003) 792–800. https://doi.org/10.1061/(ASCE)0733-9445(2003)129:6(792).

[62] C.O. Rex, W.S. Easterling, Behavior and modeling of a single plate bearing on a single bolt, Technical Report, Rep. CE/VPI-ST 96/14,. (1996).

[63] G.L. Kulak, J.W. Fisher, J.H.A. Struik, Guide to Design Criteria for Bolted and Riveted Joints, Second Edi, Search Results Web results American Institute of Steel Construction, Chicago, IL, USA, 2001.

[64] SAE International, SAE Fastener Standards Manual, 2009 Editi, Warrendale, PA, USA, 2009.

[65] G. Gravel, Étude de l'effet des hypothèses de modélisation numérique avancée sur la prédiction du comportement structural des pylônes à treillis, Université de Sherbrooke, 2020.

[66] M.A. Crisfield, A fast incremental/iterative solution procedure that handles "snap-through," Computers and Structures. 13 (1981) 55–62. https://doi.org/10.1016/0045-7949(81)90108-5.

[67] W. Petersen, Design of EHV Steel Tower Transmission Lines, Journal of the Power Division. (1962) 39–65.